PUBLISHER :

Address of Publisher & Editor's Office :

GDAŃSK UNIVERSITY
OF TECHNOLOGY
Faculty
of Ocean Engineering
& Ship Technology

ul. Narutowicza 11/12
80-952 Gdańsk, POLAND
tel.: +48 58 347 13 66
fax : +48 58 341 13 66
e-mail : office.pmr@pg.gda.pl

Account number :
BANK ZACHODNI WBK S.A.
I Oddział w Gdańsku
41 1090 1098 0000 0000 0901 5569

Editorial Staff :
Kazimierz Kempa Editor in Chief
e-mail : kkempa@pg.gda.pl
Przemysław Wierzchowski Scientific Editor
e-mail : e.wierzchowski@chello.pl
Jan Michalski Editor for review matters
e-mail : janmi@pg.gda.pl
Tadeusz Borzęcki Editor for international relations
e-mail : tadbor@pg.gda.pl
Piotr Bzura Managing Editor
e-mail : pbzura@pg.gda.pl
Cezary Spigarski Computer Design
e-mail : biuro@oficynamorska.pl

Domestic price :
single issue : 20 zł

Prices for abroad :
single issue :
- in Europe EURO 15
- overseas US$ 20

ISSN 1233-2585

POLISH MARITIME RESEARCH

in internet

www.bg.pg.gda.pl/pmr.html

POLISH MARITIME RESEARCH

No 4(54) 2007 Vol 14

CONTENTS

The papers published in this issue have been reviewed by :
Prof. W. Adamkiewicz ; Prof. Cz. Dymarski ; Prof. J. Girtler
Prof. W. Chądzyński ; Assoc. prof. T. Koronowicz
Prof. T. Szelangiewicz ; Prof. Z. Zaczek

Editorial

POLISH MARITIME RESEARCH is a scientific journal of worldwide circulation. The journal appears as a quarterly four times a year. The first issue of it was published in September 1994. Its main aim is to present original, innovative scientific ideas and Research & Development achievements in the field of :

Engineering, **Computing & Technology**, **Mechanical Engineering**,

which could find applications in the broad domain of maritime economy. Hence there are published papers which concern methods of the designing, manufacturing and operating processes of such technical objects and devices as : ships, port equipment, ocean engineering units, underwater vehicles and equipment as well as harbour facilities, with accounting for marine environment protection.
The Editors of POLISH MARITIME RESEARCH make also efforts to present problems dealing with education of engineers and scientific and teaching personnel. As a rule, the basic papers are supplemented by information on conferences , important scientific events as well as cooperation in carrying out international scientific research projects.

Scientific Board

POLISH MARITIME RESEARCH 4(54) 2007 Vol 14; pp. 3-6
DOI: 10.2478/v10012-007-0032-y

A method for selection of parameters of ship propulsion system fitted with compromise screw propeller

Jan P. Michalski, Assoc. Prof.
Gdańsk University of Technology
Polish Naval University

ABSTRACT

This paper concerns an algorithmic method for preliminary selection of parameters of ship propulsion system fitted with fixed screw propeller in the case when the ship's operation is associated with significant changes of waterway depth and width, hull resistance of the ship and its service speed. Mathematical model arguments of the considered design problem are main ship design parameters identified in the preliminary design stage. Structure of the formulated model complies with formal requirements for continuous- discrete mathematical optimization problems. The presented examples of application of the method concern an inland waterways ship fitted with compromise screw propeller optimized in the sense of minimization of fuel consumption for passing a given route distance within a given time. The elaborated method may be especially useful in designing such ships as : coasters, inland waterways ships, tugs, pushers, trawlers, mine sweepers, icebreakers etc.

Keywords : design of inland waterways ships, ship propellers, ship propulsion

INTRODUCTION AND PROBLEM DESCRIPTION

A method for selection of rational, or optimum in a given sense, technical solutions of a ship should take into account, already in the preliminary design stage, both obligatory and crucial design conditions and constraints. This paper concerns a method for determining, in the preliminary design stage, optimum values of the parameters of ship propulsion system fitted with fixed screw propeller in the case where hull resistance and service speed of the ship significantly varies during operation, that often takes place in the case of inland navigation.

Design process of inland navigation ships should takes into account the demand of adjusting the ship to future real service tasks including ship operation at significantly variable propulsion performance characteristics of the ship, whose variability results from :

- changeable hydrographic conditions in water area of ship operation – shallow waters, narrow canals of variable width, winding river bends
- significant changes of ship draught and displacement during voyage
- frequent events of ship running aground and re-floating – unavoidable in shallow waters
- hull resistance changes at various hull configurations – in the case of multi-hull arrangement.

Polish inland waterways are of small depth and often have the form of unregulated narrow river beds. In such case are fully justified the reasons for the application to inland navigation ships the propulsion systems with fixed screw propellers as they, in comparison with those with controllable pitch propellers, are characterized by :

- low manufacturing, assembling and possible repair costs of the propellers
- higher reliability and resistance against failure during stranding
- higher power conversion efficiency.

For operators of inland navigation ships the high reliability of propulsion system and easiness of its repair possible to be done even in almost any conditions along trip route are of crucial importance.

CLASSICAL PROBLEM STATEMENT

In the standard design method of preliminary selection of ship propulsion system parameters the following phases can be distinguished :

- 1st phase of the approximate determining of nominal hull resistance characteristics in function of the speed **v**, ship and waterway parameters $\overline{\mathbf{p}}$

$$R = R(v, \overline{p})$$

as well as the hull-propeller interaction coefficients, i.e. the wake fraction **w** = w(v, $\overline{p}$) and thrust deduction **t** = t(v, $\overline{p}$)

- 2nd phase of the determining of demanded power characteristics as well as geometrical parameters of screw propeller including its diameter, pitch, number of blades, and expanded blade area coefficient in function of ship speed and number of revolutions of propeller and engine; this is a basis for rational choice of an engine (-s) from producer catalogues.

In the subject-matter literature the above described design procedure is called,,thrust approach" or „naval architect's approach"; it leads to selection of propeller parameters and a specific engine of determined rated power and rotational speed. The ship's designer – in cooperation with the ship's owner and engine producer – determines permissible values of the engine's operation parameters, in particular its continuous rating, rotational speed and supercharging parameters. The selection of continuous rating parameters of the chosen engine in the form of its torque **Q** and rotational speed **n** makes it possible to select values of parameters of power transmission devices and screw propeller itself.

The above presented classical design problem may have an unambiguous solution in the case of taking the simplifying assumption consisting in an arbitrary determination of hull resistance characteristics. To this end are assumed the nominal (design) hull resistance characteristics relevant to predicted conditions, i.e. the most probable service conditions of designed ship. Hence an unambiguous value of hull resistance corresponds to the ship speed given in the ship's design assumptions, that forms the basis for the selection of parameters of propulsion system of maximum efficiency which is usually limited by necessity of satisfying a given set of design constraints.

If real ship service conditions appear different from those assumed in design procedure then the propulsion system will operate at a lower efficiency, increased specific fuel consumption, not fully utilized engine output, or with the engine overloaded by torque or rotational speed. The method of solving the classical design problems, described e.g. in [2, 3, 4], is used here as a comparative background for further considerations.

NON-STANDARD PROBLEM STATEMENT

In the case of ship propulsion system fitted with fixed screw propeller a non-standard problem of ship design theory is the designing of ship propulsion system at hull resistance characteristics significantly changing during ship service as well as at significantly changing hull -propeller interaction characteristics, **w** and **t**. The subject-matter literature does not provide a fully satisfactory algorithmic method useful in solving the so defined design problems.

The presented considerations are thought as an attempt to eliminate the gap by elaborating a method for selecting the propulsion system with fixed propeller, useful in solving design problems of ships intended for operation in the conditions when :

- water area is shallow, of changeable depth and/or width
- immersed part of ship hull undergoes intensive fouling
- ship service is associated with up- and down-stream sailing
- ship displacement significantly changes during voyage
- ship service consists in towing or pushing other objects.

Especially important is the case when the ship has to operate both in deep and shallow or restricted waters as then hull resistance characteristics much differ in each of the cases. The water area limitations influence both flow velocity distribution around the hull and ship-generated wave system (pressure distribution). Beginning from the limit speed up to critical one, hull resistance suddenly increases [6, 9]. Moreover the change in flow velocity distribution around the hull due to waterway bank effects makes the wake fraction and thrust deduction coefficients changing, thus they become variable, which seriously influences propeller performance.

The above described non-standard problem of determining the designed ship propulsion system parameters is of an utilitarian importance both technical and economical, however so far no fully satisfactory solution has been found for it in spite of the great interest paid to the problem [5, 6, 7].

The method in question exemplifies such a method for selecting the ship propulsion system parameters, which takes into account both changeable operational conditions of screw propeller and changeable hull resistance, and also arbitrary design constraints to be satisfied, and moreover which makes it possible to determine such values of the system's parameters which optimize the propulsion system in a certain sense.

MATHEMATICAL MODEL OF THE DESIGN PROBLEM

Assumptions of the method for selecting the propulsion parameters

The screw propeller designing in accordance with the classical approach [2, 3, 4] consists in such selection of its geometrical characteristics as to obtain maximum value of propulsion efficiency and full utilization of continuous rating of driving engine at a given rotational speed in ship service conditions complying with its design assumptions. Moreover, the designed screw propeller should fulfill operational reliability criteria both for the propeller itself and elements cooperating with it.

In design practice, fulfillment of reliability requirements is equivalent to selection of a suitable material for the propeller as well as of geometrical parameters of the propeller in such a way as to ensure its sufficient strength and resistance against cavitation erosion.

Continuous service output power of the engine is usually taken as its characteristic power and its relation to engine's rated power depends on engine's dynamic performance and a way of determining the rated power, which depends on a type of engine and standards applied by producers of particular engines.

The continuous service output power is assumed a little smaller than, or equal to maximum continuous rating which the engine is capable of developing at a given rotational speed and not exceeding a permissible thermal load. However the so determined output power is usually not acceptable to ship owners for the reason of values of time between engine overhauls demanded by them; hence on ship owner's request the service output power value is lowered by a few percent, and the lower output has to be developed at rated rotational speed or that somewhat lower.

Decision variables and parameters of the model

In accordance with formulation principles of the mathematical optimization problems the mathematical model of the considered design problem, built under appropriate simplifying assumptions, contains :

- a target function to be minimized (or maximized)
- constraints in the form of equalities and inequalities, resulting from technical sense of the design problem

- ❖ a vector of optimized decision variables together with permissible ranges of their determination
- ❖ a set of approximate analytical characteristics of the phenomena taken into account in the model.

The propulsion system with fixed screw propeller is considered as that commonly applied to ships operating in shallow waters [1, 6, 8].

The considered service route of the ship in question consists ***m*** waterway sections whose lengths are described by the vector $\overline{\mathbf{r}} = (r_1, r_2, \ldots r_m)$. The waterway sections differ to each other by the parameters of water area and of the ship $\overline{\mathbf{p}}_i = (p_{i,1}, p_{i,2}, \ldots)$, which significantly affect propulsion system's performance.

The hull resistance $\mathbf{R_i}(v_i, \overline{p}_i)$ in *i-th* water area of length $\mathbf{r_i}$ depends on the parameters $\overline{\mathbf{p}}_i$ and ship speed $\mathbf{v_i}$ developed over this section of the route. Moreover the hull resistance characteristics can be corrected by means of the coefficients $\boldsymbol{\xi_i}$ which represent arbitrarily assumed service margins.

Ship's speeds over particular route sections are described by the vector $\overline{\mathbf{v}} = (v_1, v_2, \ldots v_m)$ determined during optimization process, and the propulsion system efficiency $\boldsymbol{\eta}(\overline{v}, \overline{p}, \overline{s})$ over particular route sections depends on the propeller parameters $\overline{\mathbf{s}} = (s_1, s_2, \ldots)$, waterway parameters, water inflow velocity as well as parameters of ship's hull form assumed here fixed, i.e. not subjected to any correction and optimization.

In the model in question the following was assumed :

$$\overline{p}_i = (p_{i,1}, p_{i,2}, p_{i,3}) \quad \text{and} \quad \overline{s} = (s_1, s_2, s_3, s_4, s_5)$$

where :

$p_{i,1} = h_i/T$ - ratio of the depth of *i-th* route section and ship's draught
$p_{i,2} = b_i/B$ - ratio of the width of *i-th* route section and ship's breadth
$p_{i,3} = vs_i$ - current speed over *i-th* route section
$s_1 = z$ - number of propeller blades, from the set {3, 4, 5}
$s_2 = S_0/S$ - propeller expanded blade area ratio, from the set {0.55, 0.65, 0.70, 0.75}
$s_3 = D$ - propeller diameter not greater than that maximum permissible $D \le D_{max}$
$s_4 = H/D$ - propeller pitch ratio, one of the decision variables of the model, to be determined during optimization process
$s_5 = n$ - number of propeller revolutions, one of the decision variables of the model, to be determined during optimization process.

Target function to be minimized

The demanded propulsion power $\mathbf{P}(v, \overline{p}, \overline{s},)$, necessary to obtain the ship speed $\mathbf{v_i}$ over the route section $\mathbf{r_i}$, can be expressed as follows :

$$P_i = \frac{\xi_i R(v_i, \overline{p}_i)\, v_i}{\eta(v_i, \overline{p}_i, \overline{s})} = \frac{\xi_i R(v_i, \overline{p}_i)\, v_i}{\eta_p(v_i, \overline{p}_i, \overline{s})\, \xi_k(v_i, \overline{p}_i, \overline{s})\, \xi_r(v_i, \overline{p}_i, \overline{s})\, \eta_t(\overline{s})} \tag{1}$$

The fuel cost $\mathbf{K_i}$ consumed to cover the distance of the section $\mathbf{r_i}$ with the speed $\mathbf{v_i}$ is equal to :

$$K_i(v_i, \overline{p}_i, \overline{s}) = kj\, gj(s_5)\, P(v_i, \overline{p}_i, \overline{s})\, \tau(v_i) = \frac{kj\, gj(s_5)\, \xi_i R(v_i, \overline{p}_i)\, r_i(\overline{p}_i)\, [1 - w(v_i, \overline{p}_i, \overline{s})]}{\eta_p(v_i, \overline{p}_i, \overline{s})\, [1 - t(v_i, \overline{p}_i, \overline{s})]\, \xi_r(v_i, \overline{p}_i, \overline{s})\, \eta_t(\overline{s})} \tag{2}$$

where :

kj - unit fuel cost [€/t]
gj - specific fuel consumption [g/kWh]
τ_i - time period to cover the distance of *i-th* route section [h]
η_p - open –water propeller efficiency [-]
η_t - power transmission efficiency (from engine to propeller) [-]
ξ_k - hull "efficiency" characteristics [-]
ξ_r - rotational efficiency [-].

In the presented example of the method the total fuel cost $\mathbf{K_c}$ necessary the ship to cover voyage distance within the assumed time period $\boldsymbol{\tau_z}$, was taken as the criterion subjected to optimization :

$$K_c(\tau_z) = \sum_{i=1}^{m} K_i(v_i, \overline{p}_i, \overline{s}, r_i) \tag{3}$$

The set of values of propulsion system parameters, for which the set of model constraints is satisfied (set of permissible solutions) and the target function simultaneously reaches its minimum value, is considered the optimum solution of the model.

Design constraints of the model

The presented model was elaborated under the following assumptions :

➡ The voyage route of the total length **r** is consisted of **m** sections of given waterway characteristics :

$$r = \sum_{i=1}^{m} r_i \tag{4}$$

➡ The voyage duration time $\boldsymbol{\tau}$ is consisted of the ship sailing time as well as the in-advance-estimated time $\boldsymbol{\tau_0}$ – intended for stays in ports, locking operations etc :

$$\tau = \sum_{i=1}^{m} \tau_i + \tau_0 = \sum_{i=1}^{m} \frac{r_i}{v_i} + \tau_0 \tag{5}$$

➡ The voyage duration time, $\boldsymbol{\tau_z}$, determined by the design assumptions is connected with the speeds $\mathbf{v_i}$ for covering distance of particular route sections, by the following relation :

$$\sum_{i=1}^{m} \frac{r_i}{v_i} + \tau_0 \le \tau_z \tag{6}$$

➡ The permissible limits for ship's maximum speed over *i*-th route section were assumed as follows :

$$0 < v_i \le v_i^{max} \quad i = 1, 2, \ldots m \tag{7}$$

➡ Optimum propeller diameter is not to exceed that maximum permissible :

$$D(\overline{x}) \le D_{max} \tag{8}$$

➡ The range of permissible values of the propeller pitch **H** is as follows :

$$0.6 \le \frac{H}{D} \le 1.4 \tag{9}$$

➡ Minimum value of the expanded blade area ratio $\mathbf{S_0/S}$ of the propeller has to satisfy the Keller's cavitation criterion [10] :

$$\left(\frac{S_0}{S}\right)_{min} \ge \frac{(1.3 + 0.3z)\, T_r}{(p_0 - p_d)\, D^2} + k \tag{10}$$

where :
z - number of propeller blades
p_0 - water pressure at propeller axis
p_d - saturated water vapour pressure
T_r - propeller thrust
k = 0.1
D - propeller diameter.

➡ Number of propeller rotations is not to exceed that maximum permissible :

$$n \leq n_{max} \tag{11}$$

➡ Solution of the problem is searched for within the set of propellers having their hydrodynamic characteristics approximated by continuous analytical relationships. In the computer implementation of the model the characteristics of Wageningen propellers of ***Ka*** series intended for operation within **19A** nozzles, are included [11] :

$$K_T\left(J, \frac{H}{D}, \frac{S_0}{S}, z\right) \in \in \{K_T(Ka3-65)\ ,\ K_T(Ka4-55),\ K_T(Ka4-70)\ ,\ K_T(Ka5-75)\} \tag{12}$$

$$K_Q\left(J, \frac{H}{D}, \frac{S_0}{S}, z\right) \in \in \{K_Q(Ka3-65)\ ,\ K_Q(Ka4-55),\ K_Q(Ka4-70)\ ,\ K_Q(Ka5-75)\} \tag{13}$$

APPROXIMATED CHARACTERISTICS OF THE MODEL

The presented method requires to determine in advance analytical relationships which approximate selected hydrodynamic characteristics of propulsion system, and are expressed in function of the variable design arguments $\overline{x}$; in particular, it is necessary to have at one's disposal analytical representations of :

- the hydrodynamic characteristics $K_T(\overline{x})$, $K_Q(\overline{x})$, $\eta_p(\overline{x})$ of propellers
- the hull resistance characteristics $R(\overline{x})$ for particular route sections
- the hull-propeller interaction characteristics $w(\overline{x})$ and $t(\overline{x})$ for particular route sections
- the driving engine performance characteristics $P(\overline{x})$.

Analytical hydrodynamic characteristics of propellers

Making use of the data included in [11] one elaborated computer procedures for determining the analytical characteristics $K_T(\overline{x})$, $K_Q(\overline{x})$, $\eta_p(\overline{x})$ whose example graphical representation concerning Ka3 – 65 propeller ducted in 19A nozzle is shown in Fig.1.

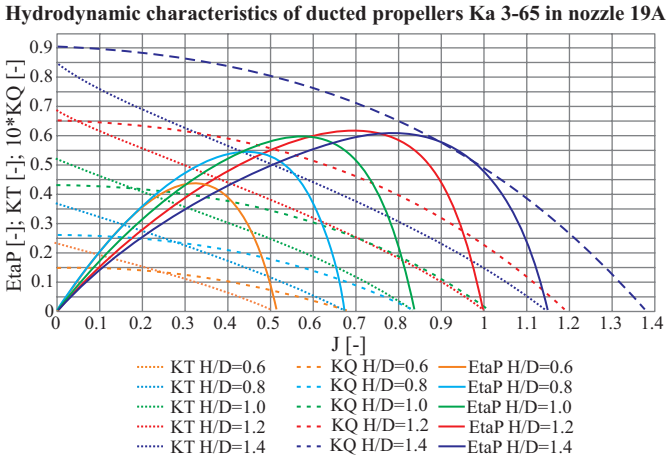

Fig. 1. *Example graphical representation of analytically approximated characteristics of propellers .*

Analytical hull resistance characteristics

On the basis of the results of hull resistance model tests [12] their analytical approximation was performed and as a result the continuous hull resistance characteristics versus ship speed and water area parameters [13] were achieved. The graphical representation of the approximated hull resistance curves is shown in Fig. 2.

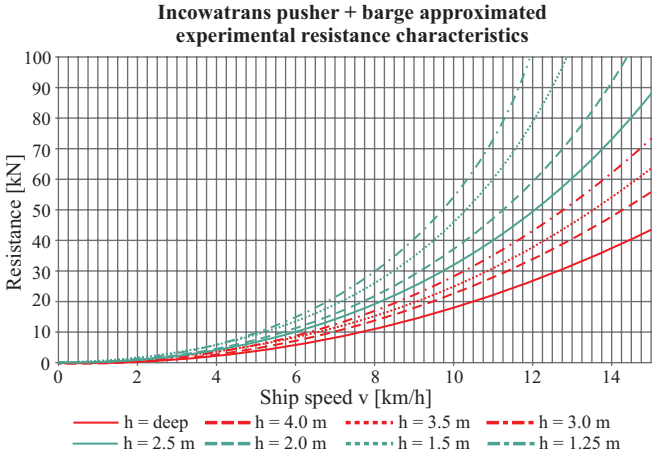

Fig. 2. *Graphical representation of the approximated hydrodynamic characteristics of hul resistance .*

Analytical characteristics of hull - propeller interaction

By making use of the elaborated method for determining the hull-propeller interaction characteristics in restricted waters [14] the characteristics of the coefficients $\mathbf{w}(\overline{\mathbf{x}})$ and $\mathbf{t}(\overline{\mathbf{x}})$ for the hull in question and particular route sections, were determined. The so obtained characteristics are presented in Fig.3 and 4, respectively.

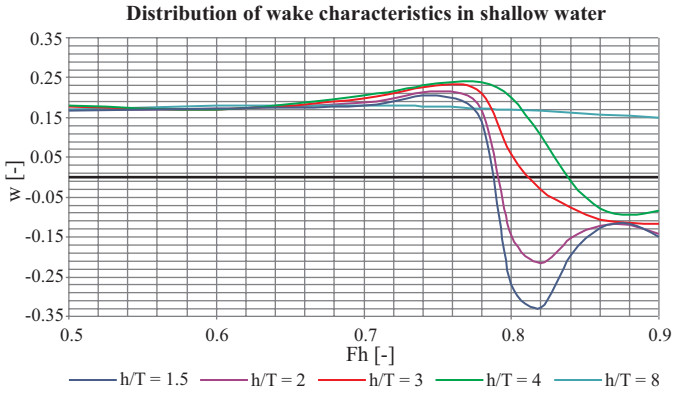

Fig. 3. *Graphical representation of the approximated hydrodynamic characteristics* $\mathbf{w}(\overline{\mathbf{x}})$.

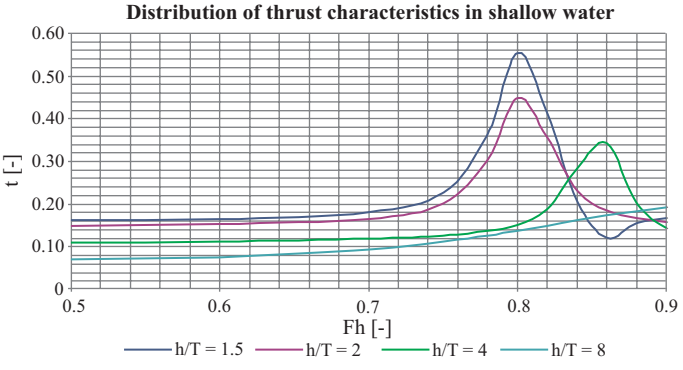

Fig. 4. *Graphical representation of the approximated hydrodynamic characteristics* $\mathbf{t}(\overline{\mathbf{x}})$.

Example of application of the method

The below presented numerical calculations were performed by means of the computer software [15]. Their results concern searching for optimum values of propulsion system parameters and speed of the ship designed within the frame of the **EU Eureka E!3065** *InCoWaTranS* Project, and intended for tourist traffic along Polish inland waterways on the route Berlin - Królewiec.

The set of input parameters for the example task

Main particulars of two-segment ship :

- Ship's name *'M/v Eureka InCoWaTranS'*
- Total length of the train (55m +55m) 110.00 [m]
- Ship breadth 9.00 [m]
- Ship draught 1.00 [m]
- Ship mass displacement 840.00 [t]
- Margin factor 1.15 [-].

Route parameters :

- Length of deep-water part of the route 250 [km]
- Depth of deep-water part of the route 5.0 [m]
- Length of shallow-water part of the route 315 [km]
- Depth of shallow-water part of the route 2.0 [m]
- Length of canals on the route 280 [km]
- Canal water depth 1.5 [m].

Screw propeller parameters :

- Characteristics of the propellers {Ka 3-65; Ka 4-55; Ka 4-70; Ka 5-75}
- Kort nozzle {No 19A}
- Maximum diameter of the propeller 1.0 [m]
- Maximum rotational speed of the propeller 600 [rpm]
- Minimum value of H/D ratio 0.6 [-]
- Maximum value of H/D ratio 1.4 [-]
- Rotational efficiency 1.05 [-]
- Power transmission efficiency 0.90 [-]
- Water density 1.0 [t/m^3]
- Immersion depth of propeller axis 0.5 [m]
- Keller's criterion constant 0.1 [-].

The constraints imposed upon permissible values of ship speed and trip duration time :

- Maximum ship speed in deep water 15.0 [km/h]
- Maximum ship speed in shallow water 10.0 [km/h]
- Maximum ship speed in canals 7.0 [km/h]
- Voyage duration time 144 [h]
- Duration time of locking operations and port stays 24 [h].

Engine parameters :

- Specific fuel oil consumption 220 [g/kWh].

Financial parameter :

- Unit fuel oil cost 325 [€/t].

Results of optimization calculations

The results obtained from the first and last iteration of optimization calculations with the use of the above given task input data, are included in Tab.1, where the first row are results of the **first iteration** (fuel cost = 1462 €), and the second row are the results of the **last iteration** (fuel cost = 877 €), and the comprehensive full report from the calculations is included in [15].

The convergence process of selected results of optimization calculations in successive iteration steps is presented in Fig.5.

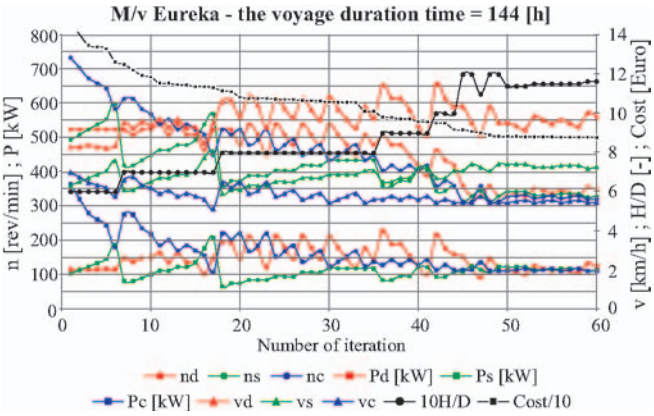

Fig. 5. *Graphical representation of convergence process of selected results of optimization calculations*

Tab. 1. *Numerical results from the first and last iteration of optimization calculations.*

Type	H/D	nd	ns	nc	vd	Eta0d	EtaPd	Rd	TNd	Pd	vs	Eta0s	EtaPs
[-]	[-]	[1/min]	[1/min]	[1/min]	[km/h]	[-]	[-]	[kN]	[kN]	[kW]	[km/h]	[-]	[-]
4	0.60	525	495	735	8.28	0.376	0.273	13.8	14.9	118	6.32	0.251	0.238
3	1.164	350	330	321	9.87	0.569	0.413	20.3	20.4	128	7.27	0.495	0.334

Rs	TNs	Ps	vc	Eta0c	EtaPc	Rc	TNc	Pc	Cavit	Jd	Js	Jc	Cost
[kN]	[kN]	[kW]	[km/h]	[-]	[-]	[kN]	[kN]	[kW]	[-]	[-]	[-]	[-]	[€]
14.7	15.1	106	7.00	0.209	0.198	38.4	39.3	365	1.01	0.30	0.24	0.18	1462
20.3	20.3	116	5.45	0.413	0.274	21.4	21.5	113	0.53	0.54	0.42	0.33	877

Description of selected items of Tab. 1. The following notation was applied : indices :

d - parameters concerning deep water
s - parameters concerning shallow water
c - parameters concerning canals.
Type: 1=Ka 3-65; 2=Ka 4-55; 3=Ka 4-70; 4=Ka 5-75;
n - rotational speed of propeller
v - ship speed
Eta0 - open -water propeller efficiency
EtaP - behind-the-hull propeller efficiency
R - hull resistance in a given water area
TN - propelling force developed by propeller
P - demanded output power of the engine in a given water area
Cavit - index of Keller's cavitation criterion (**Cavit<1** - no cavitation)
J - propeller advance ratio
Cost - total cost of fuel oil consumed to cover voyage distance within a given time period.

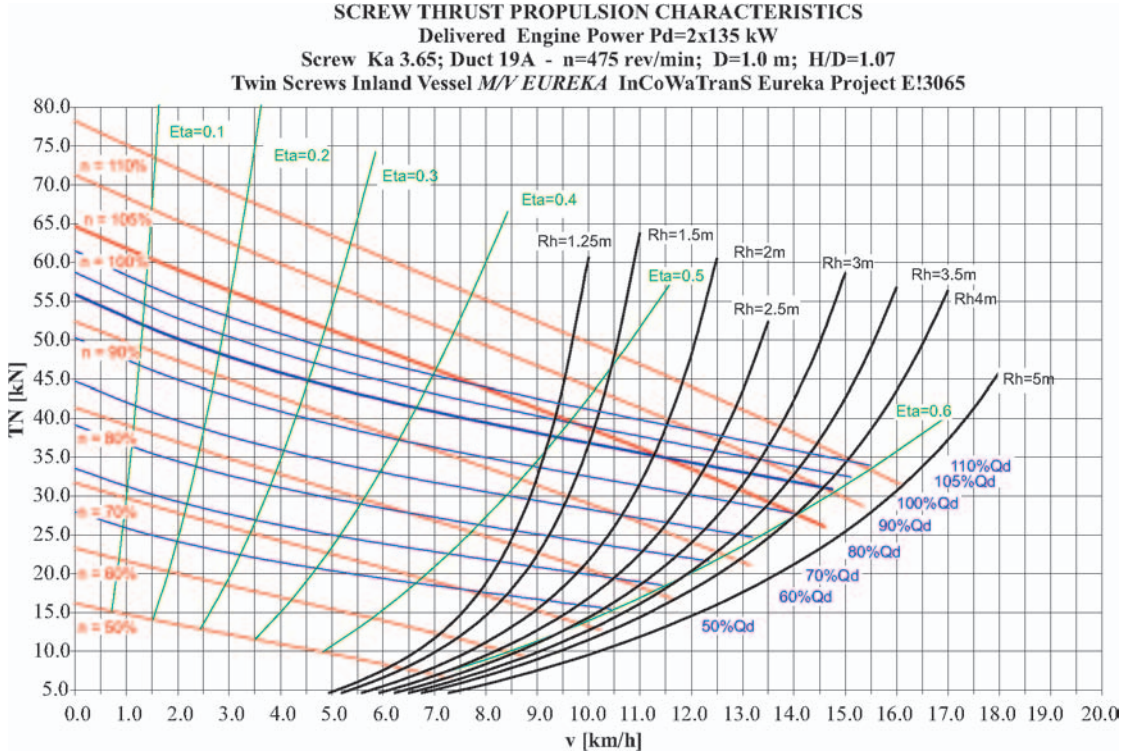

Fig. 6. Graphical representation of example characteristics of the propulsion force TN developed by the designed propulsion system.

The obtained results of optimization calculations can be used to select values of propeller parameters and an engine of appropriate output power and rotational speed, that makes it possible to elaborate characteristics of the engine and propeller and to analyze this way their interaction in changeable service conditions; so obtained characteristics are shown in Fig.6 in the form of the computer-processed diagram [15].

SUMMARY

- The computer implementation of the calculation algorithm realizing the presented mathematical model, makes it possible to effectively solve the design problem consisting in selection of optimum (here in the sense of minimizing fuel consumption cost) parameters of ship propulsion system fitted with fixed propeller, in the case of ship operating at changeable hull resistance characteristics, on a voyage route in waterways of changeable depth and width.

- The presented results concern the example in which the designed ship has to cover its assumed voyage distance within 144 h including the duration time of port stays and locking operations equal to 24 h. By changing the effective voyage duration time, different optimum values of design parameters of the propulsion system can be respectively obtained.

- The presented design method is fully algorithmic and it does not require to appeal to designer's experience and intuition, hence it can serve to objectively, effectively and immediately find complex, difficult for intuitive assessment, solutions for propulsion system design problems.

- The method may also serve as a useful tool in aiding the design process in the phase preceding model tests as well as in determining the scope of model test program.

NOMENCLATURE

b - route section width
B - ship breadth
D - propeller diameter [m]
Fh - Froude number related to depth of water area
gj - specific fuel oil consumption [g/kWh]
h - route section depth
H - propeller pitch [m]
J - propeller advance ratio [-]
k = 0.1 - constant in Keller's cavitation criterion
kj - unit fuel oil cost [€/t]
K - fuel cost
K_T - propeller thrust coefficient characteristics [-]
K_Q - propeller torque coefficient characteristics [-]
m - number of route sections
n - number of propeller rotations
$\overline{p}$ - vector of water area parameters
p_d - saturated water vapour pressure
p_i - parameter of a water area and ship
p_o - water pressure at propeller axis
P - propulsion power [kW]
r - route section length
R - hull resistance [kN]
R_i - hull resistance in i-th water area [kN]
$\overline{s}$ - vector of propeller parameters
t - thrust deduction characteristics [-]
T - propeller thrust, ship's draught
v - ship speed [km/h]
v_i - ship speed developed in i-th water area [km/h]
vs - route section current speed
Q - engine torque
w - wake fraction characteristics [-]
$\overline{x}$ - in general, vector of variable design arguments
z - number of propeller blades [-]

η - propulsion system efficiency [-]
η_p - efficiency of open - water propeller [-]
η_t - power transmission efficiency, from engine to propeller [-].
τ - voyage duration time [h]

τ_0 - duration time of port stays and locking operations [h]
τ_i - time to cover distance of i-th route section [h]
τ_z - assumed time period to cover voyage distance
ξ_k - hull "efficiency" characteristics [-]
ξ_r - rotational efficiency [-]
ξ_i - additional resistance factor in i-th water area [-].

BIBLIOGRAPHY

1. Bojko J.: *Development of US Navy* (in Polish). Bandera. February 2004
2. Kobyliński L.*: Ship propellers* (in Polish). Transport Publishing House (Wydawnictwa Komunikacyjne). Warszawa 1955
3. Carlton J.S.: *Marine Propellers and Propulsion*. Butterworth Heineman
4. Basin A.M., Miniowicz I.J.: *Teoria i rasczet grebnych wintow* (in Russian). Leningrad 1963
5. Szantyr J.: *Designing the controllable pitch propellers by means of electronic digital machine* (in Polish). 3rd Symposium on Ship Hydrodynamics – Hydrodynamic problems of ship propulsion. IMP PAN. Gdańsk 1975
6. Kulczyk J., Winter J.: *Inland waterways transport* (in Polish). Publishing House of Wrocław University of Technology (Oficyna Wydawnicza Politechniki Wrocławskiej). Wrocław 2003
7. Więckiewicz W.: *Changes of ship resistance in service versus performance of ship propeller* (in Polish). 3rd Symposium on Ship Hydrodynamics – Hydrodynamic problems of ship propulsion. IMP PAN. Gdańsk 1975
8. Basin A.M., Wjelednickij I.O., Ljakowickij A.G.: *Gidrodinamika sudow na mielkowodie (in Russian)*. Izdatielstwo Sudostroienie. Leningrad 1976
9. Żylicz A.: *Inland waterways ships* (in Polish). Maritime Publishing House (Wydawnictwo Morskie). Gdańsk 1979.
10. Dudziak J.: *Theory of ships* (in Polish). Maritime Publishing House (Wydawnictwo Morskie). Gdańsk 1988
11. Kuiper G.: *The Wageningen propeller series.* MARIN Publication. Netherlands 1992
12. Rogalski A., Grygorowicz M.: *Model test results of a tourist hotel passenger ship in deep and shallow water* (in Polish). Research report No. 126/E/2004, Faculty of Ocean Engineering and Ship Technology, Gdańsk University of Technology, 2004
13. Michalski J.P.: *Mathematical model for selecting optimum parameters of propulsion system of inland waterways ships - approximation of experimental characteristics of hull resistance* (in Polish*).* Research report No. 182/E/2005, Faculty of Ocean Engineering and Ship Technology, Gdańsk University of Technology, 2005
14. Michalski J.P.: *Calculation algorithms and DUCT_PROPELLER.VBA computer software for determining and visualizing hydrodynamic characteristics of KA screw propellers ducted in the Kort nozzle No 19A, intended for designing propulsion systems of inland waterways ships* (in Polish). Research report No. 204/E/2005, Faculty of Ocean Engineering and Ship Technology, Gdańsk University of Technology, 2005
15. Michalski J.P.: *A method for designing optimum parameters of compromise screw propellers and service speed of inland waterways ships in restricted waters* (in Polish). Research report No. 225/E/2005, Faculty of Ocean Engineering and Ship Technology, Gdańsk University of Technology, 2005

CONTACT WITH THE AUTHOR

Assoc. Prof. Jan P. Michalski
Faculty of Ocean Engineering
and Ship Technology
Gdansk University of Technology
Narutowicza 11/12
80-952 Gdansk, POLAND
e-mail : janmi@pg.gda.pl

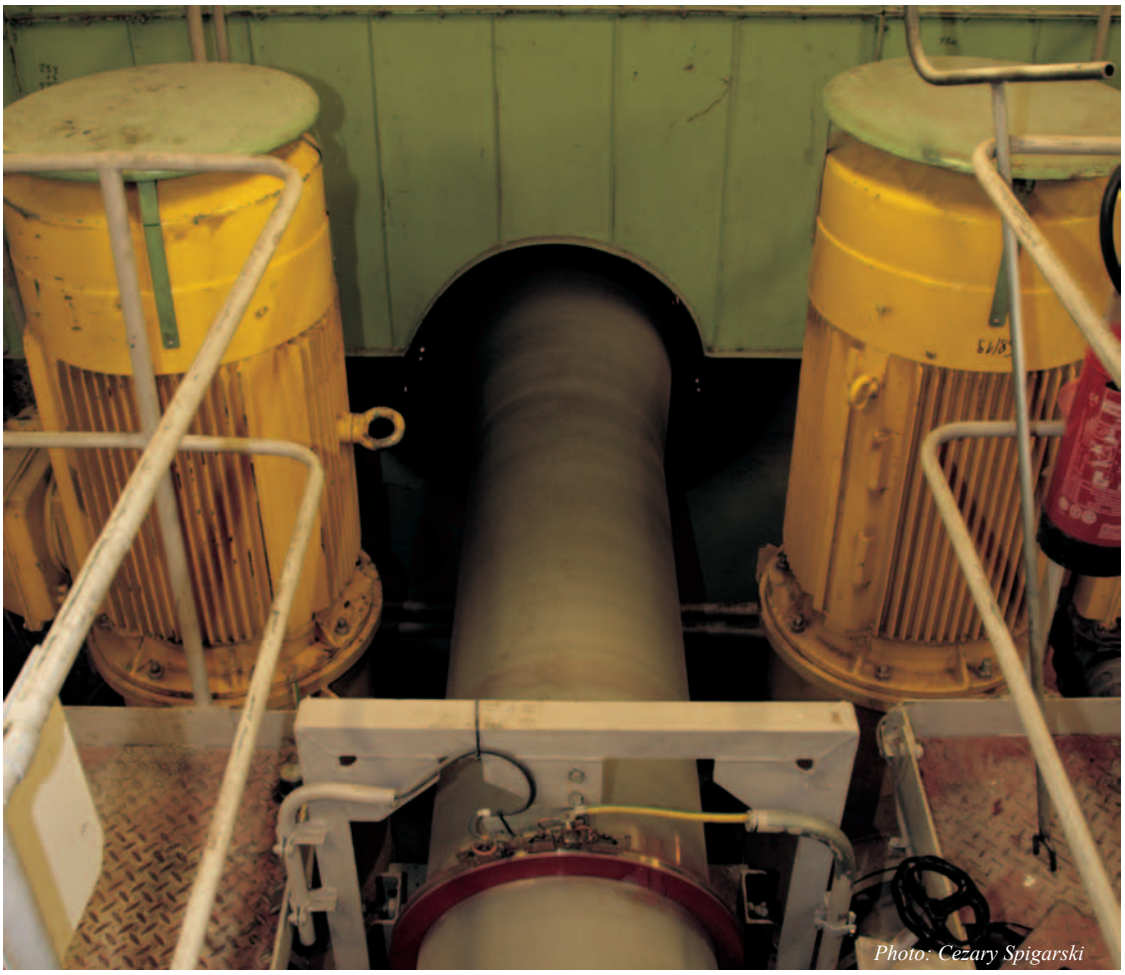

Photo: Cezary Spigarski

POLISH MARITIME RESEARCH 4(54) 2007 Vol 14; pp. 10-14
DOI: 10.2478/v10012-007-0033-x

Dynamic interaction of the cavitating propeller tip vortex with the rudder

Jan A. Szantyr,
Gdansk University of Technology

ABSTRACT

The hydrodynamic interaction between the ship propeller and the rudder has many aspects. One of the most interesting is the interaction between the cavitating tip vortex shed from the propeller blades and the rudder. This interaction leads to strongly dynamic behaviour of the cavitating vortex, which in turn generates unusually high pressure pulses in its vicinity. Possibly accurate prediction of these pulses is one of the most important problems in the hydrodynamic design of a new ship. The paper presents a relatively simple computational model of the propeller cavitating tip vortex behaviour close to the rudder leading edge. The model is based on the traditional Rankine vortex and on the potential solution of the dynamics of the cylindrical sections of the cavitating kernel passing through the strongly variable pressure field in the vicinity of the rudder leading edge. The model reproduces numerically the experimentally observed process of initial compression of the vortex kernel in the high pressure region near the stagnation point at the rudder leading edge and subsequent explosive growth of the kernel in the low pressure region further downstream. Numerical simulation of this process enables computation of the additional pressure pulses generated due to this phenomenon and transmitted onto the hull surface. This new numerical model of the cavitating tip vortex is incorporated in the modified unsteady lifting surface program for prediction of propeller cavitation, which has been successfully used in the process of propeller design for several years and which recently has been extended to include the effects of propeller – rudder interaction. The results of calculations are compared with the experimental measurements and they demonstrate reasonable agreement between theory and physical reality.

Keywords : propeller blades, rudder, cavitating, tip vortex shed

STATEMENT OF THE PROBLEM

The physical mechanisms and consequences of the interaction between ship propeller and rudder have been the focus of considerable research effort in the recent years (see for example [2, 4, 5, 6]). The results of this research show first of all that cavitation on the rudder is a fairly frequent phenomenon and that its consequences may be as important for the ship operation as cavitation on the propeller itself. Secondly, it seems that sufficiently accurate prediction of sheet cavitation on the rudder is practically possible using variety of methods, ranging from boundary element method to commercial RANS codes. However, it seems that another aspect of propeller – rudder interaction has not received sufficient attention yet. This aspect is the propeller cavitating tip vortex interaction with the rudder.

Cavitation tunnel experiments with propeller – rudder configurations show that this interaction leads to very dynamic behaviour of the sections of the cavitating kernel in the vicinity of the rudder leading edge. Examples of the selected stages of this process are shown in Figs. 1, 2, 3 and 4. Careful analysis of the photographs shows that the sections of the tip vortex cavitating kernel at first enter the high pressure area in front of the rudder leading edge stagnation point, where they undergo compression. Then they slide downstream along the rudder into the area of low pressure, where they increase their diameter and later disintegrate into a cloud of bubbles. This process may take place even when there is no sheet cavitation on the rudder. It leads to generation of additional strong pressure pulses and it may cause erosion damage on the rudder.

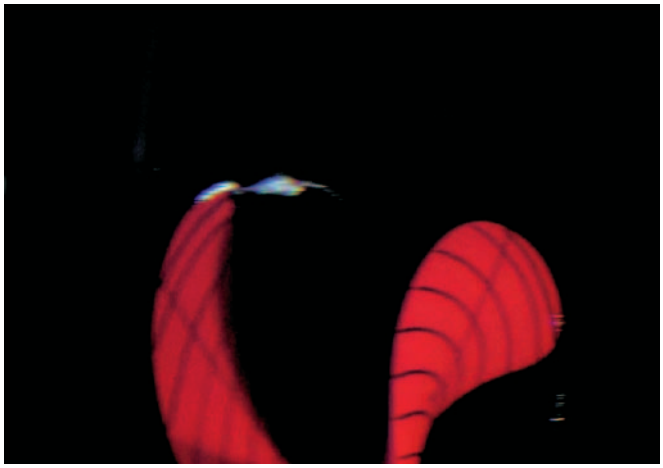

Fig.1. *Cavitating tip vortex approaching ruder – phase 1.*

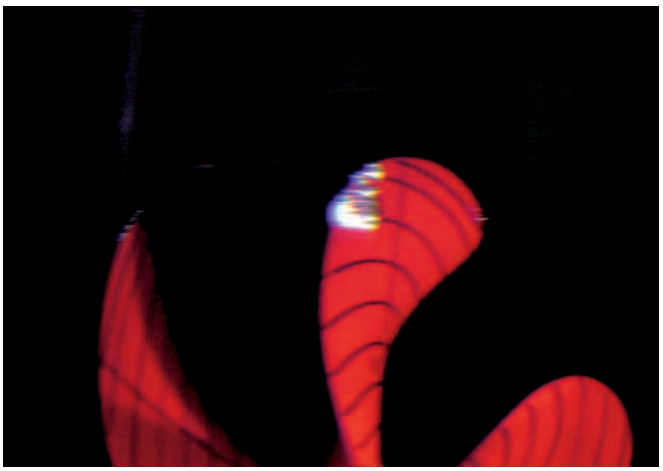

Fig.2. *Cavitating tip vortex approaching rudder – phase 2.*

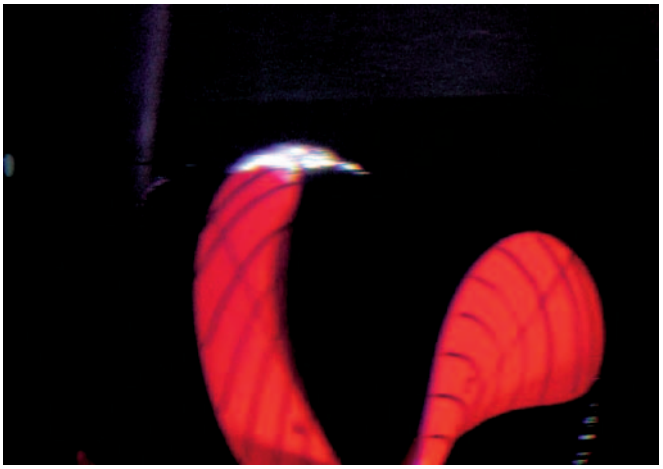

Fig.3. *Cavitating tip vortex approaching rudder – phase 3.*

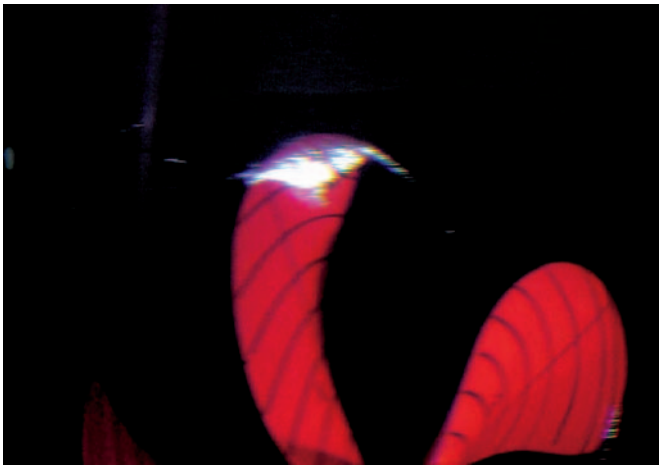

Fig.4. *Cavitating tip vortex approaching rudder – phase 4.*

Simultaneous measurements of pressure pulses on the ship hull model with and without rudder show a considerable increase of pressure harmonic amplitudes with rudder present – cf. Tab. 1. In this case all three pressure pick-ups are located along the ship symmetry plane, with point no. 1 located in front of the propeller, point no. 2 directly above propeller and point no. 3 at the rudder leading edge. The details of the model propeller rudder configuration are shown in Fig. 8. The Tab.1 includes amplitudes of the first blade frequency harmonic A1 and second harmonic A2, both re-calculated to full scale. As there was no cavitation on the rudder at zero deflection angle and no visible change in cavitation on the propeller blades due to rudder presence, this increase may be attributed to the above described dynamic interaction of the cavitating tip vortex with the rudder. A marked increase in the higher order harmonic amplitudes points to the complicated character of this interaction.

The above presented experimental evidence was the inspiration for development of the model described in [9] and this paper. The primary purpose of this model is to enable calculation of the additional pressure pulses generated by the cavitating tip vortex in interaction with the rudder.

Tab. 1. *Results of measurements, [kPa].*

Pick-up no.	With rudder		Without rudder	
	A1	A2	A1	A2
1	0.976	0.773	0.730	0.569
2	2.630	2.960	1.963	2.310
3	2.731	3.036	1.560	2.071

DESCRIPTION OF THE COMPUTATIONAL MODEL

The model of the propeller tip vortex interaction with the rudder presented in this paper was developed as an extension of the lifting surface method for prediction of unsteady propeller cavitation [7], [8]. This method was modified recently to include the unsteady hydrodynamic interaction between propeller and rudder. The original method produces the time-dependent intensity of the propeller tip vortex as the function of the variable loading of the propeller blade passing through the non-uniform velocity field of the ship wake. Typically the tip vortex is divided into sections corresponding to the angular propeller blade step of 5 deg, each section having constant vortex intensity. Geometry of the tip vortex follows the streamline, including the velocity induced by the propeller and by the rudder. The sketch of this model is shown in Fig. 5.

The extended tip vortex model is based on the following assumptions:

- the velocity and pressure fields induced by the vortex is calculated by using the Rankine vortex model
- the diameter of the Rankine vortex kernel is related to the boundary layer thickness in the tip region of the blade
- the cavitating vortex kernel of the tip vortex is divided into small sections, each of which is modelled by a circular cylinder
- dynamics of each section is modeled by a properly adapted Rayleigh-Plesset equation solved numerically in the time/space by using Runge-Kutta method
- the primary purpose of the model is to describe the first cycle of compression/rebound of the cavitating tip vortex sections, disregarding subsequent disintegration of the vortex kernel into bubble and cloud cavitation.

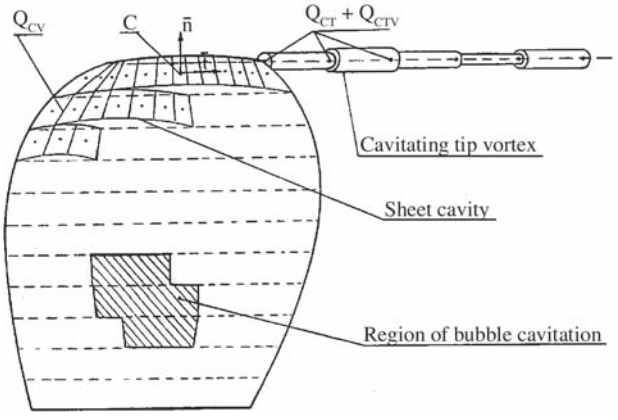

Fig. 5. *Cavitating tip vortex model in the original analysis method.*

Such simple model does not account for many of the complicated vortex flow phenomena (cf. [3]), but still is able to reproduce the basic, physically realistic dependence of the generated pressure pulses on the basic mechanisms of the propeller – rudder interaction.

In the numerical model developed under the above assumptions each element of the cavitating tip vortex is treated as an independent section of an infinite circular cylinder, filled with gas/vapour mixture and acted upon by the external pressure field which is generated due to interaction of propeller and rudder. Propeller effect is calculated by using lifting surface theory, while rudder effect is calculated by using boundary element method. Example of the pressure field calculated by using this approach in the vicinity of the rudder leading edge at zero deflection is shown in Fig. 6. This figure shows the pressure distribution in the horizontal plane located above propeller shaft and passing through the point where vortex hits the rudder. The orange and red colours show the region of reduced pressure while the shades of green and blue show the regions of increased pressure. The asymmetry of the pressure distribution despite the nominal zero rudder deflection results from the propeller induced velocity, which generates a non-zero angle of attack.

Fig. 6. *Calculated pressure field around the rudder at zero deflection.*

In the Rankine vortex model all vorticity is concentrated inside a finite diameter core, which rotates as a rigid body, while the flow around the core is irrotational. This leads to the following formulae for the tangential induced velocity:

$$V_T = \frac{\Gamma}{2\pi r} \quad \text{for} \quad r \geq R_C \tag{1}$$

$$V_T = \frac{\Gamma}{2\pi R_C}\left(\frac{r}{R_C}\right) \quad \text{for} \quad r \leq R_C \tag{2}$$

where:
Γ - the vortex circulation,
r - the radial coordinate,
R_C - the radius of the Rankine vortex core.

Vortex circulation in the above formula is taken from the unsteady lifting surface model of the propeller blade and is a function of propeller blade position. The vortex core radius is usually related to the boundary layer thickness in the tip region of the blade, in this case at the relative radius 0.95. This leads to the following approximate relation:

$$R_C = \frac{0.37C}{Re^{0.2}} \tag{3}$$

where:
Re - the Reynolds number,
C - the blade section chord length at relative radius 0.95.

Then the pressure distribution around the Rankine vortex may be determined according to the following formulae:

$$p = p_\infty - \frac{\rho\Gamma^2}{8\pi^2 r^2} \quad \text{for} \quad r \geq R_C \tag{4}$$

$$p = p_\infty - \frac{\rho\Gamma^2}{8\pi^2 R_C^2}\left[\left(\frac{R_C}{r}\right)^2 - 2\right] \quad \text{for} \quad r \leq R_C \tag{5}$$

where:
p_∞ - the pressure far away from the vortex
ρ - the water density
r - the radial coordinate.

The minimum pressure is attained in the vortex centre and its value may be determined as:

$$p_{min} = p_\infty - \frac{1}{4\pi^2}\left(\frac{\Gamma}{R_C}\right)^2 \tag{6}$$

The inception of the tip vortex cavitation is determined by analyzing the behaviour of a cavitation nuclei in the pressure field generated by the tip vortex. It is assumed that nuclei present in water are sucked due to pressure force into the vortex centre and then their dynamics is studied using the standard Rayleigh – Plesset equation for a gas-filled spherical bubble:

$$\frac{d^2R_B}{dt^2}\left[\frac{\Delta p}{\rho} - \frac{3}{2}\left(\frac{dR_B}{dt}\right)^2 - \frac{2\sigma}{\rho R_B} - \frac{4\mu}{\rho R_B}\frac{dR_B}{dt}\right]\frac{1}{R_B} \tag{7}$$

where:
R_B - the bubble radius
Δp - the pressure difference across the bubble wall
t - the time
σ - the water surface tension
μ - the dynamic viscosity coefficient.

The above given equation is solved numerically by using Runge - Kutta method with a very short time step of 1 [μs]. The pressure difference governing the bubble growth is computed in each time step from formulae (4,5,6). The initial conditions for this solution must include the initial bubble radius. In most calculations it is taken equal to 0.05 [mm], which corresponds to the typical size of cavitation nuclei present in the water. Inception of tip vortex cavitation is signalled when the bubble radius reaches the value of 0.25 [mm]. This value is in fact an empirical calibration parameter, determined on the basis of comparison of experimental and calculated inception conditions.

Once the inception of the tip vortex cavitation is diagnosed the initial radius of a cylindrical section of the cavitating kernel, just after leaving the blade, may be determined as:

$$R = \frac{\Gamma}{2\pi}\sqrt{\frac{\rho}{2(p_\infty - p_V)}} \tag{8}$$

where: p_V is the critical vapour pressure.

The dynamics of each section of the cavitating vortex kernel is calculated by using the Rayleigh-Plesset equation adapted to the cylindrical geometry. In this case the flow is treated as two-dimensional and purely vaporous content of the kernel is assumed, what leads to the following equation:

$$-\frac{d^2R}{dt^2}R\ln R-\left(\frac{dR}{dt}\right)^2\left(\ln R+\frac{1}{2}\right)+ \\ +\frac{\sigma}{\rho R}+\frac{2\mu\, dR/dt}{\rho R}=\frac{\Delta p(t)}{\rho} \tag{9}$$

where:
R - the radius of the cylindrical section of the cavitating vortex kernel
t - the time
σ - the surface tension of water
μ - the dynamic viscosity of water
ρ - the density of water
Δp - the pressure difference across the vortex kernel wall.

This equation is solved numerically by using the Runge - Kutta method. In the solution process two levels of time steps are used. The first level time step ΔT is related to the propeller blade angular step in the non-uniform inflow and typically it is of order of 5 – 10 milliseconds in full scale and 0.5 – 1.0 milliseconds in model scale. The second level time step is used in numerical solution of the dynamics equation (1) and is typically taken as Δt=0.01ΔT, i.e. 50 – 100 microseconds in full scale or 5 – 10 microseconds in model scale, although this may be varied if necessary. The external pressure acting on each vortex section is taken at the section centre and linearly approximated within each time step ΔT. The numerical solution of equation (1) is based on the initial conditions defining R and dR/dt and it yields the values of R and dR/dt at the end of each time step ΔT. These values replace the initial values for the same vortex section in the next time step. The entire procedure is illustrated in Fig. 7.

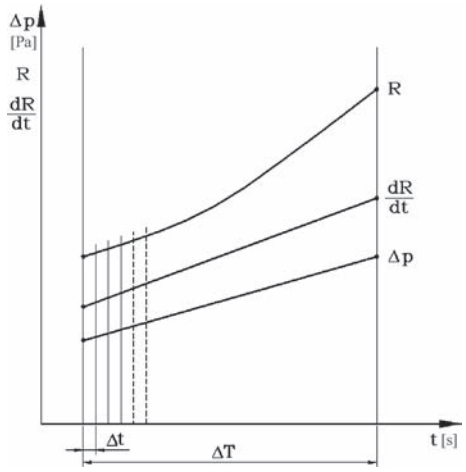

Fig. 7. *Principle of numerical solution of equation (1) for a vortex section.*

When the values of R and dR/dt are determined for each ΔT the effect of the cavitating tip vortex dynamics on the pulsating pressure field generated by the entire propeller – rudder system, may be calculated. This is done following the approach already incorporated in the propeller analysis method [8]. In this approach each cavitating tip vortex section is modelled by a point source, described by its mean value Q, constant within each ΔT and reflecting the quasi-steady displacement effect and by dQ/dt, reflecting the vortex dynamics. Both these values are employed in calculation of pressure pulses according to the linear form of the Cauchy-Lagrange equation:

$$P_H=\frac{\rho}{4\pi}\left(V_S\sum_i\frac{Q_i x_i}{l_i^3}+\sum_i\frac{Q_i}{l_i^2}\frac{dl_i}{dt}-\sum_i\frac{1}{l_i}\frac{dQ_i}{dt}\right) \tag{10}$$

where:
P_H - the pulsating pressure
V_S - the ship velocity
l - the distance from source to the calculation point
x - the component of r in direction of ship velocity.

The sources in the above given equation are calculated in the following way:

$$Q_i=\pi(R_i^2-R_{i-1}^2)\sqrt{V_S^2+(\pi Dn)^2} \tag{11}$$

$$\frac{dQ_i}{dt}=\pi\left[\left(\frac{dR_i}{dt}\right)^2-\left(\frac{dR_{i-1}}{dt}\right)^2\right]\sqrt{V_S^2+(\pi Dn)^2} \tag{12}$$

where:
D - the propeller diameter
n - the number of propeller revolutions per second

The equation for P_H yields the values of the variable part of pressure at prescribed locations for each ΔT, i.e. for each analyzed angular propeller blade positions. These values are added to the contributions from propeller hydrodynamic loading and thickness, from rudder loading and thickness and from cavitation phenomena developed on the propeller and rudder. The total pressure pulses are resolved into harmonics.

COMPARISON OF THE CALCULATED AND EXPERIMENTALLY MEASURED RESULTS

The above described numerical method was used to calculate the pressure pulsations induced by the cavitating tip vortex interacting with the rudder. The calculation was performed for the full scale configuration corresponding to the model used in the experiments presented in the Introduction. The configuration is shown in Fig. 8, while the basic data of the propeller are presented in Tab. 2.

Tab. 2. *Main data of the propeller.*

Propeller diameter			**D = 8.200 [m]**	
Number of blades			**Z = 5**	
Number of revolutions			**RPM = 99.0 [rpm]**	
r/R	**C[m]**	**P/D [-]**	**S [m]**	**M [m]**
0.25	2.2875	0.9694	-0.096	0.0979
0.4	2.5913	1.0167	-0.316	0.0834
0.5	2.7779	1.0402	-0.387	0.0715
0.6	2.9325	1.0539	-0.337	0.0632
0.7	3.0323	1.0547	-0.153	0.0578
0.8	3.0416	1.0352	0.152	0.0516
0.9	2.8226	0.9859	0.569	0.0417
0.95	2.3355	0.9494	0.834	0.0321
1.0	0.0	0.9090	1.156	0.0

where:
C – blade section chord lengths
P/D – pitch coefficients
S – skewback ordinates
M – mean line camber
r – local radius
R – propeller radius.

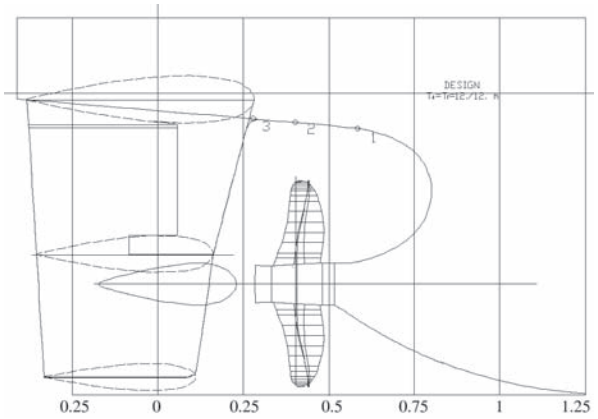

Fig. 8. *Configuration of propeller and rudder used in calculations.*

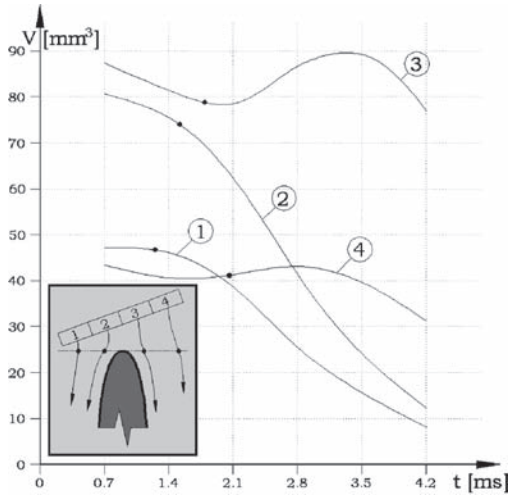

Fig. 9. *Calculated time history of selected sections of the cavitating tip vortex.*

Tab. 3. *Calculation results by using the new model*

Pickup No.	Measured with rudder	Calculated without rudder	Calculated with rudder
1	0.976	1.480	1.563
2	2.630	1.880	2.470
3	2.731	1.890	2.658

CONCLUSIONS

- The above presented model of interaction of the propeller cavitating tip vortex with the rudder incorporates the influence of the following important factors on the cavitating tip vortex dynamics:
  - structure of the non-uniform velocity field at the inflow to the propeller,
  - geometry and operating parameters of the propeller,
  - geometry, location and deflection of the rudder.
- Initial results of the calculations show that the new model is fully capable of predicting realistically the additional pressure pulses generated by the interaction of the cavitating propeller tip vortex with the pressure field around the rudder.
- The model obviously does not account for important secondary phenomena such as the disintegration of the vortex in the rebound phase, described for example by Tunc and Delale [10]. As this disintegration process dissipates energy it may be expected that the simple model above presented has the tendency to overestimate the induced pressure pulsations. This means that the calculation results should be on the "safe side".

Acknowledgement

The author would like to acknowledge kind co-operation of the Ship Design and Research Centre (CTO SA) in Gdansk which supplied the experimental results employed in this paper.

NOMENCLATURE

C – propeller blade section chord length
D – propeller diameter
l – distance from the source to the calculation point
M – propeller blade section mean line camber
n – number of propeller revolutions per second
P/D – propeller blade section pitch coefficient
P_H – pulsating pressure
p – local pressure
p_∞ – pressure far away from the vortex
p_{min} – minimum pressure at the vortex centre
p_V – critical vapour pressure
Δp – pressure difference across the wall
Q – intensity of the source modeling the vortex kernel
R – radius of the cylindrical section of the cavitating vortex kernel
R_B – radius of the spherical cavitation bubble
R_C – radius of the Rankine vortex core
Re – Reynolds number
r – radial coordinate
S – propeller blade section skewback ordinate
ΔT – time step between the consecutive blade positions
Δt – time step in the Runge-Kutta method
t – time
V_S – ship velocity
V_T – tangential velocity induced by the Rankine vortex
x – component of l in the direction of the ship velocity
Γ – vortex circulation
μ – dynamic viscosity coefficient of water
ρ – density of water
σ – surface tension of water

BIBLIOGRAPHY

1. Couty Ch., Farhat M., Avellon F.*:Physical Investigation of a Cavitation Vortex Collapse.* Proceedings of the 4th Intern. Symp. on Cavitation CAV2001, Pasadena, USA, 2001
2. Krasilnikov V.I., Berg A., Oye I.J.: *Numerical Prediction of Sheet Cavitation on Rudder and Podded Propeller Using Potential and Viscous Flow Solutions.* Proceedings of the 5th Intern. Symp. on Cavitation CAV2003, Osaka, Japan, 2003
3. Kuiper G.: *New Developments Around Sheet and Tip Vortex Cavitation on Ship Propellers.* Proceedings of the 4th Intern. Symp. on Cavitation CAV2001, Pasadena, USA, 2001
4. Lee H.S., Kinnas S.A. et al.: *Numerical Modelling of Propeller and Rudder Sheet Cavitation Including Propeller – Rudder Interaction and the Effects of the Tunnel.* Proceedings of the 5th Intern. Symp. on Cavitation CAV2001, Pasadena, USA 2001
5. Lee S.K.: *Numerical Study – Propeller/Rudder Cavitation of Fast Containership*. Proceedings of the 3rd Intern. Shipbuilding Conference, St. Petersburg, Russia, 2002
6. Shen Y.T, Remmers K.D. Jiang C.W.: *Effects of Ship Hull and Propeller on Rudder Cavitation.* Journal of Ship Research, Vol.41, No. 3, 1997
7. Szantyr J.A.: *Analytical Prediction of Propeller Cavitation*. The Naval Architect July/August 1991
8. Szantyr J.A.: *A Method for Analysis of Cavitating Marine Propellers in Non-uniform Flow.* Intern. Shipbuilding Progress Vol.41, No.427, 1994
9. Szantyr J.A.: *A Computational Model of the Propeller Cavitating Tip Vortex Interacting With the Rudder.* 6th International Conference on Cavitation CAV'06, Wageningen, The Netherlands, 24-26 September 2006
10. Tunc M., Delale C.F.*: Energy dissipation due to fission of cavitating b*ubbles. Proceedings of the 5th Intern. Symp. on Cavitation CAV2003, Osaka, Japan, 2003

POLISH MARITIME RESEARCH 4(54) 2007 Vol 14; pp. 15-17
DOI: 10.2478/v10012-007-0034-9

The effect of blade thickness on microstructure and mechanical properties of ship's sand-cast propeller

Leszek Piaseczny,
Krzysztof Rogowski
Polish Naval Academy

ABSTRACT

The microstructure and resultant mechanical properties of the MM55 manganese brass applied to ship sand - cast propeller were investigated in relation to the propeller blade section thickness. It was stated that the increase of blade section thickness from 15 mm to 45 mm resulted in the increase of the volume fraction of α-phase by 5.3% and that of κ-phase by 23.7%, the decrease of the volume fraction of β-phase by 2.9%, the 0.2% proof stress $R_{0.2}$ by 11.3%, the ultimate tensile strength R_m by 5.5% and the 5.65 $\sqrt{S_o}$ elongation A_5 by 16.8%.

Keywords: blade thickness, microstructure, sand-cast propeller

INTRODUCTION

The ship propellers range in size from small (below 2 m in diameter) to large ones (above 5 m in diameter) [1].

The specimens of most ship propeller castings constitute separately cast test bars with chemical composition and mechanical properties in line with specification for propeller cast material, Fig. 1 and 2. The test bar can be also cast in the form shown by broken line in Fig. 1 [2].

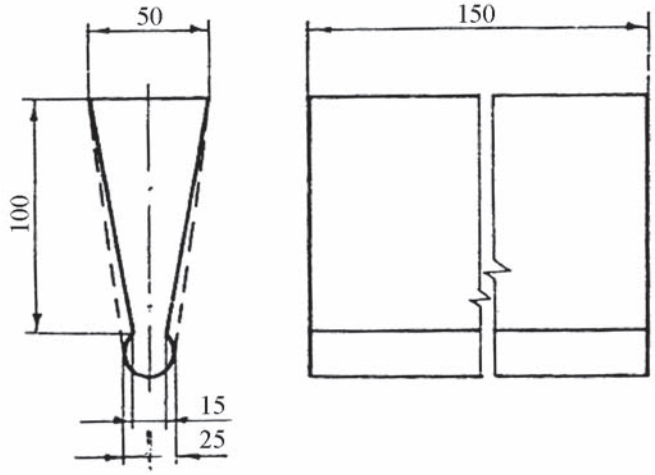

Fig. 1. *Separately cast bar for ship's propeller material testing [2]*

It is clear that the mechanical properties of the sand-cast ship propeller made of copper alloys, measured on a separately cast test bar, are intended for providing an assessment of general quality of the materials rather than for determination of the actual mechanical properties of the propeller casting, particularly when large sections are involved [3]. In large propeller casting with thick sections slower self-cooling rate is a hindrance from obtaining a microstructure to the effect that the mechanical properties of the propeller casting appear below these obtained from the cast test bar of only 25 mm diameter [4]. The lowest strength of the propeller casting material was found in the entrance of propeller blade into hub, Fig. 3; which is specially important for constructors [5].

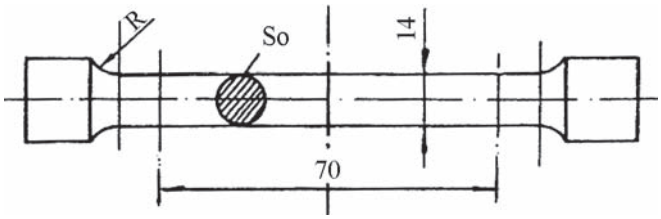

Fig. 2. *Test bar for testing mechanical properties [2]*

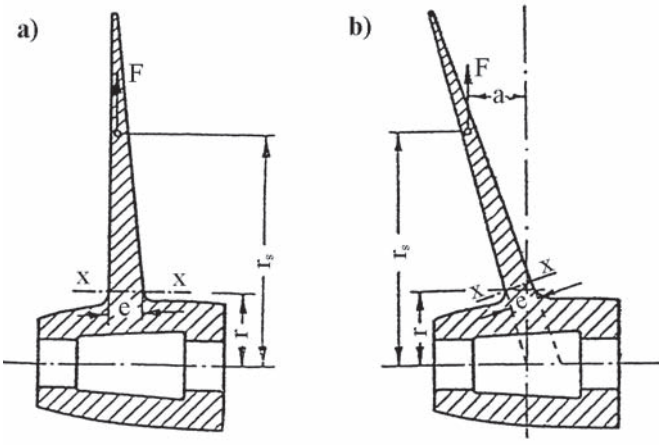

Fig. 3. *The propeller blade sections [5]:*
a) *straight blade,* ***b)*** *sloping blade*

The aim of this work is to investigate changes in microstructure and mechanical properties of ship propeller blades along with increasing thickness of their sections.

TESTED MATERIAL AND TESTING PROCEDURES

The chemical composition and mechanical properties of MM55 manganese brass used for the tested ship's propeller are included in Tab. 1 where also appropriate data taken from PN-91/H-87026 standard [6] and PRS Rules [2] are attached.

The tested ship's propeller blades are 800 mm long, 15 mm thick at 0.9 R radius and 45 mm thick at 0.25 R radius. The samples for testing microstructure and mechanical properties of ships propeller's material were cut out from centre blade section of 15 mm, 20 mm, 25 mm, 35 mm and 45 mm in thickness.

Tab. 3. Changes of phase volume fraction in microstructure of MM55 manganese brass used for ship propeller casting, along with the increasing of blade section thickness

Thickness [mm]	α- phase volume fraction [%]	β -phase volume fraction [%]	κ -phase volume fraction [%]
15	100	100	100
20	104.32	97.58	116.30
25	106.21	96.52	120.00
35	103.90	97.82	114.07
45	105.32	97.02	123.70

Tab. 1. Chemical composition and mechanical properties of the tested MM55 manganese brass used for ship's propeller casting

Item	Chemical composition [%]								$R_{0.2}$ MPa	R_m MPa	A_5 %
	Cu	Sn	Zn	Pb	Mn	Fe	Al.	Ni			
Tested material	54.5	-	41.3	0.02	3.4	1.0	0.21	-	275	488	25.6
Required by PN-91/H-87026	53-58	Max 0.5	Balance	Max 0.5	3.6-4.0	0.5-1.5	Max 0.5	Max 0.5	Min 180	Min 450	Min 15.0
Required by PRS rules	52-62	Max 1.5	35-40	Max 0.5	0.5-4.0	0.5-2.5	0.5-3.0	Max 0.5	175	440	20.0

TEST RESULTS AND DISCUSSION

The results of tensile tests are listed in Tab. 2.

Tab. 2. Mechanical properties of MM55 manganese brass used for the tested propeller

Blade thickness [mm]	$R_{0.2}$ [MPa]	R_m [MPa]	A_5 [%]	HV20
15	275	488	25.6	177
20	259	482	25.8	171
25	263	484	23.6	165
35	248	477	23.1	149
45	244	461	21.3	146

The results are also graphically shown in Fig. 4.

It can be observed that along with the increasing of blade thickness the ultimate tensile strength R_m of the blade material decreased initially slowly and then quickly. Similar are the changes of the 5.65 $\sqrt{S_o}$ elongation A_5 of the material, which become stable when the blade section thickness approaches 45 mm. The 0.2% proof stress $R_{0.2}$ and hardness HV20 decreased initially quickly and became stable at the blade section thickness close to 45 mm. All the changes of mechanical properties of propeller's casting material resulted from the decreasing of self-cooling rate of propeller casting along with increasing blade section thickness.

The metalographic examinations showed that with the increasing of the blade section thickness the microstructure of the manganese brass used for the propeller casting was also changing, as presented in Tab. 3 and illustrated in Fig. 5 and 6.

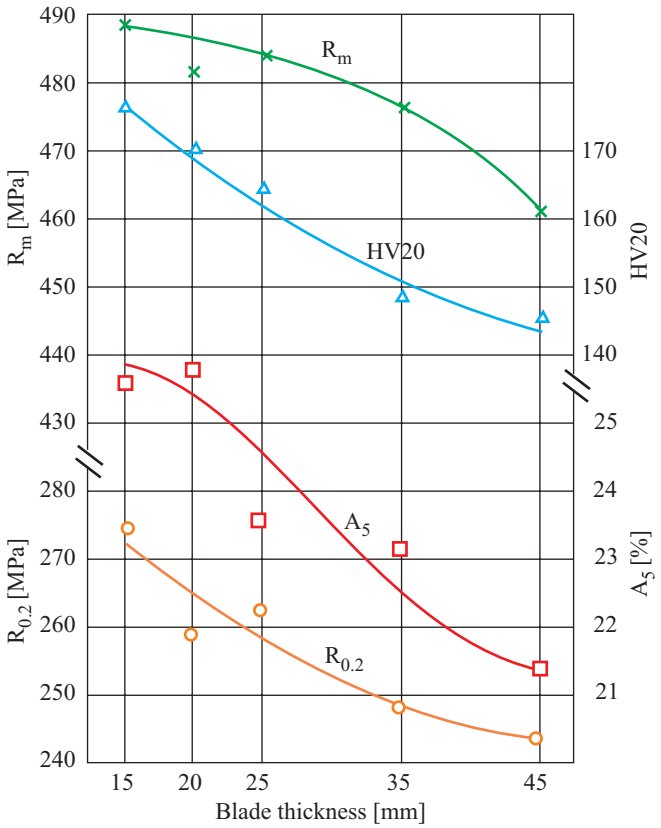

Fig. 4. Changes of mechanical properties of MM55 manganese brass used for ship propeller casting in function of increasing blade section thickness

The increase of the blade section thickness resulted not only in the volume fraction of the phase in microstructure but also in the increased areas of α-phase precipitates. Fig. 7

shows the number of α -phase precipitates in relation to thickness of propeller blade section. It can be observed that in the microstructure the number of precipitates of 0-500 μm^2 area diminished and that of precipitates of 1001-5000 μm^2 are increased along with decreasing self-cooling rate.

The course of microstructure changes in MM55 manganese brass used for ship propeller casting resulted from the decreasing of self-cooling rate of casting along with the increasing of blade section thickness.

Fig. 5. *Micrograph of MM55 manganese brass used for ship propeller casting, at the blade section of 15 mm in thickness. Magnification : 240x.*

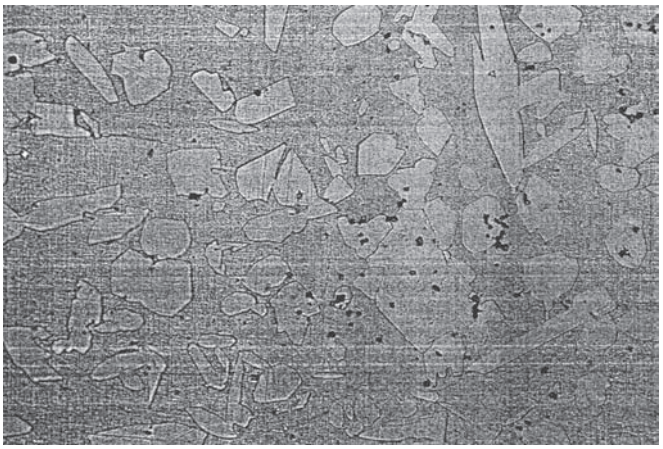

Fig. 6. *Micrograph of MM55 manganese brass used for ship propeller casting, at the blade section of 45 mm in thickness. Magnification : 240x.*

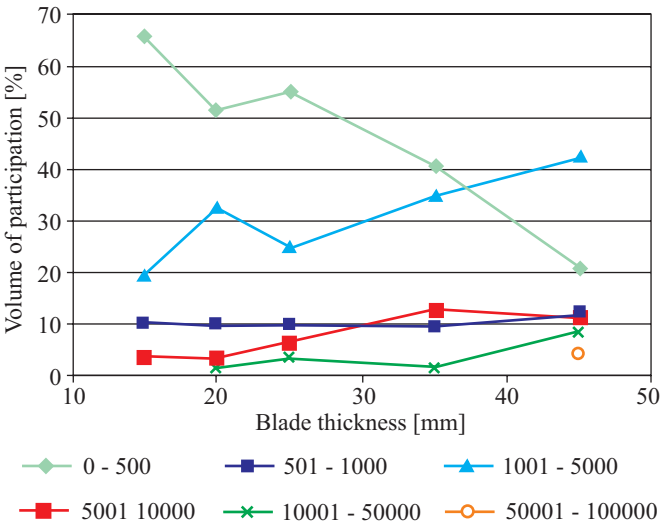

Fig. 7. *Volume of precipitation in relation to thickness of ship propeller blade section*

CONCLUSIONS

The performed tests showed that the increasing - from 15 mm to 45 mm - of blade section thickness of the ship sand - cast propeller made of MM55 manganese brass resulted in :

- An increase of the volume fraction of hard and short κ- phase in the material's microstructure, and a simultaneous decrease of the mechanical properties of the material.
- The following decrease of particular properties was observed : the 0.2% proof stress $R_{0.2}$ – by 5.3%, the ultimate tensile strength R_m –by 5.5 %, 5.65 $\sqrt{S_o}$ elongation A_5 - by 16.8%, and HV20 hardness - by 17.5%.

BIBLIOGRAPHY

1. Meyne K.: *Propellerfertigung-Propellerwerkstoffe-Propellerfestigkeit.* Schiff u. Hafen, Jg. 26, H. 3, 1974
2. Polish Register of Shipping : *Rules for the construction and classification of sea-going ships, Part 13, Materials* (in Polish), Gdańsk 2002
3. Wenschot P.: *The properties of Ni-Al bronze sand cast ship propeller in relation to section thickness.* Naval Engineers Journal, September 1986
4. Couture A.: *Literature survey on the properties of cast Ni-Al and Mn-Ni-Al bronzes*. AFS International Cast Metal Journal, June 1981
5. Ruseckij A.A., Žučenko M.M., Dubrovin O.V.: *Sudovyje dvižiteli* (in Russian) Sudostroenie. Leningrad 1971
6. PN-91/H-87026 Polish standard : *Cu- alloys for casting. Kinds* (in Polish), Warszawa 1991.

CONTACT WITH THE AUTHORS

Prof. Leszek Piaseczny
Mechanic-Electric Faculty,
Polish Naval University
Śmidowicza 69
81-103 Gdynia, POLAND
e-mail : lpias@amw.gdynia.pl

POLISH MARITIME RESEARCH 4(54) 2007 Vol 14; pp. 18-23
DOI: 10.2478/v10012-007-0035-8

Mean long-term service parameters of transport ship propulsion system

Part I
Screw propeller service parameters of transport ship sailing on a given shipping route

Tadeusz Szelangiewicz
Katarzyna Żelazny
Szczecin University of Technology

ABSTRACT

During ship sailing on a given shipping route in real weather conditions all propulsion system performance parameters of the ship change along with changes of instantaneous total resistance and speed of the ship. In this paper results of calculations are presented of distribution function and mean statistical values of screw propeller thrust, rotational speed and efficiency as well as propulsion engine power output and specific fuel oil consumption occurring on selected shipping routes. On this basis new guidelines for ship propulsion system design procedure are formulated.

Keywords: thrust, efficiency and rotational speed of screw propeller, long-term prediction, shipping route, design working point of screw propeller

INTRODUCTION

A crucial element of design process of transport ship propulsion system is selection of its design parameters, i.e. determination of a speed value for which screw propeller should be designed and determination of a thrust value which should be developed by this propeller at the assumed speed. Correct selection of the design speed is specially important for ships fitted with fixed pitch propellers (most often applied to transport ships) as only at that design speed such propeller is able to use full engine power output.

The service speed at which the designed ship has to operate in real weather conditions on a given shipping route, should be assumed as the design speed.

The way of calculation of the mean long-term service speed and the mean long-term resistance of the ship is presented in [1, 2, 3].

The design working point of screw propeller is associated with the following design parameters : ship speed and propeller thrust. Selection of such point is very important with a view of correct operation of propulsion system. In this point screw propeller efficiency should reach as - high - as possible value. For screw propellers interacting with piston combustion engines the design point is usually placed half way between the points A and B (Fig. 1), that generally ensures correct operation of the propulsion system in the point B, i.e. in service conditions (real weather conditions).

Instantaneous service speed of ship and its total resistance depend on instantaneous weather conditions occurring on a given shipping route. Hence working parameters of the screw propeller designed and applied to propel the ship will be changeable depending on weather parameters and assumed criteria of propulsion system control [4]. Knowing statistical data on wind and waves occurring on a given shipping route as well as long-term distribution function of ship speed [3] on the route, one can determine long-term distribution functions of working parameters of the screw propeller and hence mean statistical location of its working point on a given shipping route.

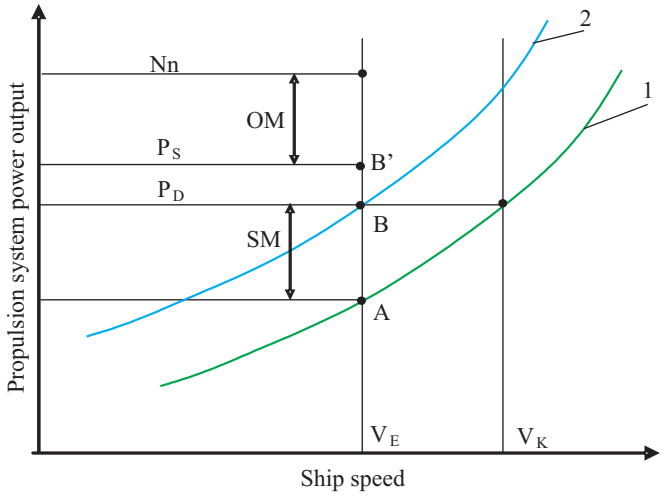

Fig. 1. *Predicted service speed of ship*
Nn *– nominal power output of engine,* P_S *– shaft-line power,* P_D *– power delivered to propeller cone,* V_K *– contractual speed of ship,* V_E *– predicted service speed of ship,* ***1*** *– still-water propeller curve for clean ship hull,* ***2*** *– predicted propeller curve with service margin, in real conditions,* ***OM*** *– operational margin,* ***SM*** *– service margin.*

Therefore this paper presents calculations - performed for designed ships and their propulsion systems together - of long-term service parameters of screw propeller and mean service location of its working point as well as discussion on how it would influence its design working point.

SERVICE PARAMETERS OF SCREW PROPELLER

The service parameters of screw propeller to be calculated for a ship sailing on a given shipping route are the following:

- ⇨ the propeller thrust T
- ⇨ the propeller rotational speed n_p
- ⇨ the free-propeller efficiency η_0.

The thrust of the behind-the-hull propeller is expressed as follows :

$$T = \frac{R_C}{1-t} \tag{1}$$

where:

R_C − total resistance of ship to motion in waves
t − thrust deduction.

The free-propeller thrust can be calculated by using the formula :

$$T = K_T \rho_w D_p^4 n_p^2 \tag{2}$$

where:

D_p − propeller diameter,
n_p − propeller speed,
K_T − thrust ratio which – for typical B-Wageningen screw propellers of given parameters : (P/D) (A_E/A_0), (Z) – is approximated with the use of the expression:

$$K_T = A_0 + A_1 \cdot J + A_2 \cdot J^2 + A_3 \cdot J^3 \tag{3}$$

where:

A_0, A_1, A_2, A_3 − coefficients of polynomial approximating propeller thrust characteristic, dependent on (P/D), (A_E/A_0), (Z)

J − advance ratio:

$$J = \frac{V[1-w(V)]}{D_p \cdot n_p} \tag{4}$$

where:

w(V) − wake fraction dependent on the ship speed V.

On the propeller in operation the torque Q is generated:

$$Q = K_Q \rho_w D_p^5 n_p^2 \tag{5}$$

where:

K_Q − torque ratio which − for a given propeller − can be expressed as follows:

$$K_Q = B_0 + B_1 \cdot J + B_2 \cdot J^2 + B_3 \cdot J^3 \tag{6}$$

where:

B_0, B_1, B_2, B_3 − coefficients of polynomial approximating propeller torque, dependent on the propeller parameters : (P/D), (A_E/A_0), (Z).

The free-propeller efficiency (free of ship hull) is equal to:

$$\eta_0 = \frac{K_T}{K_Q} \cdot \frac{J}{2\pi} \tag{7}$$

During calculations of the propeller service parameters, propeller thrust changes due to ship's rolling motion and resulting excitations to propeller were taken into account; the influence of ship roll on propeller thrust decrease was presented in [2].

The behind-the-hull propeller loads its propulsion engine with the torque (5). The relationship between the propeller torque and propulsion engine output is as follows:

$$Q = \frac{P_D}{2\pi n} \tag{8}$$

where:

P_D − power delivered to the propeller
n − engine speed (for slow-speed engines where a reduction gear is not applied : $n = n_p$), and :

$$P_D = N \cdot \eta_{LW} \cdot \eta_R \cdot \eta_P \tag{9}$$

N − engine power output
η_R − rotative efficiency
η_{LW} − shaft-line efficiency
η_P − efficiency of reduction gear (if applied).

The calculations of the service parameters of screw propeller were performed for the propulsion engine whose working area is limited by its characteristics [2].

PREDICTION OF MEAN STATISTICAL SERVICE SPEED OF SCREW PROPELLER OF SHIP SAILING ON A GIVEN SHIPPING ROUTE

Instantaneous values of propeller service parameters

During ship sailing in waves the ship is loaded by additional resistance components due to wind, waves, sea surface currents, and possible rudder blade deviations [1]. The additional resistance forces make propeller speed and thrust changing; new values of propeller speed and thrust are searched for in such a way as to keep engine working point within its working area. Searching for the working point at given criteria, e.g. at maintaining a given ship speed or reaching the maximum one without engine overloading, is performed in the same way as the searching for of instantaneous ship speed [2, 3].

On the basis of the solution of the non-linear set of equations presented in [2], at first instantaneous values of propeller speed and ship speed are determined and if all criteria are satisfied then instantaneous values of propeller thrust and efficiency are calculated.

Mean statistical values of screw propeller service parameters of ship sailing on a given route

In the case of screw propeller - like in calculating the mean statistical value of ship service speed - its parameters depend on statistical parameters of waves and wind, and assumed ship course angles and speeds on a given shipping route. Therefore the probability of ship being in a given situation while sailing in waves on a given shipping route is the following :

$$p_w = f_A \cdot f_S \cdot f_\mu \cdot f_{HT} \cdot f_V \cdot f_\psi \tag{10}$$

where:

f_A – probability of staying the ship in the sea area A
f_S – probability of staying the ship in the sea area A during the season S
f_μ – occurrence probability of the wave direction μ in the sea area A during the season S
f_{HT} – occurrence probability of wave of the parameters (H_S, T_1), propagating from the direction μ
f_V, f_ψ – probability of the event that ship will sail with the speed V and the course angle ψ, respectively.

For each situation for which the probability p_w is calculated, the instantaneous working point of propeller, determined by the instantaneous ship speed V_i and the instantaneous propeller speed n_{pi}, is calculated. Different instantaneous values of V_i and n_{pi} may yield the same value of the advance ratio J_i acc. (4) and - in consequence - instantaneous values of the thrust T_i and the propeller efficiency η_{0i}.

The total occurrence probability P_T of given values of propeller thrust and efficiency is as follows :

$$P_{TT} = \sum_{A=1}^{n_A}\sum_{S=1}^{n_S}\sum_{\mu=1}^{n_\mu}\sum_{H,T=1}^{n_{HT}}\sum_{V=1}^{n_V}\sum_{\psi=1}^{n_\psi} p_{T_i}[T_i(\Delta R_i)] \qquad (11)$$

where:

P_{TT} – total occurrence probability of a given value of the thrust T_i
$T_i(\Delta R_i)$ – instantaneous value of the propeller thrust in function of the instantaneous additional resistance
n_A, n_S, n_μ, n_{HT}, n_V, n_ψ – number of : sea areas crossed by the ship, seasons of the year, values of wave direction, wave parameters and ship course angle, respectively.

All instantaneous values of propeller service parameters are grouped into classes (intervals of a width appropriate to a given parameter and number of its calculation results).

Calculating the distribution function of occurrence probability of instantaneous propeller thrust, $f(T_i)$, or that of occurrence probability of instantaneous propeller speed, $f(n_{pi})$, or that of occurrence probability of instantaneous propeller efficiency, $f(\eta_{0i})$, one can determine the mean, long-term value of propeller thrust (or – analogously – propeller speed and efficiency) for a given shipping route :

$$\overline{T} = \frac{\sum_{i=1}^{n_T} P_{TT} \cdot T_i(\Delta R_i = \text{const})}{\sum_{i=1}^{n_T} P_{TT}} \qquad (12)$$

where:

n_T – number of intervals containing similar instantaneous values of propeller thrust.

From the expressions similar to (12) the mean, long-term value of propeller speed, $\overline{n}_p$, or that of propeller efficiency, $\overline{\eta}_0$, can be calculated.

PARAMETERS OF THE SHIPS AND SHIPPING ROUTES FOR WHICH THE CALCULATIONS WERE PERFORMED

The calculations of the mean statistical service parameters of screw propeller were performed for the ships and shipping routes whose parameters were given in [3].

RESULTS OF CALCULATIONS

Results of the calculations for the selected ship and shipping routes are presented in the form of :

- histogram of propeller thrust and its mean statistical value
- histogram of propeller speed and its mean statistical value
- histogram of propeller efficiency and its mean statistical value
- mean statistical propeller working point,
- probability distribution function of long-term occurrence of given values of propeller rotational speed and ship service speed.

All the calculations were performed under the assumption that engine's power output reaches at most 0.9 N_n.

In the below attached figures the calculation results are presented for K1 containership [3] and the two very different shipping routes : 5b - "easy" one and 2b - „difficult" one - in the sense of occurrence of long-term weather parameters.

MEAN STATISTICAL WORKING POINT OF SCREW PROPELLER

Presented in Fig. 2, the histograms of propeller thrust, speed and efficiency show that propeller service parameters depend to a large extent on shipping route weather parameters. The most interesting is the distribution of the free-propeller efficiency η_0, the mean statistical value of propeller efficiency on a given route, $\overline{\eta}_0$, and its comparison with that in still water, η_0, Fig. 3 and 4.

Ship: K1 - assumed service speed = 8.44 [m/s]
- probability of maintaining the assumed speed P_{VE}

Thrust histograms

Route no. 2b - P_{VE} = 0.50

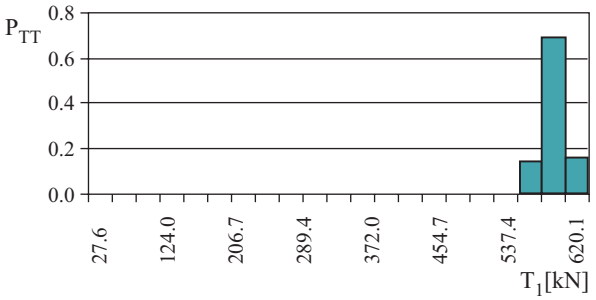

Thrust in still water T = 579 [kN]
Mean thrust $\overline{T}$ = 593 [kN]

Route no. 5b - P_{VE} = 0.83

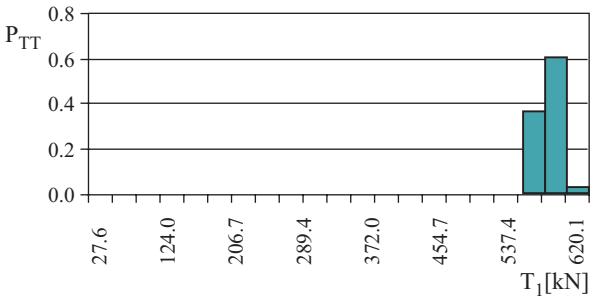

Mean thrust $\overline{T}$ = 582 [kN]

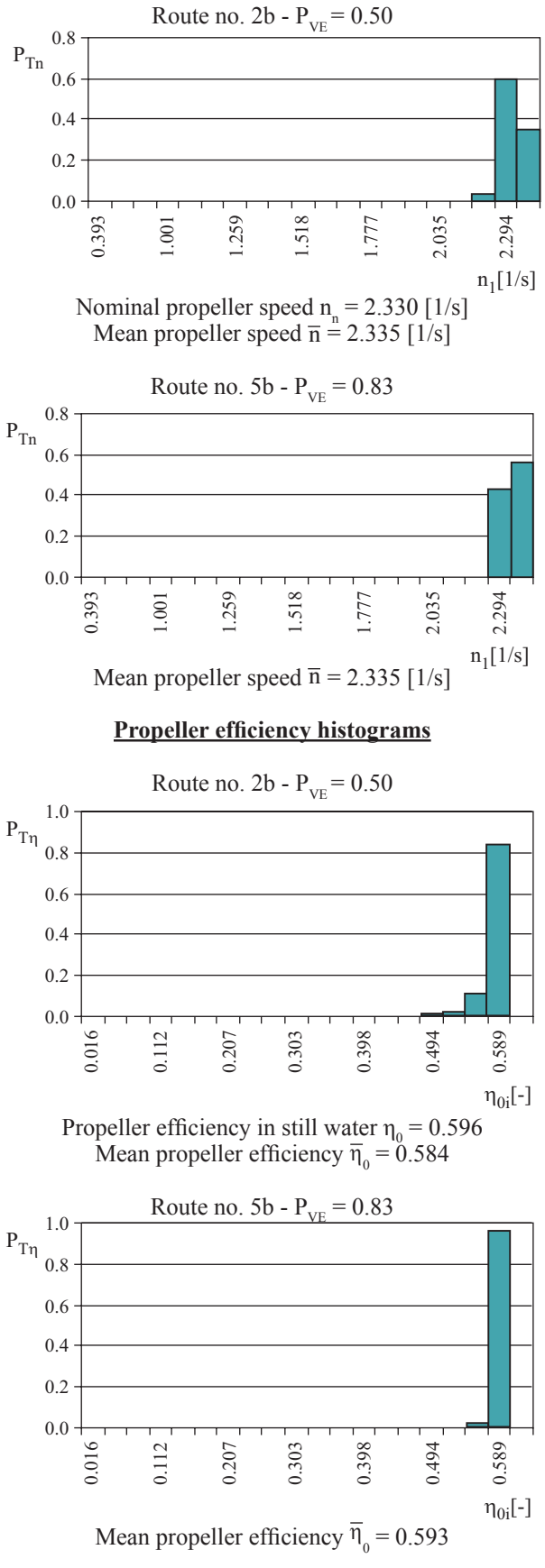

Fig. 2. *Histograms and mean statistical values of thrust, speed and efficiency of propeller for K1 ship sailing on 2 b and 5 b shipping routes*

The enlarged fragment of the propeller efficiency characteristic together with the depicted mean statistical values of propeller efficiency for various shipping routes makes it possible to determine values of propeller design parameters for a selected ship sailing on a given route. For ship which sails on many shipping routes appropriate mean efficiency value can be calculated from mean statistical efficiency values for the ship on particular shipping routes.

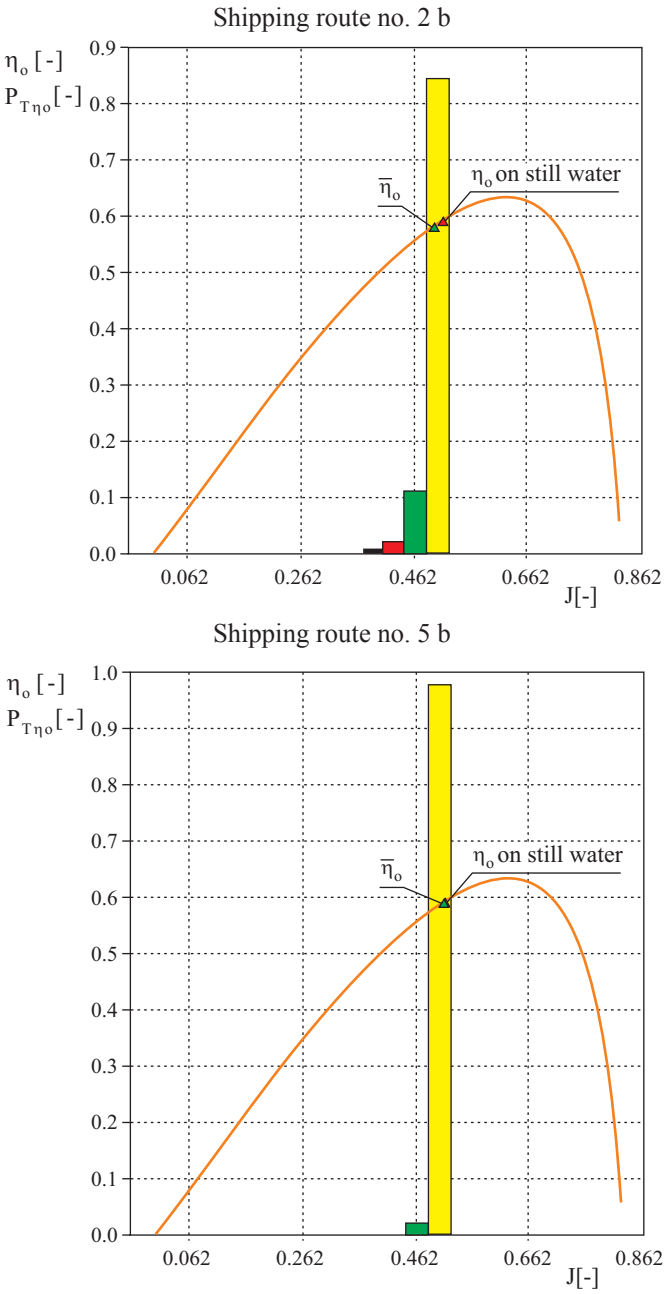

Fig. 3. *Histogram, mean statistical value of propeller efficiency on a given shipping route and propeller still-water efficiency for K1 ship*

On the basis of the calculation results of the mean statistical values of propeller efficiency (Fig. 4), were calculated the mean statistical working points of the propeller, presented on the power output – ship speed diagram (Fig. 6). On comparison of Fig.6 and Fig. 1 it can be clearly stated that the design working point is not only located between the points A and B (Fig. 1) but also its location depends on the mean statistical service speed of ship on a given shipping route hence it also depends on statistical weather parameters on the shipping route in question These problems are planned to be further investigated so as to make it possible to elaborate design guidelines for screw propeller of ship sailing on a given shipping route. The presented figures yield one important information, namely :

it is rather improbable that during ship sailing on a given route in real weather conditions the advance ratio J could reach a value greater than that in still water conditions.

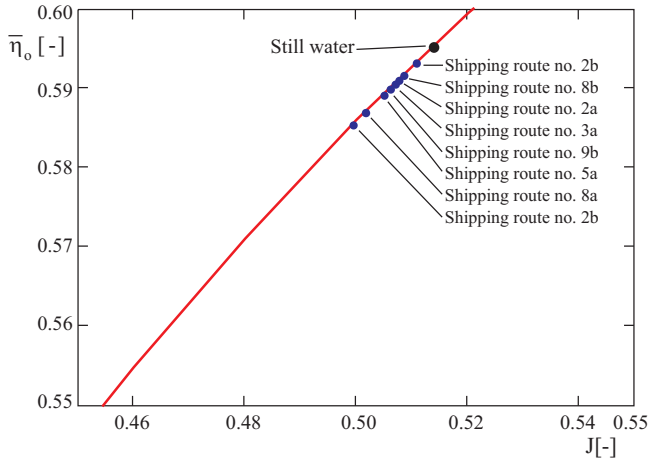

Fig. 4. *Influence of shipping route [3] (weather parameters on a given shipping route) on mean statistical value of propeller efficiency for K1 ship*

Shipping route no. 2 b

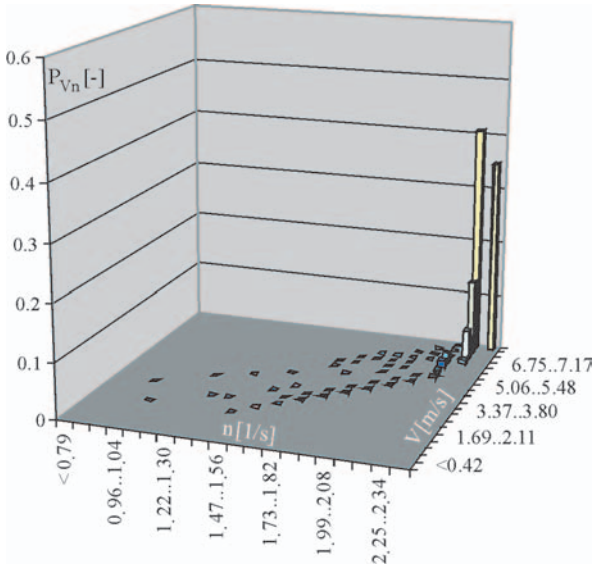

Shipping route no. 5 b

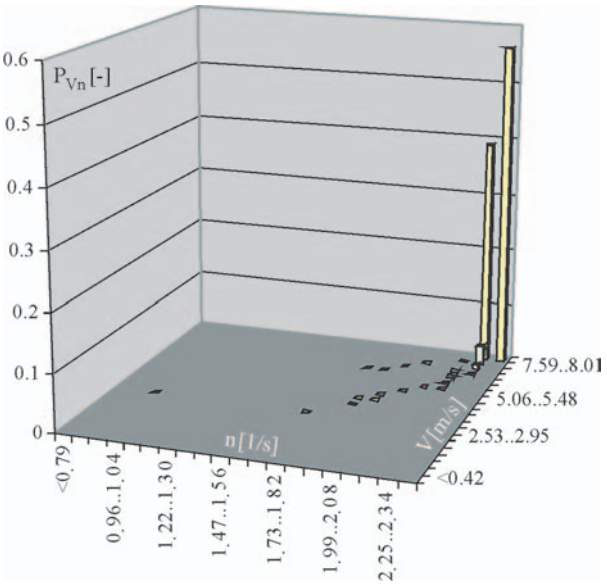

Fig. 5. *Occurrence probability of given values of propeller speed and ship speed on a given shipping route for K1 ship*

Efficiency of a given screw propeller depends on its rotational speed and ship speed (advance ratio J). Fig. 5 shows which is the occurrence probability of the pairs of propeller rotational speed – ship speed values for two selected shipping routes.

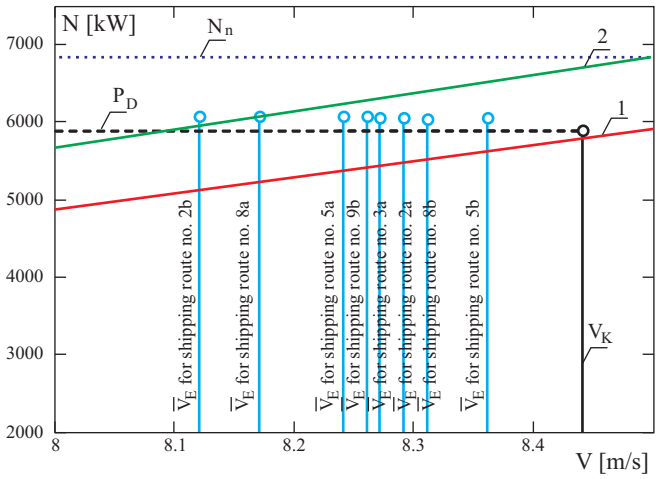

Fig. 6. *Mean statistical working point of K1 ship propeller, depending on the mean statistical ship service speed $\overline{V}_E$ on various shipping routes. **1** – still-water propeller curve; **2** – propeller curve containing the service margin SM = 15%; P_p – power delivered to propeller cone at ship's contractual speed in still water conditions; N_n – nominal power output of propulsion engine; $\overline{V}_E$ – mean statistical long-term value of ship service speed on a given shipping route; V_K – contractual speed of ship*

NOMENCLATURE

(A_E/A_0) – coefficient of developed area of propeller blades
A_0, A_1, A_2, A_3 – coefficients of polynomial approximating propeller thrust characteristic
B_0, B_1, B_2, B_3 – coefficients of polynomial approximating propeller torque characteristic
D_p – propeller diameter
f_A – probability of staying the ship in the sea area A
f_{HT} – occurrence probability of wave of the parameters (H_S, T_1), propagating from the direction μ
f_S – probability of staying the ship in the sea area A during the season S
f_V, f_φ – probability of the event that ship will sail with the speed V and the course angle ψ, respectively
f_μ – occurrence probability of the wave direction μ in the sea area A during the season S
H_S – significant wave height
J – propeller advance ratio
J_i – instantaneous advance ratio
K_T – propeller thrust ratio
K_Q – propeller torque ratio
N – propulsion engine power
N_n – nominal propulsion engine power
n – propulsion engine speed
n_p – propeller (rotational) speed
n_{pi} – instantaneous propeller speed
$\overline{n}_p$ – long-term, mean statistical propeller speed
$n_A, n_S, n_\mu, n_{HT}, n_V, n_\psi$ – number of : sea areas crossed by the ship, seasons of the year, values of : wave direction, wave parameters and ship course angle, respectively
P_D – power delivered to propeller cone
P_S – shaft-line power
P_{Vn} – occurrence probability of given values of propeller speed and ship speed
P_{VE} – probability of maintaining a given value of ship speed
P_{Tn} – occurrence probability of a given value of propeller speed
P_{TT} – occurrence probability of a given value of propeller thrust T_i
$P_{T\eta 0}$ – occurrence probability of a given value of propeller efficiency

p_w – probability of being the ship in a given situation
Q – propeller torque
R_C – total ship resistance to motion
T_i – instantaneous thrust of propeller
$\overline{T}$ – long-term mean statistical value of propeller thrust
t – propeller thrust deduction
V – ship speed
V_E – ship service speed
$\overline{V}_E$ – mean statistical ship service speed
V_K – contractual ship speed
Z – number of propeller blades
w – wake fraction
η_0 – free -propeller efficiency
η_{0i} – instantaneous propeller efficiency
$\overline{\eta}_p$ – long-term mean statistical propeller speed
η_R – rotative efficiency
η_{LW} – shaft-line efficiency
μ – geographic direction of wave
ρ_w – water density
ψ – geographic angle of ship course.

BIBLIOGRAPHY

1. Szelangiewicz T., Żelazny K.: *Calculation of Mean Long-Term Service Speed of Transport Ship, Part I : Resistance of Ship Sailing on Regular Shipping Route in Real Weather Conditions*, Polish Maritime Research, No 4/2006
2. Szelangiewicz T., Żelazny K.: *Calculation of Mean Long-Term Service Speed of Transport Ship, Part II : Service speed of ship sailing on regular shipping route in real weather conditions*, Polish Maritime Research, No 1/2007
3. Szelangiewicz T., Żelazny K.: *Calculation of Mean Long-Term Service Speed of Transport Ship, Part III : Influence of shipping route and ship parameters on its service speed*. Polish Maritime Research, No 2 /2007
4. Żelazny K.: *Numerical prediction of mean long-term service speed of transport ship* (in Polish). Doctoral thesis, Maritime Technology Faculty, Szczecin University of Technology, Szczecin 2005

CONTACT WITH THE AUTHORS
Prof. Tadeusz Szelangiewicz
Katarzyna Żelazny, D.Sc., Eng.
Faculty of Marine Technology,
Szczecin University of Technology
Al. Piastów 41
71-065 Szczecin, POLAND
e-mail : tadeusz.szelangiewicz@ps.pl

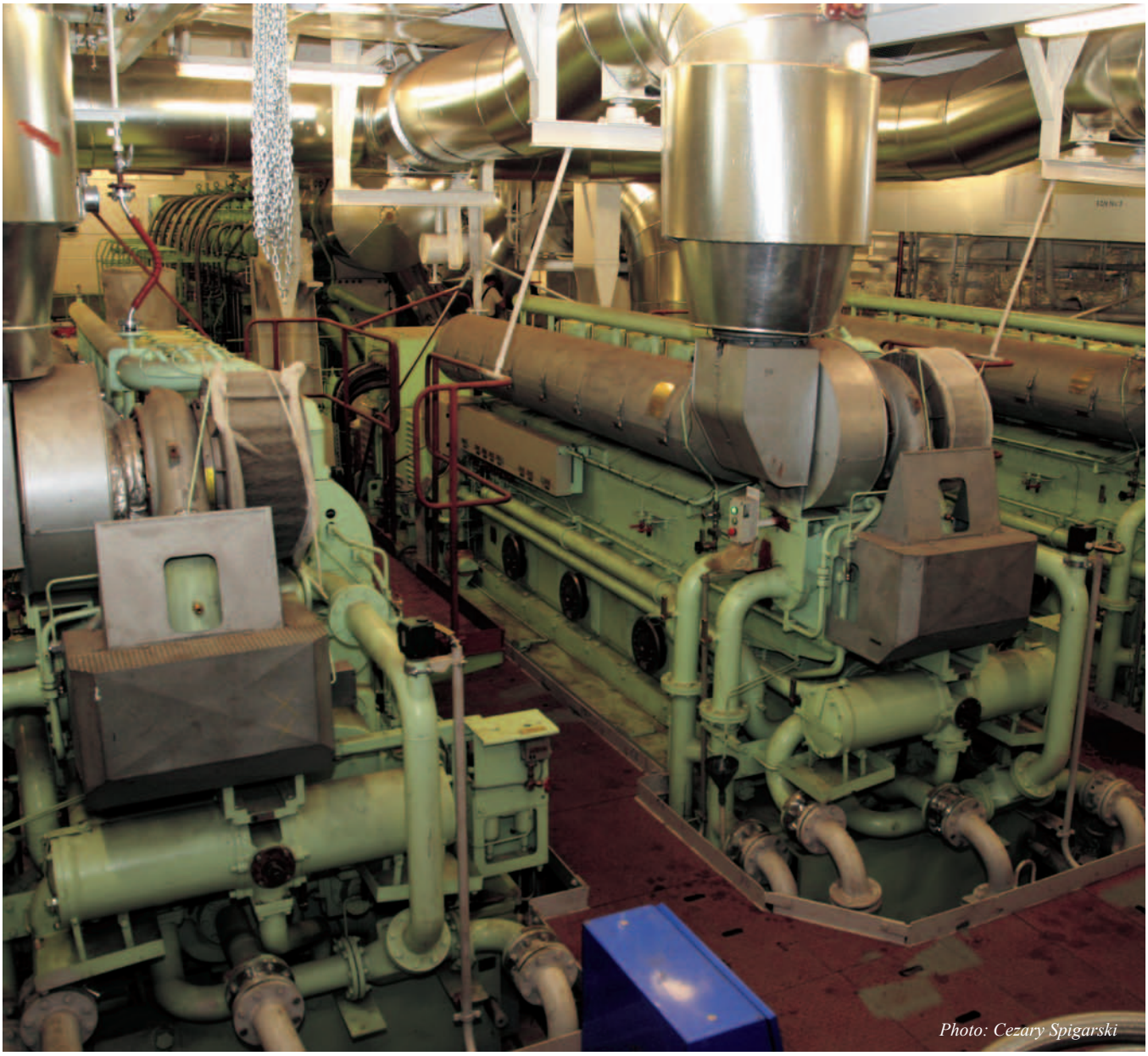
Photo: Cezary Spigarski

POLISH MARITIME RESEARCH 4(54) 2007 Vol 14; pp. 24-30
DOI: 10.2478/v10012-007-0036-7

Prediction of power demand for ship motion control system of sea mining ship fitted with tubular winning system

Monika Bortnowska,
Szczecin University of Technology

ABSTRACT

One of the crucial systems of sea mining ship for poly-metallic concretions is its motion control system (SMC). Power of such system depends on sea environment characteristics and main dimensions of the ship. It can be expected that it will have important influence on total power of the ship's power plant and in effect on the mining ship's dimensions. In this paper is presented one of the possible ways of preliminary estimation of design power of SMC system for sea mining ship. Since details of design solution of such system for the ship in question are unknown (ships of the kind have not been built so far) the presented results should be considered to be the first estimation of the order of the power demand.

Keywords: sea mining ship, tubular winning system, action of sea environment, thrust of ship propellers, power of ship motion control system.

INTRODUCTION

Mining process of poly-metallic concretions from seabed is assumed to be carried out by using three basic elements: a bottom gathering vehicle, tubular winning system (called further also TW system) and floating winning unit.

One of the concepts of the mining facility for the concretions – most often taken into consideration - is that composed of a conventional single-hull ship providing possible storing the concretions in its holds, equipped with a vertical tubular winning system and self-propelled gathering device.

The mining ship makes correct functioning both the bottom gathering vehicle and tubular winning system, possible (by supporting them and delivering electric power).

During the mining process the vehicle moving over seabed will gather the concretions and pass on them to the TW hydraulic system. The mining ship to which the pipe of the TW system is hung, will have to monitor the gathering vehicle's motions, moving with a steady speed and keeping course within a corridor of a given width (Fig.1).

Like other ocean engineering floating units the mining ship, to fulfill its functions often in heavy environmental conditions is to be fitted with an appropriate system for its motion control. The system has to ensure not only keeping the ship's position and course by means of special propellers [e.g. azimuthing ones like in the case of dynamic positioning systems (DSP)] but also to make continuous and precise moving the mining ship along a given trajectory possible, coping with unfavourable action of sea environment (wind, sea current, waves), resistance to motion of the ship and tubular winning system.

Such mining ship's motion control system (called further shortly SMC system) is crucial because of :

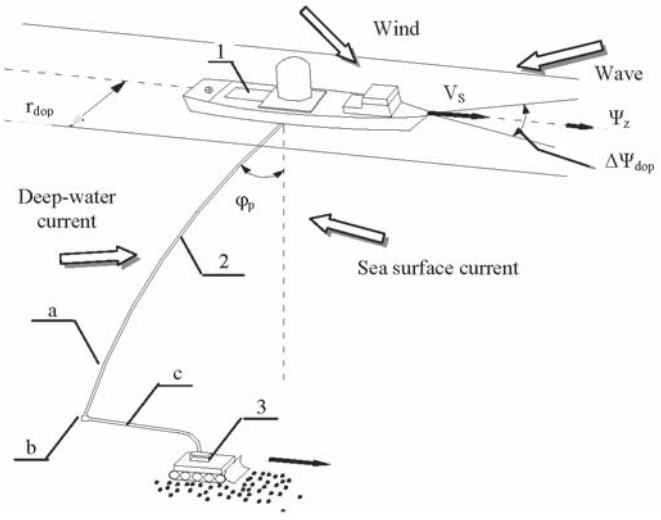

Fig.1. *Motion control of mining ship moving along a given trajectory within a corridor.*
Notation *: **1** – mining ship, **2** – tubular winning system: **a** – vertical pipe, **b** – buffer, **c** – horizontal elastic pipe of zero-buoyancy (for the compensating of buffer's position changes against the gathering vehicle), **3** – bottom gathering vehicle (negligible influence of the mining ship - winning device system is assumed due to compensating action of horizontal elastic pipe between the buffer and gathering vehicle)*
V_s – ship speed

- ⇨ realization of main functions of the ship moving over deep--water areas
- ⇨ large power demand (the motion control system's power is expected to be large as compared with that of the whole electric power plant)
- ⇨ investment and service costs of the ship

⇨ volumetric subdivision and design parameters of the ship: displacement, deadweight etc.

Value of the power delivered to propellers should be such as to obtain resultant thrust value sufficient to balance (without using redundant propellers) resultant action of sea environment in the most unfavourable weather conditions with taking into account resistance of the mining ship and lowered winning pipe. The value directly depends on :

- hydro-meteorological parameters in zone of operation, i.e.: the average wind velocity V_A, average sea current velocity V_C (both surface and deep-water one), significant wave height H_S
- main parameters of the ship, its dimensions and its surface areas (above- and under-water) first of all
- technical parameters of TW system (outer diameter of the pipe, Dr_z, its length l_r)
- assumed ship motion speed and accuracy of keeping its position and course.

As information on already designed and built mining ships are still lacking a preliminary design of such ship was used [1] to estimate demanded power for the SMC system in question. On this basis was selected one of the ship's versions characterized by its main dimensions, parameters, areas etc.

POWER COMPONENTS OF SMC SYSTEM FOR SEA MINING SHIP FITTED WITH TW SYSTEM

The total power of SMC system for mining ship, N_{SS}, is composed as follows:

$$N_{SS} = N_B + N_R + N_S \quad (1)$$

where:

N_B - power necessary for generating the thrust of propellers to balance sea environment action [kW]
N_R - power necessary for towing the TW system N_R [kW]
N_S - power necessary for generating the thrust of propellers to balance ship hull resistance to motion [kW].

In Fig. 2 the overall schematic diagram is presented of the estimation procedure of SMC system power in the preliminary phase of mining ship design.

SEA ENVIRONMENT ACTION TO MINING SHIP

Sea mining ship is more exposed to detrimental action of sea environment than transport ships because it is intended for many-year service at open sea. Hence the greatest disturbances during its motion control will result from :

- ★ wind action
- ★ sea wave action
- ★ sea current action (surface and deep-water)
- ★ resistance of ship hull and TW system (resulting from speed of ship and sea current).

Along with design practice, in determining maximum values of thrust and power of SMC system the most unfavourable action of sea environment to the ship is assumed. To this end it was assumed that wind and waves are directed perpendicularly to ship's plane of symmetry, i.e. $\beta_{Ay} = \beta_{Wy} = 90°$ and sea current - in opposite direction to ship motion, i.e. $\beta c_x = 180°$ (Fig. 3).

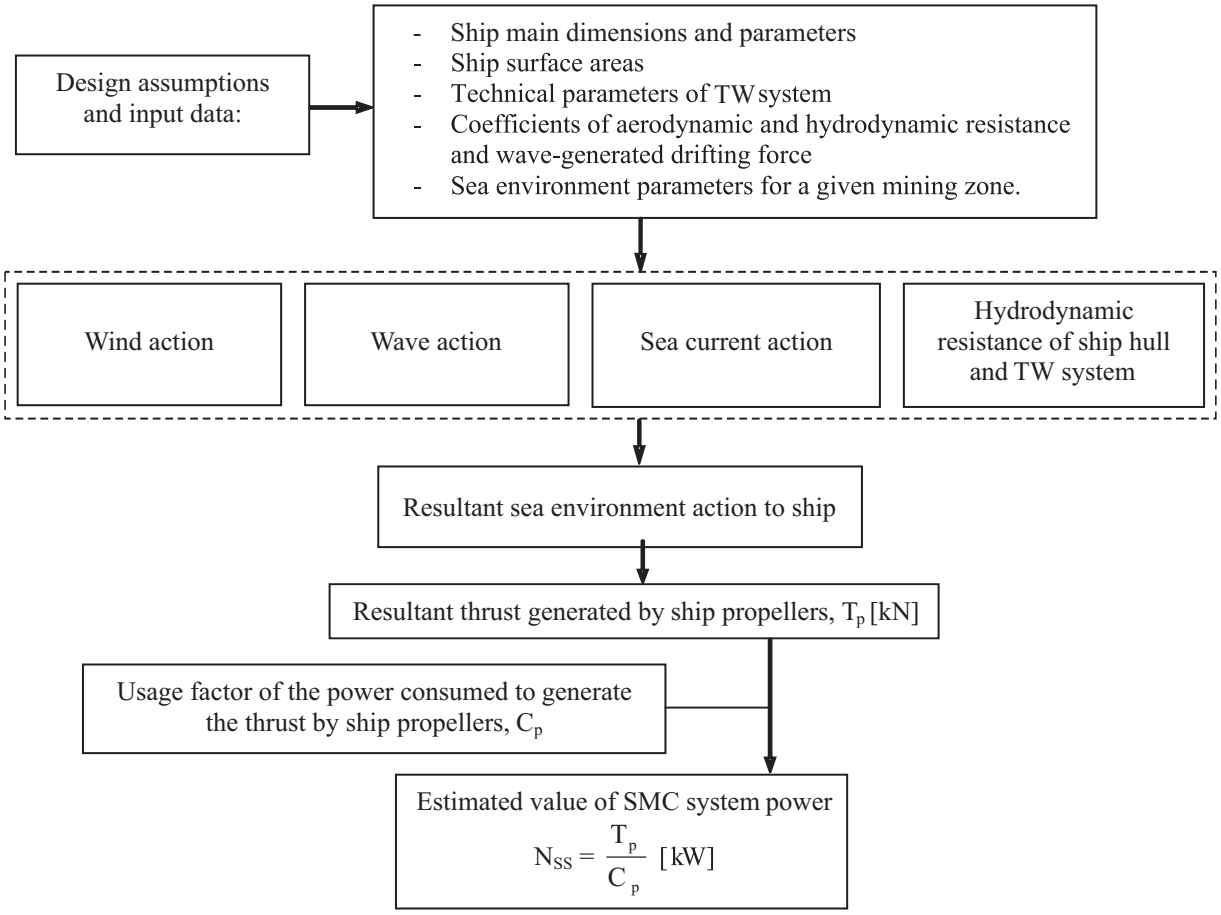

Fig. 2. *Overall schematic diagram for estimation of SMC system power*

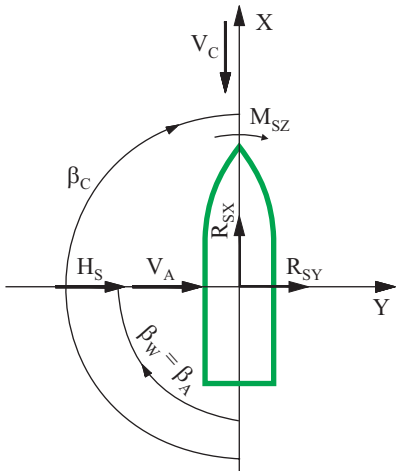

Fig. 3. Directions of sea environment action to ship

WIND ACTION TO MINING SHIP

In designing the SMC system the wind action is calculated for its average velocity and assumed direction with respect to the ship. Under the assumption that the wind is directed perpendicularly to the ship's plane of symmetry, i.e. $\beta_{Ay} = 90°$ the average wind action was calculated by using the following formula :

$$R_{Ay} = \frac{1}{2}\rho_A S_y V_{RA}^2 C_{Ay}(\beta_{RA}) \qquad (2)$$

where:

V_{RA} – average wind velocity [m/s], (Fig. 4)
S_y – windage lateral area [projected to ship's plane of symmetry (PS)] [m^2]
β_{RA} – wind direction angle with respect to ship [°], (Fig. 4)
C_{Ay} – aerodynamic resistance coefficient of above-water body of ship.

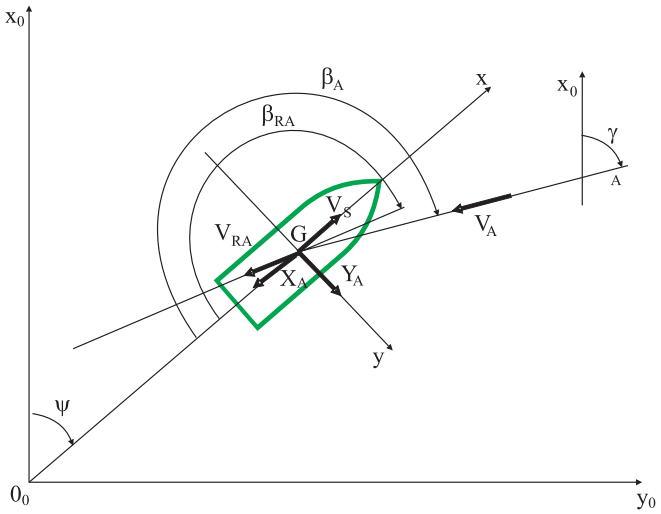

Fig. 4. Coordinate frame, velocities and directions of ship and wind

The relative wind velocity which appears in Eq. (1), is the average vectorial sum of the average absolute wind velocity and the velocity opposite to ship speed. The relative wind velocity can be calculated by means of the following formulae:

$$V_{RA} = \sqrt{V_{RAx}^2 + V_{RAy}^2}$$
$$V_{RAx} = -V_A \cos\beta_A - V_s \qquad (3)$$
$$V_{RAy} = -V_A \sin\beta_A$$

$$\beta_{RA} = \text{arc tg}\frac{V_{RAy}}{V_{RAx}} \qquad (4)$$

where:

V_A – average real wind velocity [m/s]

The wind action to moving ship can be calculated if the wind parameters (V_A) aerodynamic resistance coefficients C_{Ay} [5] (obtained from a ship of similar dimensions or model tests) for a given velocity V_S and ship course angle ψ, are known.

As the mining ship will move at very low speeds it was assumed that the relative wind velocity and direction is equal to the absolute wind velocity and direction.

SEA WAVE ACTION TO MINING SHIP

In the determining of power demand for SMC system propellers, second-order actions which are non-linear and depend on square of wave ordinate, are taken into account. The wave-generated, second-order forces are also called wave-generated drifting forces.

The average irregular-wave action to moving ship, at $\beta_{Wy} = 90°$, were calculated by means of the following formula:

$$R_{Wy} = 2\rho_w g \frac{B^2}{L}\int_0^\infty C_{Wy}(\omega/\beta_w, V)\, S_{\zeta\zeta}(\omega)\, d\omega \qquad (5)$$

where:

B, L – ship breadth and length [m], respectively
C_{Wy} – coefficient of regular -wave -generated drifting force, dependent on the wave direction angle with respect to ship, β_w, and ship's speed V_s
ω – regular wave frequency [s^{-1}]
β_w – wave direction angle with respect to ship [°], (Fig. 5)
$S_{\zeta\zeta}$ – irregular -wave spectrum density function dependent on the significant wave height H_s and average wave period T_1 [m^{2}s].

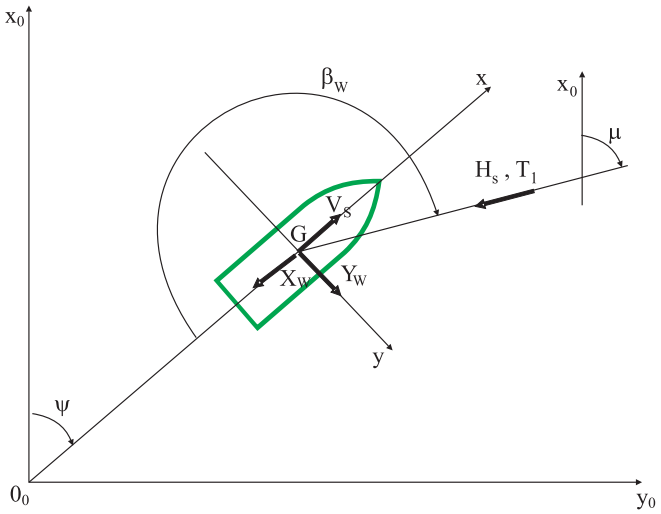

Fig. 5. Wave action to moving ship

For the calculations the ITTC standard function of wave energy spectrum density was assumed.

Assuming values of the wave parameters (H_s , T_1) and coefficients of wave-generated drifting force, C_{wy} , (determined from a ship of similar under-water body) for a given ship speed V_S and course ψ, one can calculate the wave action to moving ship.

ACTION OF SEA SURFACE CURRENT AND WATER RESISTANCE TO MINING SHIP IN MOTION

The average quasi-static action of sea surface current and water resistance to under-water body of mining ship at $\beta c_x = 180°$ was calculated by using the following formula:

$$R_{Cx} = \frac{1}{2}\rho_W F_x V_{RV}^2 C_{Cx}(\beta_{RV}) \tag{6}$$

where:

F_x – head area of underwater portion of ship hull surface (projected to midship plane) [m²]
V_{RV} – relative ship speed [m/s], (Fig. 6)
C_{Cx} – hydrodynamic resistance coefficient of underwater body of ship, dependent on the angle β_{RV} (Fig. 6)
β_{RV} – relative ship's speed direction angle [°].

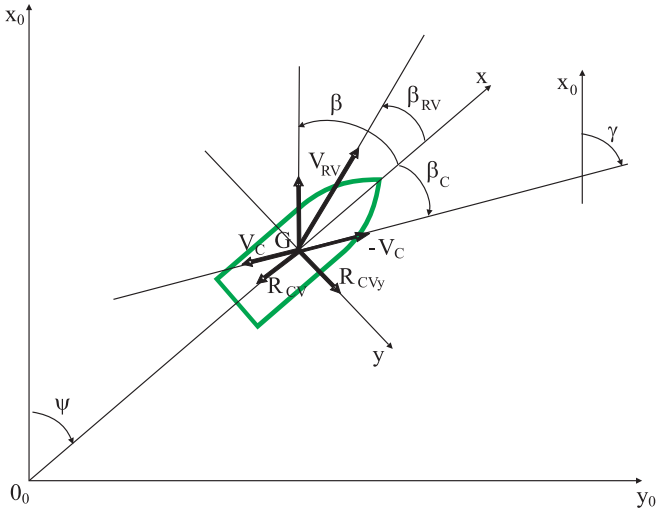

Fig. 6. Sea current and drifting ship directions

In calculations of the relative ship speed V_{RV} and the direction angle β_{RV} the sea surface current velocity V_C and its direction angle β_C should be taken into account.

The relative ship speed can be calculated according to the following formulae:

$$\begin{aligned} V_{RV} &= \sqrt{(V_{RV_X})^2 + (V_{RV_Y})^2} \\ V_{RVx} &= V_x - V_C \cos\beta_C \\ V_{RVy} &= V_y + V_C \sin\beta \\ \beta_{RV} &= \operatorname{arc\,tg}\frac{V_{RV_Y}}{V_{RV_X}} \end{aligned} \tag{7}$$

where:

$V_x = V\cos\beta$, $V_y = V\sin\beta$ − ship speed components
β − ship drift angle [°], (Fig. 6)
V_C − sea surface current velocity [m/s], (Fig. 6).

WATER RESISTANCE AND DEEP - WATER CURRENT ACTION TO TW SYSTEM

TW system resistance depends on speeds of its motion and deep-water sea currents which continuously flow in determined directions, with determined velocities and at determined water depths. Hence the currents can act to the TW system pipe hung in water at various depths, in various, even opposite, directions.

The deep-water current velocity, ship speed and hydrodynamic resistance coefficients constitute the crucial factors affecting the TW system resistance to motion.

Such factors as weight of the pipes of which the TW system is composed, interaction of concretions floating through the system, or local deformations and vertical deflections of the TW installation are neglected since from the research on dynamic behaviour of TW system [6] it results that in the calculation phase in question they have no influence on the preliminary estimation of power demand for SMC system.

The average action of water and deep-water current to TW system was calculated by using the following equation:

$$R_R = \frac{1}{2}\rho_w Dr_z l_r V_{RVg}^2 C_D(R_e) \tag{8}$$

where:

Dr_z – outer diameter of the pipe [m]
l_r – length of the pipe [m]
C_D – hydrodynamic resistance coefficient dependent on the Reynolds number R_e.

Along with water depth changing the sea water physical parameters (such as dynamic viscosity, temperature, density) are also changing, and in consequence – the Reynolds number. Because of large discrepancies in research results on the changeability of the coefficient $C_D = f(R_e)$ and lack of its precise definition, the results of Achenbach`s analyses [2] were taken into consideration.

The velocity field of deep-water currents, combined with the motion speed of TW system, yields the relative water velocity V_{RV}:

$$\begin{aligned} V_{RVg} &= \sqrt{(V_{RV_X})^2 + (V_{RV_Y})^2} \\ V_{RVx} &= V_x - V_{gł}\cos\beta_{gł} \\ V_{RVy} &= V_y + V_{gł}\sin\beta_{gł} \\ \beta_{RV} &= \operatorname{arc\,tg}\frac{V_{RV_Y}}{V_{RV_X}} \end{aligned} \tag{9}$$

where:

$V_{gł}$ − resultant velocity of deep-water current [m/s],
V_{RVg} − relative water velocity [m/s].

MAXIMUM RESULTANT ACTION OF SEA ENVIRONMENT TO MINING SHIP

In compliance with designing practice, the most unfavourable direction of sea environment action to ship (Fig. 3) was assumed for calculation of power demand for the SMC system. Therefore in the calculations influence of the external moments M_{Az}, M_{Wz}, M_{Cz}, was neglected as values of the moments are minimum at the assumed angles $\beta_A = \beta_W = 90°$. They attain maximum values at an oblique action of wind and wave but in such case values of power demand for the SMC system propellers are smaller.

The maximum resultant action of sea environment to mining ship is due to wind, waves, sea currents and water resistance, and for the made assumptions (Fig. 3) it is a sum of particular components of axial and lateral actions :

$$\begin{aligned} R_{Sx} &= R_{Cx} + R_{Rx} \\ R_{Sy} &= R_{Ay} + R_{Wy} \end{aligned} \tag{10}$$

where:

R_{Ay} – component of wind action to above-water portion of mining ship's hull

R_{Wy} – component of wave-generated drifting force action to mining ship's hull

R_{Cx} – component of resultant water-flow action to mining ship's hull, due to sea surface current and ship's speed

R_{Rx} – component of water action to TW system (due to deep-water currents and the system's motion speed).

THRUST AND POWER DEMAND FOR THE SMC SYSTEM

Having the components of resultant sea environment action to the mining ship during keeping its position and course along a given trajectory, one is able to determine the components of resultant thrust generated by propellers of the SMC system, which balance the action. In the preliminary design phase it was assumed that for so large ships as mining ones and so large electric power demanded for them, the total resultant thrust, T_S, of the SMC system propellers is equal to :

$$T_{Sx} = a_x * R_{Sx}$$
$$T_{Sy} = a_y * R_{Sy} \qquad (11)$$

where:

R_{Sx} , R_{Sy} – components of resultant action of sea environment

a_x, a_y – additional resultant thrust of propeller to balance inertia and damping forces resulting from slow-changeable motions of the ship.

Components of the resultant thrust generated by propellers of the SMC system are sums of thrusts generated by its particular propellers. Power delivered to every propeller of the system can be approximately determined from the following relationship :

$$N_P = \frac{T_P}{C_P} \qquad (12)$$

where:

T_P – thrust generated by every propeller of the SMC system [kN]

C_P – usage factor of propeller power for generating the thrust.

Because of low speeds of the ship the power demanded for the propellers used in the SMC system will be calculated by applying the usage factor of propeller power for generating the thrust.

Propellers used in such systems are special ones; they are adjusted to operation at low speeds (even equal to zero), zero advance ratio and small values of wake fraction.

In the preliminary design phase when data on type, diameter, revolutions and pitch of ship propellers and on engine - propeller interaction are still unknown it is not possible to precisely estimate values of the factor C_p in function of ship speed. As it results from performed preliminary analyses, influence of ship speed on C_p factor value is negligibly small within the speed range of 0.257 ÷ 1.285 m/s, hence its average value was assumed irrespective of ship speed.

Power demand for SMC system during mining operations is equal to the total power demanded by all the propellers used to generate the thrust necessary to balance sea environment action:

$$N_{SS} = \Sigma N_P \text{ [kW]} \qquad (13)$$

The total thrust of propellers, this way determined, corresponds with the conditions for selecting the power source characteristics, i.e. the satisfying of maximum design power demand.

ESTIMATION OF THRUST AND POWER OF SMC SYSTEM PROPELLERS FOR PURPOSES OF PRELIMINARY DESIGN OF SEA MINING SHIP

In the calculations was used the preliminary design concept of the sea mining ship whose main parameters are given in Tab. 1.

Tab. 1. *Values of main parameters of sea mining ship acc. [1]*

	Main parameters of sea mining ship	
Design assumptions	Yearly mining rate of wet concretions [10^6 t / year]	1.750.000
	Period of storing the concretions in holds [days]	10
	Operational period [days/year]	292
	Average density of concretions [t/m^3]	2
Parameters and main dimensions of the ship	Length b.p. L_{pp} [m]	215.6
	Breadth B [m]	40.68
	Hull depth H [m]	19.37
	Draught T [m]	12.83
	Hull block coefficient C_B [-]	0.83
	Displacement Δ [t]	96250
	Deadweight P_N [t]	75469
	Load capacity [t]	61130
	Windage lateral area of ship, S_y [m^2]	3850
	Lateral area of under-water surface of ship, F_y [m^2]	2980
	Head area of under-water surface of ship, F_x [m^2]	512

To calculate at first sea environment action to the mining ship fitted with TW system and then trust and power of SMC system, the formulae (1) ÷ (13) and the following assumptions were used:

- the design weather conditions in the assumed zone of mining operations, in three variants :
  - **Variant 1**: V_A = 18 m/s ; H_S = 5 m ; V_C =1.1 m/s; $V_{gł}$ = 0.55 m/s,
  - **Variant 2**: V_A = 22 m/s ; H_S = 6 m ; V_C = 1.1 m/s; $V_{gł}$ = 0.55 m/s,
  - **Variant** 3: V_A = 26 m/s ; H_S = 7 m ; V_C = 1.1 m/s; $V_{gł}$ = 0.55 m/s,

- the mining ship speed range : $V_S = 0.5 \div 2.5$ kn
- the TW system technical parameters : $Dr_z = 0.28$ m, $l_r = 4600$ m acc. [2]
- ship's main parameters and surface areas acc. [1]
- values of the coefficients : $C_{Ay} = 0.96$ and $C_{xC} = 0.85$ acc. [5].

The range of design sea environmental conditions results from some optimization analyses (which was not a subject of this research).

Maximum sea environmental conditions in which the mining ship is intended to operate are assumed on such level as to obtain a rational value of operational costs and an optimum form of the whole process. Hence for the calculations only a certain range of design sea environmental conditions was assumed by using the results of the research on influence of weather conditions on design criteria [9].

RESULTS OF THE CALCULATIONS

Sea environment action to sea mining ship

In Tab. 2 are presented the calculation results of the wind action R_{Ay}, that of wave, R_{Wy}, and of surface current, R_{Cx}, to sea mining ship for different sea environmental conditions.

Tab. 2. *The calculation results of the wind, wave and surface current actions to sea mining ship*

	Sea environmental conditions - variant 1			Sea environmental conditions - variant 2			Sea environmental conditions - variant 3		
V_s [m/s]	R_{Ay} [kN]	R_{Wy} [kN]	R_{Cx} [kN]	R_{Ay} [kN]	R_{Wy} [kN]	R_{Cx} [kN]	R_{Ay} [kN]	R_{Wy} [kN]	R_{Cx} [kN]
0.257	764	856	411	1143	1232	411	1595	1678	411
0.514	765	857	581	1144	1233	581	1596	1679	581
0.771	765	859	781	1144	1234	781	1597	1680	781
1.028	766	860	1010	1146	1235	1010	1598	1681	1010
1.283	767	861	1267	1147	1237	1267	1600	1683	1267

The calculation results of the hydrodynamic resistance of TW system, R_R , and ship hull resistance to motion, R_T , in function of ship speed are given in Tab. 3.

Tab. 3. *Ship hull resistance to motion and TW system resistance to motion and deep-water currents*

Ship speed V_S [m/s]	Hull resistance R_T [kN]	TWS resistance R_r [kN]
0.257	4.0	515
0.514	13.0	917
0.771	28.0	1446
1.028	48.0	2107
1.283	73.0	2892

Values of the total resistance of mining ship hull, R_T, for the assumed and controlled speed values during mining operations, were calculated by means of the Holtrop - Mennen method.

Thrust and power output of the SMC system propellers

The calculation results of thrust of ship propellers and main components of power of SMC system are presented in function of ship speed in Tab. 4 and Fig. 7.

Tab. 4. *Values of thrust of ship propellers and main components of power of SMC system*

Ship speed	Thrust components [kN]			Thrust T [kN]	Power components [kW]			Power N_{SS} [kW]
	T_B (*)	T_R	T_S		N_B (*)	N_R	N_S	
0.257	3868	541	4.0	4413	19341	2705	5.0	22051
0.514	4049	963	14.0	5026	20244	4814	35.0	25130
0.771	4261	1519	29.0	5809	21305	7593	113.0	29045
1.028	4504	2212	50.0	6766	22517	11062	259.0	33830
1.283	4778	3037	77.0	7892	23888	15185	492.0	39460

(*) Thrust and power calculated for the sea environmental conditions - variant 3

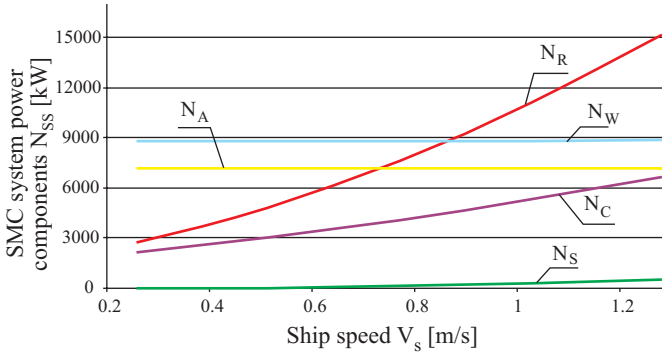

Fig. 7. *The SMC system's power components : N_A, N_W, N_C, N_S, N_R*

CONCLUSIONS

- In this paper is presented an analysis of estimation of maximum design power of a ship motion control (SMC) system intended for the preliminarily designed ship for mining Fe-Mn concretions, described in [1].
- The factors crucial for the generating of motion disturbances of the ship fitted with tubular winning (TW) system during its movement along a given trajectory within a corridor, i.e. action of wind, wave, sea currents (surface and deep--water), resistance of ship hull and TW system, have been specified.
- On the basis of the performed analytical calculations it can be stated that the largest share in the power necessary for the SMC system is attributed to that for towing the TW system. The towing power (Fig. 7) increases dynamically along with ship speed and reaches large values. Hence one of the main operational problems will be to provide such large values of the power N_R as well as to find an appropriate technical solution for towing the deeply immersed pipe.
- And, the smallest share is associated with the power necessary to generate propellers' thrust to overcome ship hull resistance to motion; it results from very low values of the ship's speed. Hence it can be assumed negligible.
- Due to its power demand the SMC system will constitute one of the largest power consumers out of those installed in the whole power system. Taking into consideration that the percentage share of the system's power in the total power balance amounts to about $60 \div 80$ % one can suppose that the total output of the electric power plant installed onboard the mining ship will be of the order of a few dozen megawatts.

NOMENCLATURE

a_x, a_y – additional resultant propeller thrust to balance inertia and damping forces resulting from slow-changeable motions of the ship
B – ship breadth [m]
C_{Ay} – aerodynamic resistance coefficient [-]
C_B – hull block coefficient [-]
C_{cx} – hydrodynamic resistance coefficient of under-water portion of ship hull [-]
C_D – hydrodynamic resistance coefficient [-]
C_p – usage factor of the power consumed to generate thrust by ship propellers
C_{Wy} – coefficient of drifting force generated by regular wave [-]
Dr_z – outer diameter of wining system's pipe [m]
F_x,F_y – areas of under-water hull surface projected to midship plane and ship plane of symmetry, respectively [m^2]
g – earth gravity acceleration [m/s^2]
H – ship hull depth [m]
H_S – significant wave height [m]
l_r – length of the pipe
l_y – length of winning system's pipe [m]
L_{pp} – ship length between perpendiculars [m]
N_A – power for generating the thrust necessary to balance wind action [kW]
N_B – power for generating the thrust necessary to balance sea environmental action (wind + wave + current) [kW]
N_C – power for generating the thrust necessary to balance sea current action [kW]
N_P – power [kW]
N_R – power for towing the winning system pipe [kW]
N_S – power for generating the thrust necessary to balance hull resistance to motion [kW]
N_{SS} – total power of ship motion control system [kW]
N_W – power for generating the thrust necessary to balance wave–generated drifting force [kW]
P_N – ship deadweight [t]
R_{Ay} – component of wind action to above-water portion of mining ship hull [kN]
R_{Rx} – component of water action to tubular winning system [kN]
R_{Wy} – component of wave-generated drifting force action to mining ship hull [kN]
R_{Cx} – component of resultant water - flow action to ship hull, due to sea surface current and ship speed [kN]
R_R – resistance of tubular winning system to motion [kN]
R_T – total resistance of ship hull [kN]
S_x, S_y – windage areas projected to midship plane and plane of symmetry, respectively [m^2]
$S_{\zeta\zeta}(\omega)$ – wave energy spectrum density [m^{2}s]
T – ship draught [m]
T_p – thrust of propellers of ship motion control system [kN]
T_{Sx}, T_{Sy} – components of resultant thrust of propellers of ship motion control system, necessary to balance sea environment action to ship, [kN]
V_S – ship speed [m/s]
V_A – average wind velocity [m/s]
V_C – sea surface current velocity [m/s]
V_{gl} – resultant velocity of deep-water current [m/s]
V_{RA} – relative wind velocity [m/s]
V_{RV} – relative current velocity [m/s]
V_{RVg} – relative water-flow velocity [m/s]
V_{RVx}, V_{RVy} – components of relative water-flow velocity [m/s]
β – ship drift angle [°]
β_A – wind direction angle with respect to ship [°]
β_C – sea current direction angle with respect to ship [°]
β_{RA} – relative wind direction angle [°]
β_{RC} – relative current direction angle [°]
β_{RV} – relative drift angle [°]
β_W – wave direction angle with respect to ship [°]
ρ_A – air density [t/m^3]
ρ_w – sea water density [t/m^3]
Δ – ship displacement [t]
ω – frequency of harmonic wave component (linear regular wave) [s^{-1}].

BIBLIOGRAPHY

1. Bortnowska M.: *A method of estimation of power demand for motion control system of floating unit during operation of mining Fe-Mn concretions, applicable in preliminary designing* (in Polish). Doctor's thesis, Szczecin University of Technology, 2006
2. Cheng B., Chung J.S.: *Application of Thrusts to Elastic Joints on Long Vertical Pipe in 3-D Nonlinear Motions – Part II: Numerical Examples by MSE an FEM Results*, International Offshore and Polar Engineering Conference Montreal, Canada, May 24-29, 1998
3. Hogben N., Lumb F. E.: *Ocean Wave Statistics, National Physical Laboratory,* London 1967
4. Неизвнесимстнов Я. В., Глумов И. Ф.: *Инженерная геология рудной провинции Кларион-Клиппертон в тихом океане*, Труды, Том 197, Наука, Санкт-Петерсбург, 2004
5. A group of authors, Brix J. Ed.: *Manoeuvring Technical Manual*. Hamburg, 1993
6. Szelangiewicz T.: *Research on dynamic behaviour of a winning facility for mining the concretions from seabed* (in Polish). Research report 5T12C 012 25, Faculty of Maritime Technology, Szczecin University of Technology, Szczecin 2006
7. Sobota J.: *Estimation of power demand for winning the concretions from seabed* (in Polish). *Interoceanmetal* Common Enterprise, Szczecin 2003
8. Szelangiewicz T.: *Research on influence of displacement and main dimensions of a base ship for underwater operations on power of ship's dynamic positioning system* (in Polish), Proceedings of 4th Conference on Design and Construction of Ocean Engineering Objects, Ocean Engineering Committee, Scientific Technical Session, SIMP Shipbuilding Section, Szczecin 1987
9. Szelangiewicz T.: *Influence of weather conditions on design criteria for ocean engineering units* (in Polish). Proceedings of 8th International Symposium on Ship Hydromechanics, Wrocław 1989.

CONTACT WITH THE AUTHOR

Monika Bortnowska, Ph. D.
Faculty of Marine Technology,
Szczecin University of Technology
Al. Piastów 41
71-065 Szczecin, POLAND
e-mail : mwojciechowska@ps.pl
tel.: (091) 449 47 20

POLISH MARITIME RESEARCH 4(54) 2007 Vol 14; pp. 31-39
DOI: 10.2478/v10012-007-0037-6

Application of artificial neural networks to approximation and identification of sea-keeping performance of a bulk carrier in ballast loading condition

Tomasz Cepowski
Szczecin Maritime University

ABSTRACT

This paper presents an application of artificial neural networks to approximation and identification of additional wave-generated resistance, slamming and internal forces depending on ship motion and wave parameters. The analysis was performed for a typical bulk carrier in ballast loading conditions. The investigations were carried out on the basis of ship response data calculated by means of exact numerical methods. Analytical functions presented in the form of artificial neural networks were analyzed with a view of their accuracy against standard values. Possible ways of application of the artificial neural networks were examined from the point of view of accuracy of approximation and identification of the assumed ship response parameters.

Keywords : ship, ship sea keeping qualities, artificial neural networks, slamming, additional wave generated resistance, internal forces, shear forces, bending moments, wave parameters, approximation, identification, assessment

INTRODUCTION

Various optimization methods of ship design parameters or operational ones are often applied to problems associated with ship designing and operation. Economic profits are the main criteria for which target functions are usually formulated. And, ship sea-keeping qualities are usually used as constraints for ship design or shipping route since they first of all influence ship safety. To this end various approaches are applied. In the publications [1,4] assessment of sea-keeping qualities was presented in terms of the operational effectiveness index E_T, which expresses probability of the event that ship response to given wave conditions will not exceed an assumed level:

$$E_T = \Sigma_A \Sigma_S \Sigma_\mu \Sigma_{HT} \Sigma_V \Sigma_\psi [P(\Omega = 1)] \qquad (1)$$

where:

E_T – the operational effectiveness index under assumptions that:
- Ship will operate in a given sea region with the frequency f_A
- It will operate in that region with the frequency f_S in each season of the year
- In a given season and sea region waves of f_μ frequency propagating from μ directio, will occur
- For μ- direction waves of the parameters H_S (significant height) and T (significant period) will occur with the frequency f_{HT}
- On its shipping route the considered ship will move with the speed V and course angle ψ with the frequencies f_V and f_ψ, respectively
- Permissible criterion values assumed for selected sea-keeping qualities will not be exceeded.

Ω – a function which usually takes the values:
- 0 – in the case when ship response exceeds its permissible criterion value
- 1 – in the case when ship response does not exceed its permissible criterion value

P – probability of the event that the function Ω will take the value equal to 1 for given wave and ship motion parameters.

In Eq.1 a crucial element is the function Ω which makes it possible to assess sea-keeping qualities quantitatively. In Fig. 1 the classical algorithm for determining the function Ω is presented (algorithm no 1). In the first phase, values of sea-keeping qualities are calculated by using exact numerical methods or approximating functions. In the second phase, values of the function Ω are determined on the basis of the criteria for the sea-keeping qualities.

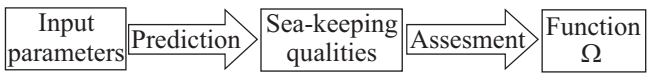

Fig. 1. *Algorithm no. 1 for determining the function Ω*

In this work another approach is proposed, namely that based on using only one phase for direct determining the function Ω instead of two (prediction and assessment). The algorithm described further as the algorithm no. 2, is presented in Fig. 2. The artificial neural networks are there applied to identify values of the function Ω.

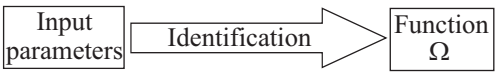

Fig. 2. An alternative algorithm for determining the function Ω

In this work a comparative analysis of both the approaches is performed, i.e.:

- ✦ Prediction (approximation) of sea-keeping qualities
- ✦ Identification of sea-keeping qualities (values of the function Ω).

Assumptions

The investigations were performed for B-517 bulk carrier of the following particulars:

- ♦ Overall length: Lc = 198 m
- ♦ Length between perpendiculars: Lpp = 185 m
- ♦ Breadth: B = 24.4 m
- ♦ Design draught: T = 11 m
- ♦ Block coefficient of immersed part of ship hull: $C_B = 0.82$
- ♦ Water-plane coefficient: $C_{WL} = 0.87$.

The ship's hull form is presented in Fig. 3.

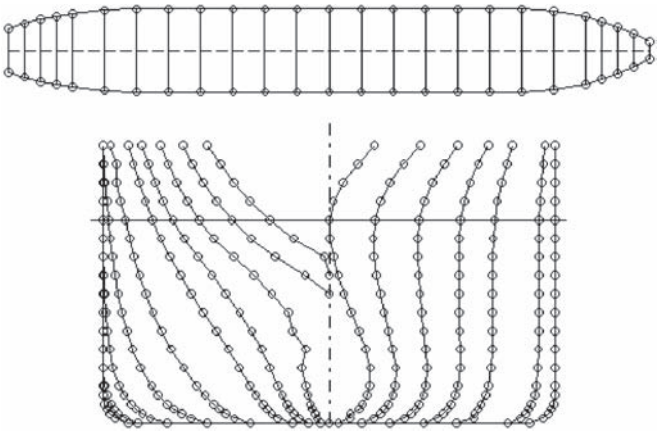

Fig. 3. Body lines of B-517 bulk carrier

The following ballast loading condition was taken into consideration:

- ✶ mass of ballast: 1830 t
- ✶ mass of stores: 1240 t (50 % of full mass of stores).

At this loading condition the ship obtained the following stability parameters:

- ➢ Displacement: D = 18069 t
- ➢ Average draught: Tm = 4.79 m
- ➢ Trim: t = -1.15 m
- ➢ Initial transverse metacentric height: GM = 3.27 m
- ➢ Propeller immersion ratio: Pr = 150 %.

In Fig. 4 the ship's curve of weights is presented for the analyzed loading condition.

- ➢ In the investigations were taken into account the sea-keeping qualities which influence ship safety most detrimentally. In the general case of transport ship to such qualities the following belong acc. [1, 4]: rolling. slamming, green water shipping on the deck, propeller emerging, vertical accelerations on the bridge and bow. And, only slamming is of importance for the considered bulk carrier in the assumed load condition (in view of the values of trim, transverse metacentric height and propeller immersion ratio).
- ➢ Moreover, structural safety problems associated with longitudinal strength can appear on the bulk carriers of the kind. Therefore in the analysis:
- ➢ slamming and
- ➢ internal forces (bending moments and shear forces at selected frame stations) were taken into consideration.

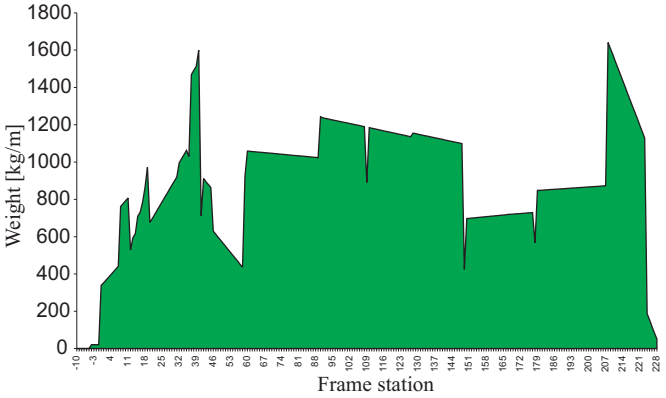

Fig. 4. Curve of weights for B-517 bulk carrier in the ballast loading condition and 50 % amount of stores

Additionally it was decided to analyze possible application of artificial neural networks to approximation and identification of additional ship resistance to motion in waves.

In the investigations the following operational parameters of the ship were taken into account:

- ⇨ the ship's speed V ranging from 0 to 15 knots, every 5 knots
- ⇨ the wave encounter angle Ω = 0° (following waves), 15°, 30°, 60°, 75°, 90°, 105°, 120°, 150° 175°, 180° (heading waves)
- ⇨ the significant wave height H_s ranging from 1 to 9 m, every second m
- ⇨ the characteristic wave period $T_s = 6 \div 20$ s, every second s.

Model (reference) values for approximation were calculated with the use of SEAWAY software based on exact numerical methods.

The SEAWAY software utilizes the two-dimensional flow theory and calculates ship motions in regular and irregular waves. Tests of accuracy of the software, presented in [2,3], show high accuracy of its calculation results.

APPROXIMATION AND IDENTIFICATION OF SEA-KEEPING QUALITIES BY MEANS OF ARTIFICIAL NEURAL NETWORKS

The functions ψ which serve for approximation and identification of ship's response, can be found in accordance with the following formula:

$$X \xrightarrow{\Psi} Y \qquad (2)$$

where:

X – set of assumed (input) operational parameters

Y – set of response(output) values calculated with the use of exact methods

Ψ – searched-for analytical function in the form of an artificial neural network, serving for approximation or identification of ship's response.

The phase of searching for the best network was composed of the following steps:

- ➲ determination of the best structure of the network by using genetic algorithms
- ➲ teaching the network

- testing the network
- accuracy assessment of the network's approximation on the basis of the testing results.

For teaching the neural networks 50 % of all the data at most were utilized so as not to cause the over-teaching of the network.

For the approximation accuracy assessment were used teaching and testing errors which can be determined in accordance with Eq. (3):

$$RMS = \sqrt{\frac{(\Psi_w - \Psi)^2}{n}} \tag{3}$$

where:
RMS – error value
Ψ_w – model values used for teaching or testing the neural network
Ψ – values calculated by using the neural network
n – number of records.

The neural networks elaborated for approximation and identification of:

- additional wave- generated resistance
- internal forces
- slamming

are presented below.

The neural networks were elaborated with the use of the software *STATISTICA Neural Networks*.

Additional wave-generated resistance

Approximation

The best network approximating additional wave-generated resistance appeared a MLP network of 4x7x1 structure (Fig. 5) characterized by:

- the high value of the correlation coefficient R = 0.95
- the value of RMS teaching error = 48 kN
- the value of RMS validation error = 54 kN
- the value of RMS testing error = 52 kN.

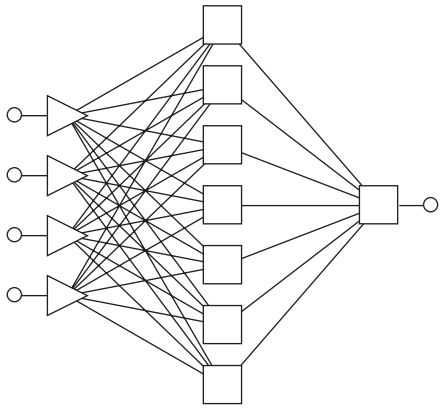

Fig. 5. *Schematic diagram of the MLP artificial neural network of 4x7x1 structure for approximation of additional wave-generated resistance of B-517 bulk carrier in ballast loading condition*

The searched-for function approximating the additional wave-generated resistance R, elaborated by means of the above mentioned neural network, is presented in the analytical form of Eq. (4):

$$R = \frac{\left(\frac{1}{1+e^{-([\beta, V, Hs, T_S]\times S+P)\times A-B)}} \times C - \alpha_0\right) - \alpha_1}{\alpha_2} \tag{4}$$

where:
R – additional wave-generated resistance [kN]
V – ship speed [kn]
β – wave encounter angle [deg]
T_S – characteristic wave period [s]
H_S – significant wave height [m]

A – matrix of weighting values:

3.061	3.060	-9.035	-8.150	5.422	0.389	-7.598
0.985	1.097	0.878	0.772	0.452	3.646	0.721
1.774	2.427	0.651	1.253	-0.847	-1.871	2.031
-6.194	-4.738	1.153	0.450	0.498	1.449	-0.269

B – vector of threshold values:

[6.082 5.747 -2.717 -2.682 2.524 -3.422 -2.742]

C – column vector of weighting values:

[-4.896 2.781 2.685 -5.144 -0.182 1.02 2.286]

S – matrix of coefficients:

0.0056	0	0	0
0	0.067	0	0
0	0	0.1250	0
0	0	0	0.0714

P – vector of displacement values:

[0 0 -0.1250 -0.4286]

α_0, α_1, α_2 – coefficients of the following values:

$\alpha_0 = 0.454$, $\alpha_1 = 0.3749$, $\alpha_2 = 0.0005$

Fig. 6 presents comparison of the approximation of the additional wave-generated resistance calculated from Eq. (4) with the values calculated by using the exact methods included in the SEAWAY software. For the test was assumed the ship's speed being beyond the speed range taken into account during modelling the neural network and described by Eq. (4). From the comparison it results that the function described by Eq. (4) is characterized by a relatively high extrapolating accuracy within that range of wave and ship motion parameters.

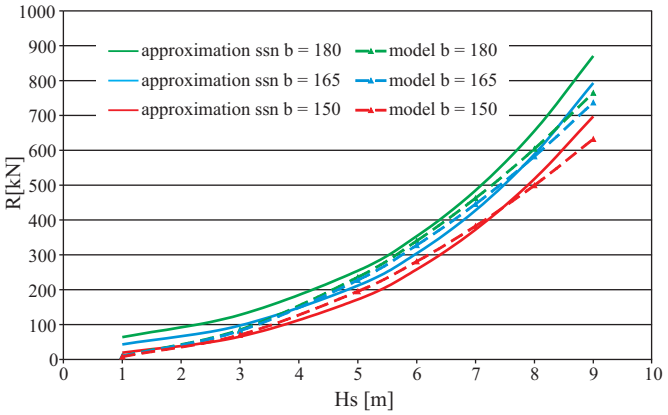

Fig. 6. *Approximation of the additional wave – generated resistance R, V = 20 knots, Ts = 14 s, Hs = var, b = var*

Identification

In this part of investigations were elaborated the artificial neural networks which make it possible to identify the additional wave-generated resistance expressed in the form of the four-state nominal function Ω_R equal to:

- R_1 – thrust (for the additional wave-generated resistance R<0 kN)

- ☆ R_2 – lack of the resistance (for values of R = 0 ÷ 30 kN)
- ☆ R_3 – a small value of the resistance (for values of R = 30 ÷ 100 kN)
- ☆ R_4 – a large value of the resistance (for values of R exceeding 100 kN).

The best artificial neural network which made it possible to identify the additional wave-generated resistance appeared to be the MLP network of 4x15x4x1 structure, characterized by the statistics shown in Tab. 1.

Tab.1. *Statistics applied to classification problems of the artificial neural network identifying the additional wave-generated resistance of B-517 bulk carrier in ballast loading condition*

Number of events	Teaching set				Validating set				Testing set			
	R1	R2	R3	R4	R1	R2	R3	R4	R1	R2	R3	R4
Total	124	541	182	253	83	354	106	139	73	340	109	160
Correct	124	536	161	235	83	352	93	133	73	337	98	151
Erronous	0	5	21	18	0	2	13	6	0	3	11	9
Indeterminate	0	0	0	0	0	0	0	0	0	0	0	0

The above mentioned artificial neural network can be analytically presented by means of Eq. (5) and (6):

$$\Omega_R = \begin{cases} R_1 \Leftrightarrow \alpha_1 = 1 \\ R_2 \Leftrightarrow \alpha_2 = 1 \\ R_3 \Leftrightarrow \alpha_3 = 1 \\ R_4 \Leftrightarrow \alpha_4 = 1 \end{cases} \tag{5}$$

where:

Ω_R – additional wave – generated resistance in the form of the four-state nominal variable: R_1 – resistance thrust, R_2 – lack of resistance, R_3 – small resistance, R_4 – large resistance

$\alpha_1, \alpha_2, \alpha_3, \alpha_4$ – initial values of the artificial neural network, determined on the last- but- one layer, calculated from Eq. (6):

$$\begin{bmatrix} \alpha_1 \\ \alpha_2 \\ \alpha_3 \\ \alpha_4 \end{bmatrix} = \left(1+\exp\left(-\left(\frac{1}{1+e^{-([\beta, V, Hs, T_S]\times S+P)\times A-B)}}\times C - D\right)\right)\right)^{-1} \tag{6}$$

where:

V – ship's speed [kts]
β – wave encounter angle [deg]
T_S – characteristic wave period [s]
H_S – significant wave height [m].

A – matrix of weighting values:

-4.8	10.8	-4.3	13.8	-10.9	-9.7	11.1	-35.8	8.1	-27.9	-2.7	-8.2	-24.4	24.5	-4.0
-1.9	-11.0	-2.5	25.4	-5.2	-3.7	14.6	1.6	-9.1	-41.8	-7.4	2.6	-2.9	-5.0	-7.9
-6.3	-20.5	2.2	-0.6	-16.9	19.0	-3.8	-1.9	11.2	-0.9	-3.9	-4.9	-7.8	-2.7	-1.6
7.4	16.0	8.4	1.6	14.9	9.7	2.2	4.2	-6.2	1.4	-2.6	-23.2	11.6	11.8	1.3

B – vector of threshold values:

[-3.9 2.9 -2.5 7.3 -7.4 -7.0 4.2 -18.8 4.8 -12.3 -5.3 -2.1 -18.6 3.7 -1.7]

C – matrix of weighting values:

0.9	0.9	-0.8	-14.2	-0.3	-2.2	-5.5	5.5	3.6	16.5	4.6	2.7	-1.0	-2.5	4.3
11.9	-5.5	-5.8	7.2	18.2	-12.2	-13.9	22.5	2.6	-45.6	1.5	16.3	-7.1	14.4	-3.2
-2.2	18.8	-1.8	-16.3	-27.3	12.9	5.0	-7.8	-1.9	-9.5	-4.4	-7.6	15.7	-5.6	-5.4
-15.6	-15.1	11.5	-3.9	-5.8	25.5	0.9	-23.9	-3.9	-4.1	3.8	-5.3	-8.3	-17.4	0.7

D – column vector of weighting values:

[4.5 3.1 3.1 -0.9]

S – matrix of coefficients having the same values as in Eq. (4)
P – vector of displacements having the same values as in Eq. (4).

Slamming

Appproximation

The best network approximating occurrence probability of slamming appeared MLP network of 4x2x1 structure, characterized by:

- the correlation coefficient R = 0.9
- the RMS teaching error = 0.95 %
- the RMS validation error = 0.76 %
- the RMS testing error = 0.96 %.

The searched-for function approximating the occurrence probability of slamming, P_S, elaborated by means of the above mentioned neural network, is analytically presented in the form of Eq. (7):

$$P_S = \frac{\left(\frac{1}{1+e^{-([\beta, V, Hs, T_S]\times S+P)\times A-B)}}\times C-\alpha_0\right)}{\alpha_1} \tag{7}$$

where:

P_S – slamming occurrence probability [%],
V – ship's speed [kn]
β – wave encounter angle [deg]
T_S – characteristic wave period [s]
H_S – significant wave height [m]

A – matrix of weighting values:

$$\begin{vmatrix} 5.628 & 6.929 \\ 2.297 & 2.483 \\ 6.812 & 6.551 \\ -8.117 & -13.530 \end{vmatrix}$$

B – vector of threshold values:

[12.929 14.016]

C – vector of weighting values:

[4.7 -4.249]

S – matrix of coefficients having the same values as in Eq. (4)
P – vector of displacements having the same values as in Eq. (4).

α_0, α_1, α_2 – coefficients having the values as follows:

$\alpha_0 = 0{,}0032$, $\alpha_1 = 0{,}0476$.

In Fig. 7 is presented extrapolation of the slamming occurrence probability P_S calculated from Eq. (7) compared with the values calculated by using the exact method implemented in the SEAWAY software. From the comparison it results that the function described by Eq. (7) is characterized by a relatively high accuracy as far as extrapolation is concerned.

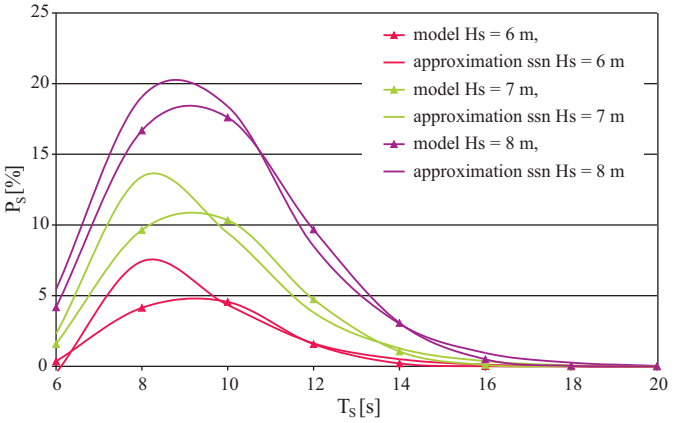

Fig. 7. Approximation of the slamming occurrence probability P_S, V = 20 knots, b = 165°, [T_S, H_S] = var

Identification

In this part of the investigations was elaborated the artificial neural network which makes it possible to assess occurrence of slamming in the form of the two-state nominal variable Ω_S taking the values:

- „0" – if slamming value does not exceed a dangerous threshold (not greater than 3%)
- „1" – if slamming value exceeds a dangerous threshold (greater than 3%).

The best artificial neural network which made it possible to identify values of the function Ω_S appeared to be the MLP network of 4x18x1 structure, characterized by the statistics shown in Tab. 2.

Tab.2. Statistics applied to classification problems of the artificial neural network identifying values of the function Γ_S for B-517 bulk carrier in ballast loading condition

Number of events	Teaching set		Validating set		Testing set	
	$\Omega_S = 0$	$\Omega_S = 1$	$\Omega_S = 0$	$\Omega_S = 1$	$\Omega_S = 0$	$\Omega_S = 1$
Total	53	1047	34	648	27	655
Correct	51	1029	34	641	27	638
Erronous	2	18	0	7	0	17
Indeterminate	0	0	0	0	0	0

The above mentioned artificial neural network can be analytically presented by means of Eq. (8):

$$\Omega_S = \left(1+\exp\left(-\left(\frac{1}{1+e^{-([\beta, V, Hs, T_S]\times S+P)\times A-B)}}\times C-1\right)\right)\right)^{-1} \tag{8}$$

where:

Ω_S – slamming in the form of the two-state nominal variable: „0" – slamming not exceeding a permissible value, „1" – slamming exceeding a permissible value; V – ship's speed [knots]; β – wave encounter angle [deg]; T_S – characteristic wave period [s]; H_S – significant wave height [m].

A – matrix of weighting values:

$$\begin{vmatrix} -0.30 & -4.99 & 4.04 & -0.44 & -12.37 & 1.98 & -1.19 & 1.49 & -0.02 & 1.44 & -18.98 & 5.57 & -3.32 & -22.70 & -3.23 & 10.89 & 1.05 & -0.01 \\ -5.38 & -3.48 & 0.44 & 4.64 & -0.01 & 5.49 & -0.66 & -5.27 & -3.72 & -3.05 & -0.04 & -0.75 & 5.67 & 0.85 & -3.63 & -2.73 & -6.87 & -3.05 \\ 0.28 & -2.01 & -2.13 & -3.02 & -9.46 & 14.45 & 3.40 & 4.27 & -0.43 & -1.58 & -5.94 & 0.71 & 5.39 & 8.02 & -3.02 & -12.61 & -6.41 & 3.25 \\ -1.43 & -6.37 & 0.11 & 6.16 & 14.80 & -15.77 & 6.75 & 6.97 & 3.34 & 5.12 & 10.65 & -1.48 & 5.55 & 10.66 & -0.01 & 0.38 & -1.84 & -2.57 \end{vmatrix}$$

B – vector of threshold values:

[0.65 5.60 -4.12 0.65 -8.81 10.51 1.37 0.23
1.06 2.82 -13.07 -10.73 -0.11 -4.74 2.39
-5.11 -1.25 -0.88]

C – column vector of weighting values:

[-2.91 -9.63 11.63 -4.31 23.06 -27.36 -9.65
-3.31 1.27 2.64 23.11 15.06 -5.59 20.2 -3.78
16.21 5 1.18]

S – matrix of coefficients having the same values as in Eq. (4)

P – vector of displacements having the same values as in Eq. (4).

Internal forces

In the investigations were taken into consideration shear forces and bending moments for B 517 bulk carrier in irregular waves, occurring at frame stations where an appropriate longitudinal strength of the ship in still water is required.

Approximation

For the approximation of shear forces and bending moments in irregular waves at selected frame stations of the ship was used the set of MLP neural networks having the structures and statistical parameters shown in Tab. 3 and 4.

Tab.3. *Structure and statistics of artificial neural networks approximating, at selected frame stations, shear forces of B-517 bulk carrier in ballast loading condition*

Frame stations	Distance from A.P. [m]	Structure of network	Coefficient of correlation R	RMS validation error [kN]
41	33.21	4x7x1	0.98	427.8
59	49.41	3x12x1	0.98	623.3
90	77.31	4x15x1	0.98	484.4
109	94.41	4x6x1	0.97	496.9
128	111.51	4x11x1	0.99	374.0
149	130.41	4x9x1	0.98	692.0
178	154.51	4x4x1	0.96	1143.4
208	175.51	4x6x1	0.97	358.5

Tab.4. *Structure and statistics of artificial neural networks approximating, at selected frame stations, bending moments of B-517 bulk carrier in ballast loading condition*

Frame stations	Distance from A.P. [m]	Structure of network	Coefficient of correlation R	RMS validation error [kN]
41	33.21	4x9x1	0.97	6460.3
59	49.41	4x11x1	0.98	13681.1
90	77.31	4x7x1	0.98	28725.3
109	94.41	4x8x1	0.98	27335.0
128	111.51	4x6x1	0.98	30878.2
149	130.41	4x8x1	0.98	31132.8
178	154.51	4x15x1	0.97	12484.2
208	175.51	4x15x1	0.96	2236.0

In Fig. 8 through 11 are presented extrapolations of shear forces and bending moments obtained by means of the artificial neural networks, compared with values calculated with the use of the exact methods implemented in the SEAWAY software. From the tables it results that the above mentioned extrapolations are characterized by a relatively high accuracy.

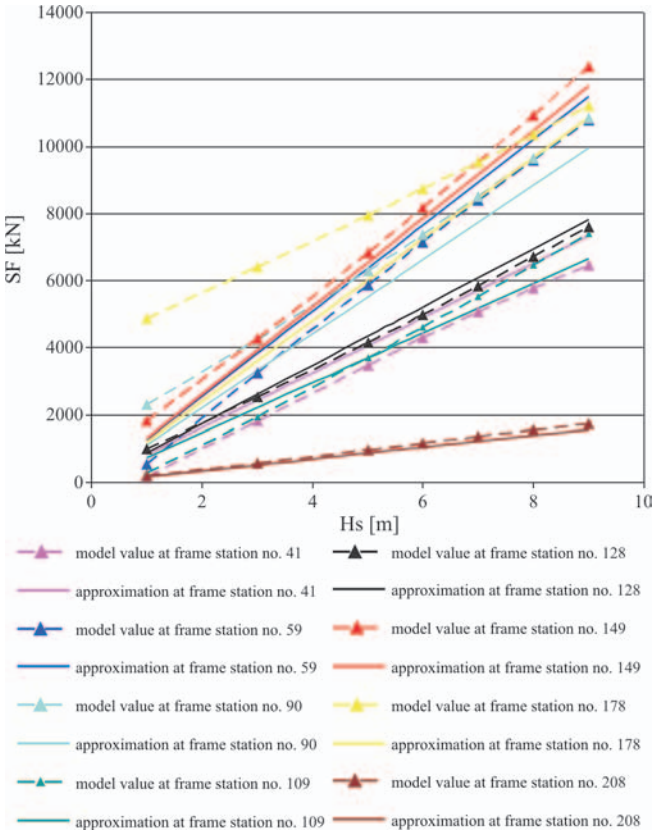

Fig. 8. *Approximation of the shear forces SF at: V = 20 kn., b = 0°, T_S = 12 s, H_S = var.*

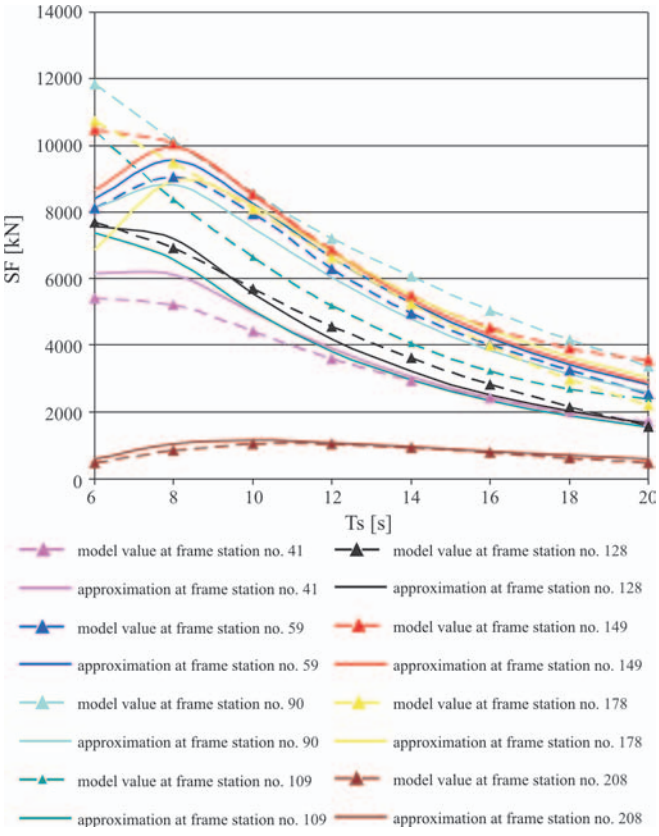

Fig. 9. *Approximation of the shear forces SF at: V = 20 kn., b = 0°, H_S = 6 m, T_S = var.*

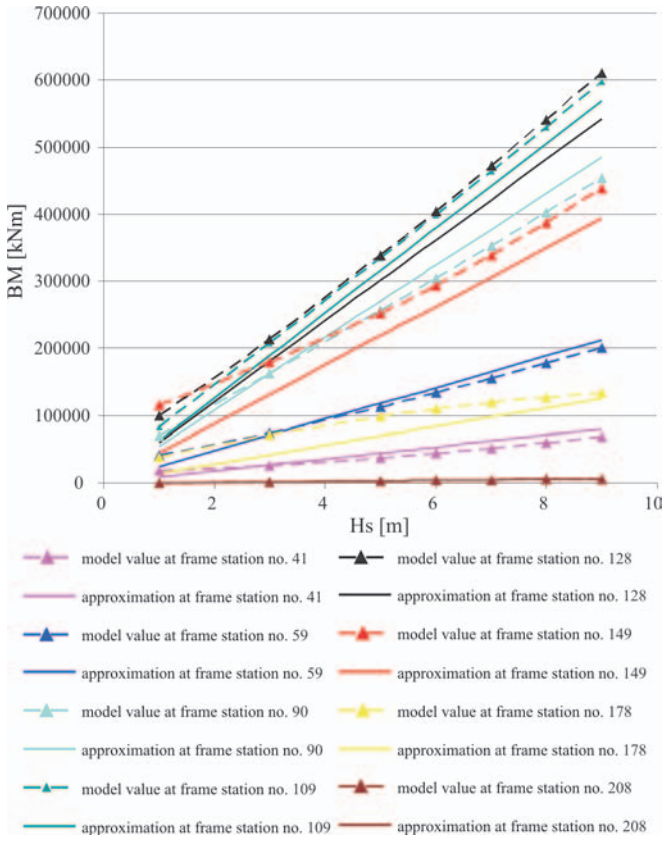

Fig. 10. *Approximation of the bending moments BM at: V = 20 kn., b = 0°, T_S = 12 s, H_S = var.*

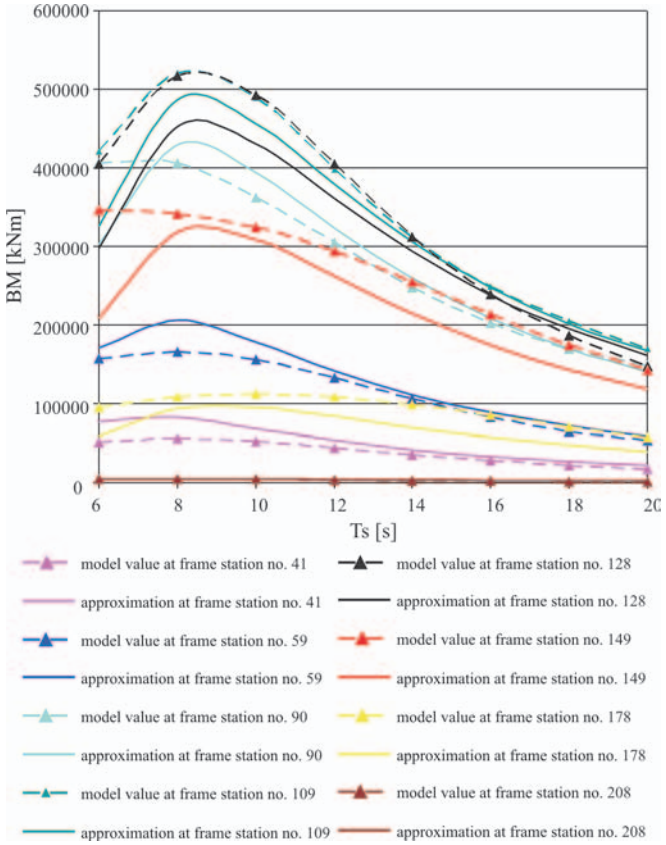

Fig. 11. *Approximation of the bending moments BM at: V = 20 kn., b = 0°, H_S = 6 m, T_S = var*

Identification

In this part of the investigations was elaborated the artificial neural network which makes it possible to assess occurrence of the internal forces expressed in the form of the two-state function Ω_S taking the values:

- „1" – if values of internal forces do not exceed the criterion ones IF_{crit}
- „0" – if values of internal forces exceed the criterion ones IF_{crit}

As the criterion $IF_{crit.}$ for internal forces of the ship in irregular waves were assumed the permissible still water internal forces $IF_{s.w.crit}$ for B-517 bulk carrier, lessened by instantaneous values of the still water internal forces $IF_{s.w.}$ of the ship in ballast loading condition, i.e:

$$IF_{crit} = IF_{s.w.crit.} - IF_{s.w} \tag{9}$$

where:

IF_{crit} – permissible internal force for ship in irregular waves

$IF_{s.w.crit.}$ – permissible internal force for ship in still water (harbour state) taken from the ship's technical documentation

$IF_{s.w}$ – calculated instantaneous value of still water internal force for ship in ballast loading condition.

The values of the still water internal forces were calculated with the use of the author's computer program *Kalkulator*. The instantaneous values of still water internal forces, permissible values of internal forces both in still water and irregular waves, are presented in Tab. 5 and 6.

Tab. 5. *Values of shear forces of B-517 bulk carrier, at selected frame stations*

Frame station	Instantaneous value in still water [kN]	Permissible value in still water [kN]	Permissible value in irregular waves [kN]
41	17678	43262	25584
59	18237	48667	30431
90	10987	48667	37680
109	9261	48667	39407
128	8888	48667	39780
149	3698	48667	44969
178	3640	60812	57173

Tab.6. *Values of bending moments of B-517 bulk carrier, at selected frame stations*

Frame station	Instantaneous value in still water [kN]	Permissible value in still water [kN]	Permissible value in irregular waves [kN]
41	67042	1471500	1404458
59	256198	1471500	1215302
90	456106	1471500	1015394
109	507354	1471500	964146
128	543111	1471500	928389
149	531996	1471500	939504
178	361773	1471500	1109727

The best artificial neural network which made it possible to assess values of internal forces, appeared the MLP network of 4x13x1 structure, characterized by the statistics shown in Tab. 7.

Tab. 7. Statistics applied to classification problems of the artificial neural network predicting values of the function Ω_{IF} for B-517 bulk carrier in ballast loading condition

Number of events	Teaching set		Validating set		Testing set	
	$\Omega_{IF} = 0$	$\Omega_{IF} = 1$	$\Omega_{IF} = 0$	$\Omega_{IF} = 1$	$\Omega_{IF} = 0$	$\Omega_{IF} = 1$
Total	100	1100	109	1091	6	58
Correct	98	1086	108	1070	6	58
Erronous	2	14	1	21	0	0
Indeterminate	0	0	0	0	0	0

The above given artificial neural network can be presented by means of Eq. (10):

$$\Omega_{IF}=\left(1+\exp\left(-\left(\frac{1}{1+e^{-([\beta,V,Hs,T_S]\times S+P)\times A-B)}}\times C-13.4\right)\right)\right)^{-1} \tag{10}$$

where:
Ω_{IF} – internal forces in the form of the following two-state nominal variable:
- „1" – if values of internal forces do not exceed the criterion ones
- „0" – if values of internal forces exceed the criterion ones

V – ship speed [kn]
β – wave encounter angle [deg]
T_S – characteristic wave period [s]
H_S – significant wave height [m].
S – matrix of coefficients having the same values as in Eq. (4)
P – vector of displacements having the same values as in Eq. (4).

COMPARATIVE ANALYSIS OF APPROXIMATION AND IDENTIFICATION OF SEA-KEEPING QUALITIES

In this part of investigations was performed the comparative analysis of approximation and identification accuracy of the elaborated neural networks for ship speed values beyond the range of those assumed for building the networks.

The tests were carried out on the basis of the following set of input parameters:

- the ship's speed V = 20 knots
- the wave encounter angle β = 0° (following waves), 15°, 30°, 60°, 75°, 90°, 105°, 120°, 150°, 175°, 180° (heading waves)
- the significant wave height H_s ranging from 1 to 9 m, taken every second m
- the characteristic wave period T_s ranging from 6 to 20 s, taken every second s the set contained 616 cases altogether.

Next, making use of the algorithms no. 1 and 2 as well as the elaborated neural networks one determined values of the function Ω for each case contained in the above mentioned set. In Tab. 8 are presented the numbers of correct and erroneous classifications in relation to model values of the function Ω, and in Fig. 12 - the percentage specification of correct classifications.

Tab. 8. Numbers of correct and erroneous classifications for the testing set identifying values of the function Ω

	Correct classifications		Erroneous classifications	
	Algorithm no. 1	Algorithm no. 2	Algorithm no. 1	Algorithm no. 2
Additional resistance	300	494	316	122
Slamming	587	605	29	11
Internal forces	507	533	109	83

From Tab. 8 and Fig. 12 it results that the elaborated artificial networks have relatively good extrapolating properties for the investigated range of data. Moreover it turned out that the application of algorithm no. 2 for determining values of the function Ω gives more exact solution. It may result from that

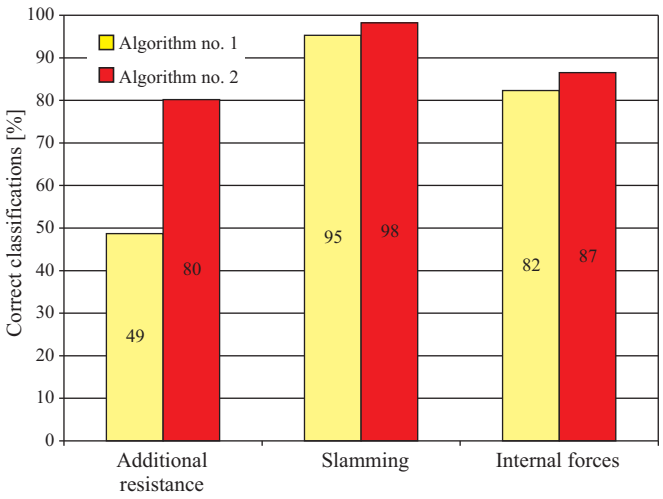

Fig. 12. Percentage specification of correct classifications

A – matrix of weighting values:

0.738	-1.339	2.036	2.076	26.157	0.773	-7.942	-4.118	-9.894	-7.184	-1.009	-7.160	-6.680
2.190	-1.415	-6.310	0.941	-0.995	0.584	-2.556	0.355	0.785	-10.104	-3.078	0.785	-3.075
2.194	-2.695	1.947	-6.437	-0.925	1.667	-7.545	-1.524	1.468	-1.545	-12.164	2.023	1.068
6.907	-1.163	2.876	-6.349	8.502	1.077	-17.785	0.998	12.706	2.509	16.332	-0.846	1.631

B – vector of threshold values:

[1.809 -0.318 4.836 -5.008 8.845 -0.744 -7.992 -3.162 -2.815 -16.438 -5.014 8.071 -7.596]

C – column vector of weighting values:

[-16.403 2.25 -10.425 7.202 16.795 -3.703 14.176 0.613 10.288 13.271 18.094 -7.28 -2.349]

the accuracy of approximation or extrapolation is influenced by the range of input data which is rather narrow in the case of the function Ω. When the function Ω is two-state one the accuracy of both the tested algorithms is close to each other (with outnumbering algorithm no. 2). And, when the function Ω is multi-state one (four-state one in the case of additional resistance) the accuracy of algorithm no. 2 greatly increases.

SUMMARY

- In this work were elaborated the artificial neural networks which make it possible to approximate and identify selected sea-keeping qualities of B-B17 bulk carrier in ballast loading condition. The analysis was focused on:
  - additional wave-generated resistance
  - slamming
  - shear forces and bending moments at selected frame stations depending on ship's motion and wave parameters.
- The elaborated artificial neural networks were characterized by high accuracy within a wide range of values of ship motion and wave parameters.
- The undertaken investigations were mainly aimed at making comparison of approximation and identification possibilities of artificial neural networks in assessing sea-keeping qualities. It turned out that more exact solutions were achieved by using the neural networks for identification of sea-keeping qualities. Such approach may find application in determining the operational effectiveness index E_T given by Eq. (1) in the case of problems associated with ship design and operation.

BIBLIOGRAPHY

1. Karppinen T.: *Criteria for Seakeeping Performance Predictions*, ESPOO 1987
2. Journée J.M.J.: *Verification and Validation of Ship Motions. Program SEAWAY*, Report1213a, Delft University of Technology, The Netherlands, 2001
3. Journée J.M.J.: *Theoretical Manual of SEAWAY*, Report1216a, Delft University of Technology, The Netherlands, 2001
4. Szelangiewicz T.: *Ship's Operational Effectiveness Factor as Criterion for Cargo Ship Design Estimation,* Marine Technology Transaction, Polish Academy of Sciences, Branch in Gdańsk, Vol. 11, 2000.

CONTACT WITH THE AUTHOR

Tomasz Cepowski, D.Sc.,Eng.
Institute of Marine Navigation,
Maritime University of Szczecin
Wały Chrobrego 1/2
70-500 Szczecin, POLAND
e-mail : cepowski@am.szczecin.pl

Photo: Cezary Spigarski

POLISH MARITIME RESEARCH 4(54) 2007 Vol 14; pp. 40-46
DOI: 10.2478/v10012-007-0038-5

Identification of hydro-acoustic waves emitted from floating units during mooring tests

Eugeniusz Kozaczka,
Gdansk University of Technology
Jacek Domagalski, **Grażyna Grelowska**, **Ignacy Gloza**
Naval University of Gdynia

ABSTRACT

Measurements of hydro-acoustic noise emitted from vessels are a.o. a subject of the tests carried out in the control measurement ranges of the Navy. The measurements are performed both on anchored and floating vessels. Acoustic field of vessels is changing along with their speed changing and is associated with acoustic activity of wave sources installed in vessel's hull (main engines, electric generating sets, reduction gears, pumps, shaft-lines, piping, ventilating ducts etc) as well as hydro-dynamic sources such as screw propellers and water flow around the hull [5, 7]. Vibration energy generated by the onboard devices is transferred through ship structural elements to water where it propagates in the form of hydro-acoustic waves of a wide frequency band.

Keywords: identification, propagation, hydro-acoustics

INTRODUCTION

Identification of sources of underwater noise generated by moving vessel in which various devices are installed, is a complex problem [2, 3, 4, 6]. Vibration energy propagating through ship structural elements interfers with acoustic waves emitted by various sources, that additionally complicates their identification.

One of the methods for identifying ship - generated underwater noise is examination of its spectrum. On the basis of such investigations can be selected characteristic components of the spectrum associated with running ship's mechanisms and devices as well as continuous spectrum which reflects work of cavitating ship propeller, turbulent flow in piping systems, fans, friction in slide bearings etc. It is rather hard to practically identify underwater noise. Ship-borne noise is mixed with environmental technical noise propagating from remote ships, shipbuilding and port facilities. There are also natural noise sources such as waves, wind and rain.

An additional difficulty in identifying acoustic spectrum components may be that various shipboard devices may emit waves of similar of identical frequencies.

This paper presents results of identification tests of a ship on the basis of measurements of underwater noise and vibration of main engines and electric generating sets, recorded in main and auxiliary engine rooms. The tests were carried out in two phases. In the first phase, mooring tests of the ship were performed. They consisted of simultaneous measurements of vibrations recorded on board and acoustic pressure - in water depths. After that cycle of the tests ship measurements were carried out on a dynamic testing range. Their results will be published later.

MOORING TESTS OF THE SHIP

The measurements were carried out in Gdańsk Bay waters in the area free from disturbances generated by marine industry, merchant and naval ports and fairways. Schematic diagram of the testing range is presented in Fig. 1.

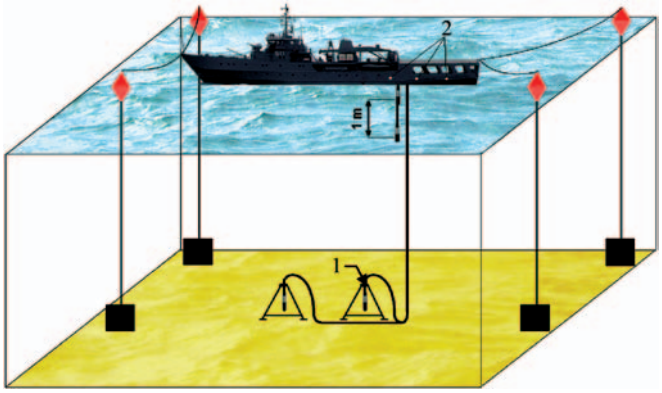

Fig. 1. *Schematic diagram of the testing range for moored ship's investigations.* ***Notation****: **1** - hydrophones, **2** - accelerometers.*

The investigation was aimed at selecting characteristic components of the spectrum, associated with work of particular ship machines and devices. Frequencies of the components were determined by comparing spectral density of vibration

power and that of underwater noise. To this end was used the coherence function which - for two signals : v(t) and p(t) - is defined as follows [1, 2]:

$$\gamma^2_{pv}(f_k) = \frac{\left|G_{pv}(f_k)\right|^2}{G_p(f_k)G_v(f_k)} \qquad (1)$$

where:

G_p, G_v - spectral density values of the signals $p(t_n)$, $v(t_n)$, respectively

G_{pv} - mutual spectral density value of the signals $p(t_n)$, $v(t_n)$.

The coherence function takes values from the interval :

$$0 \le \gamma^2_{pv}(f_k) \le 1 \qquad (2)$$

Zero - value means that there is no casual relation between the signals, and one-value - that the signals come from the same source.

The tests were commenced from the measurements of main engine vibrations and underwater noise resulting from the vibrations. Next the tests were performed of the electric generating sets and remaining devices installed onboard and which influence ship acoustic field structure.

The assumed measurement method makes it possible to find the components of power density spectrum which uniquely characterize the tested ship.

Vibrations of ship propulsion systems and electric generating sets were measured by means of piezo-electric acceleration indicators which were fixed to ship hull and engine seatings by using screw joints, in order to make transmission characteristics as broad as possible. The accelerometers were screwed to the under-frame of the engine in the places of its connection with the frame. Another accelerometers were screwed to the ship's hull directly below the former accelerometers. The so selected fixing places of accelerometers made it possible to investigate vibration energy resulting from work of engines and transferred directly to the under-frame and further through the ship's hull to surrounding water.

Schematic arrangement plan of the measurement points is presented in Fig. 2.

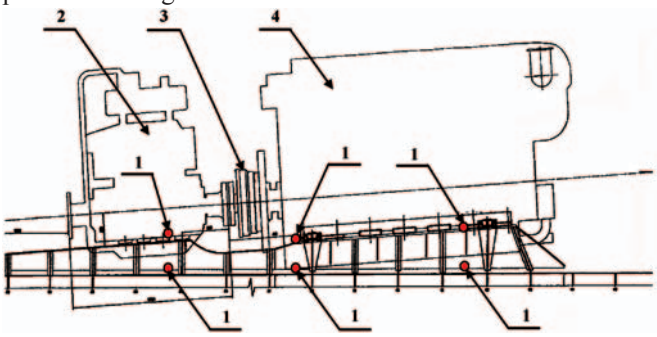

Fig. 2. *Schematic arrangement plan of the measurement points.* ***Notation****: **1** - accelerometers, **2** - reduction gear, **3** - coupling (of elastic connection with main engine and rigid one with shafting), **4** - 6ATL 25R engine.*

The ship's propulsion system is consisted of two 6ATL 25R Cegielski – Sulzer non-reversible main engines, two four-blade CP propellers and a reduction gear. On the ship two shaft- lines supported by three slide bearing each, are installed.

RESULTS OF THE TESTS OF THE RIGHT MAIN ENGINE RUNNING AT 750 RPM SPEED

The tests were performed for both propulsion systems at the rotational speed of main engines : 600, 750, 800, 850 [rpm]. To record and process signals the following instrumentation produced by B &K firm was applied : the 8101 measuring hydrophones, 2626, 2628 and 2636 measuring amplifiers, 2308 X -Y recorder, and 2145 two-channel frequency analyzer. The analyzer makes it possible to measure vibrations, acoustic pressure and rotational speed as well as to process recorded signals. Operational correctness of the vibration measuring system was checked in advance by means of the 4294 calibrating exciter. The exciter constitutes a small-size source of vibration intended for the field calibration of measuring systems, having the rms value of signal constant, equal to 10 [mms^{-2}] ± 3 [%] at 159.2 [Hz] (1000 [rad/s]). And, operational correctness of the noise measuring system was checked by using the 4223 hydrophone calibrator. It serves for calibrating the hydrophones together with the measuring system in field conditions. The reference signal is equal to 151 [dB] ÷ 166 [dB] against 1 [μPa] at 250 [Hz]; and the calibration accuracy: ± 0.3 [dB].

In this paper - for the reason of a vast amount of data obtained from the measurements - are included only those dealing with the tests of the right main engine at 750 rpm as well as of both main engines at 600 rpm.

In Fig. 3 is presented the spectrum of acoustic signals and vibrations elaborated in the frequency band up to 100 [Hz] at 0.25 [Hz]resolution.

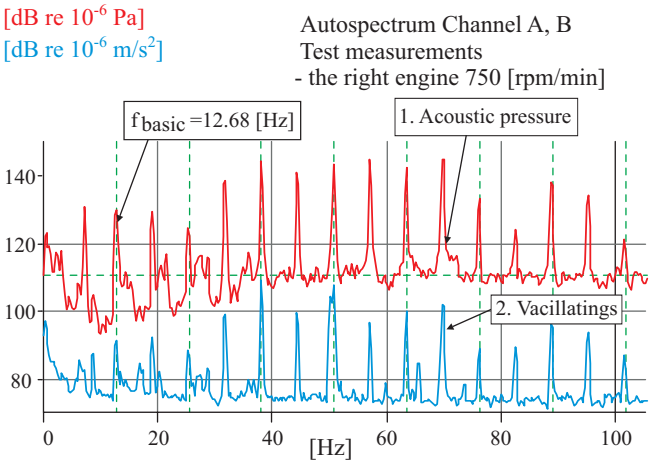

Fig. 3. *Spectrum of underwater noise and vibrations.* ***Notation****: **1** - Acoustic pressure measured under the ship's hull in the place of main engine seating, **2** – Vibrations measured at the seating of the right main engine.*

In the figure the upper spectrum represents changes of acoustic pressure in function of its frequency. The signals were recorded by the acoustic indicator placed under the ship in the distance of about 3.5 m from the hull. Changes of vibration acceleration in function of its frequency are presented in black colour. The vibrations were recorded at the engine seating. Additionally is showed the fundamental frequency of 12.68 [Hz] resulting from main engine rotation, as well as the subsequent harmonics. In the spectra can be observed the characteristic components which appeared at the same frequencies. To settle similarity of the recorded signals the coherence function showed in Fig. 4, was determined. On the function's diagram several characteristic components of the function, whose values are close to 1, can be observed.

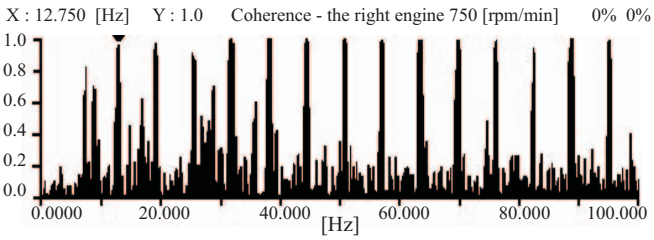

Fig. 4. *Coherence function of underwater noise and vibrations*

Determination of accurate value of rotational speed of the main engine made it possible to calculate frequencies associated with rotations of shaft-line, screw propeller and firings occurring in the main engine. The frequencies together with the subsequent harmonics are presented in Tab. 1.

Tab.1. *Vibration frequencies and subsequent harmonics of the engine calculated by using its real rotational speed.*

Source of vibration	Vibration frequency [Hz]		Subsequent harmonics [Hz]
Unbalanced moving parts of main engine	$f_n = kf_o$	12.68	25.36, 38.04, 50.72
Fuel violent combustion in cylinders	$f_z = kz_c f_o s$	6.34, 12.68, 19.02, 5.36, 31.70, 8.04	44.38, 50.72, 57.06, 63.40, 69.74, 76.08, 82.42, 88.76, 95.10
Unbalance of shaft-line	$f_w = \frac{kf_o}{2 \cdot 1.77}$	3.58	7.16, 10.74, 14.32
Unbalance of screw propeller	$f_s = 4\frac{kf_o}{1.77}$	28.66	57.32, 85.98

Notation:
k = 1,2,3,...,n, subsequent harmonics
f_n - main engine unbalance frequency
f_z - frequencies of firing in main engine cylinders
f_o - fundamental frequency $f_o = \frac{n}{60}$
n - rotational speed [rpm]
f_w - shaft-line unbalance frequency
f_s - propeller unbalance frequency
s - stroke factor (0.5 – for 4-stroke engine)
z_c - number of cylinders
1.77 - reduction ratio of transmission gear.

Results of identification of wave frequencies associated with combustion processes occurring in engine cylinders, as well as with shaft-line and propeller operation are presented in Tab. 2 and 3.

Tab.2. *List of frequencies associated with combustion processes occurring in main engine cylinders*

Frequency [Hz]		Coherence	Frequency [Hz]		Coherence
1	2	3	1	2	3
12.68	12.75	1	57.06	57.00	1
19.02	19.00	1	63.40	63.25	1
25.36	25.25	0.9	69.74.	69.50	1
31.70	31.75	1	76.08	76.00	1
38.04	38.00	1	82.42	82.25	0.9
44.38	44.25	1	88.76	88.50	1
50.27	50.50	1	95.10	95.00	1

Tab. 3. *List of frequencies associated with shaft-line and screw propeller rotation.*

Shaft-line			Screw propeller		
Frequency [Hz]		Coherence	Frequency [Hz]		Coherence
1	2	3	1	2	3
7.16	7.25	0.8	28.66	28.50	0.7

Notation:
1 - values of vibration frequencies calculated on the basis of the real rotational speed of the main engine (equal to 760,8 [rpm]),
2 - values of vibration frequencies taken from the spectrum shown in Fig. 3.
3 - values of the coherence function of underwater noise and vibrations.

Basing on the tests performed on the right main engine running at the rotational speed of 750 [rpm] one can evidence the relation occurring between vibrations of the ship devices and underwater noise.

In Fig. 3 the spectra of vibration accelerations and acoustic pressure are presented. In both diagrams distinct components of the same frequencies, resulting from operation of the main engine, rotating shaft-line and screw propeller, can be observed. The professional PULSE LABSHOP software of B&K firm, used for signal processing, made it possible to exactly determine the frequency resulting from rotation of the main engine's shaft. On the basis of this frequency (12.68 [Hz]) the real rotational speed (760.8 [rpm]) of the tested engine was determined during signal recording. Knowing values of spectral densities of acoustic pressure and vibrations one compared the signals by using the coherence function (Fig. 4). In this figure can be observed the characteristic components of values close to one, which unambiguously confirm the relation between vibrations generated by working engine, shaft-line and screw propeller and underwater noise.

The same testing method was used for the tests of main engines and auxiliary devices carried out at the remaining rotational speeds.

RESULTS OF THE TESTS OF BOTH MAIN ENGINES RUNNING AT 2*600 RPM SPEED

Identification of structure of ship acoustic field generated by two main engines of similar masses and running at almost the same rotational speed, is a complex issue. The summed up vibration energy resulting from work of the engines is transferred through ship structural elements to surrounding water and recorded by accelerometers placed at particular engines, that additionally makes their identification more difficult. The spectrum obtained from the tests is presented in Fig. 5.

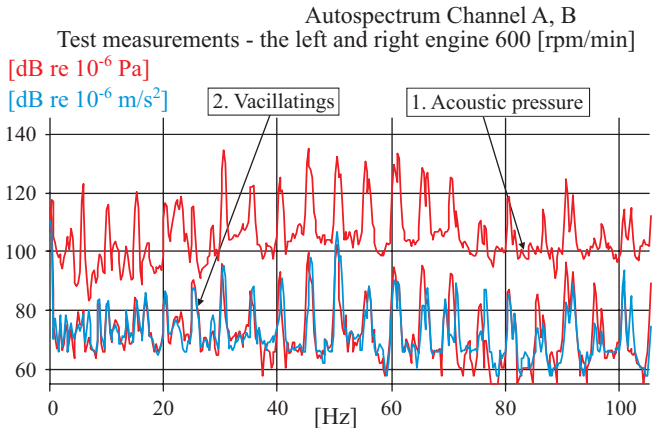

Fig.5. *Spectrum of underwater noise and vibrations of the left and right main engine running at the rotational speed n = 2*600 [rpm].*
Notation*: **1** - Acoustic pressure measured under the ship's hull in the place of main engine seating, **2** - Vibrations of the left and right main engine measured at their seatings.*

In the acoustic pressure spectrum, the characteristic components generated by the considered propulsion systems,

can be observed. It can be seen that in the spectrum over 30 [Hz] frequency appear double stripes which are more and more distinct along with frequency increasing. The phenomenon resulted from that the investigated wave sources operated at different rotational speeds (of 610.8 [rpm] – the left engine and of 602.4 [rpm] – the right engine). The fundamental frequencies of the engines are contained within 0.25 [Hz] band width of the filter used for signal processing (i.e. 10.18 [Hz] - the fundamental frequency of the left engine and 10.04 [Hz] – that of the right engine). The subsequent harmonics are displaced to each other by more than 0.25 [Hz] that can be observed in the presented spectrum (e.g. 61.08 [Hz] - the harmonic associated with operation of the left engine, 60.24 [Hz] - that associated with operation of the right engine).

From the performed tests it results that in the underwater noise of the frequency band up to 30 [Hz] the characteristic components generated by the left and right engine, can be identified. To this end was performed the analysis of the signals in the frequency band from 3.5 [Hz] to 28.5 [Hz] with 31.25 [mHz] resolution, presented in Fig. 6 where the frequencies associated with operation of the right engine are marked red and those associated with the left engine – blue.

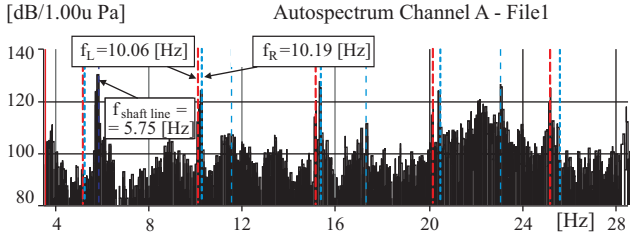

Fig. 6. *Underwater noise spectrum recorded on the ship in the mooring stage at the rotational speed of the main engines n = 2*600 [rpm]*

The fundamental frequencies of running main engines and shaft-lines, obtained from the noise spectrum are as follows:

- resulting from unbalanced moving parts of the right engine - f_R = 10.06 [Hz]
- resulting from unbalanced moving parts of the left engine - f_L = 10.19 [Hz]
- resulting from unbalance of the shaft-line of the right propulsion system - $f_{linii\ wałów}$ = 5.69 [Hz]
- resulting from unbalance of the shaft-line of left propulsion system - $f_{shaft\ line}$ = 5.75 [Hz].

To perform identification of vibration spectrum against underwater noise spectrum the above described coherence function was elaborated. The obtained results of the identification of acoustic waves is presented in Tab. 4 and 5.

Basing on the tests performed on the main engines running at the rotational speed n = 2*600 [rpm] one can evidence the relation occurring between vibrations and underwater noise. It is also possible to identify sources of the waves in surrounding water.

Values of the coherence function containing frequencies associated with combustion processes occurring in cylinders of main engines, are contained within the interval from 0.5 to 1 – for the right engine. The values unambiguously confirm the relation between vibrations and underwater noise. Similar values for the left engine are contained within the interval from 0.2 to 1. The following values : 0.4 for 10.25 [Hz], frequency, 0.3 for 20 [Hz], 0.3 for 50.25 [Hz] and 0.2 for 85 [Hz] did not confirm satisfactorily occurrence of a relation between that signals. The remaining values of the coherence function contained in the interval from 0.5 to 1 did confirm the relation. The frequencies associated with running the shaft-lines and screw propeller were determined from real values of rotational speed of main engines. The results are presented in Tab. 4. The obtained values of the coherence function, associated with vibrations generated by the shaft-lines and those with acoustic pressure are as follows : 0.8 for the left propulsion system and 0.9 for the right one. Similar values associated with running screw propellers are for these propulsion systems : 0.6 and 0.7, respectively. They also confirm occurrence of the relation between vibrations and noise.

Tab. 4. *List of frequencies associated with combustion processes occurring in cylinders of main engines*

Frequency [Hz]		Coherence	Frequency [Hz]		Coherence
1	2	3	1	2	3
Right engine					
10.19	10.25	0.9	56.05	56.00	1
15.29	15.50	0.9	61.14	60.25	1
20.38	20.50	0.7	66.24	66.25	1
25.48	25.25	0.5	71.33	71.25	0.9
30.57	30.75	1	76.43	76.25	0.9
35.67	35.75	1	81.52	81.50	1
40.76	40.75	0.9	86.61	86.75	0.9
45.86	46.00	1	91.71	91.75	0.9
50.95	51.00	1	96.81	96.75	0.8
Left engine					
1	2	3	1	2	3
10.06	10.25	0.4	55.33	55.25	1
15.09	15.00	0.5	60.36	60.25	1
20.12	20.00	0.3	65.39	65.25	0.9
25.15	25.00	0.9	70.42	70.25	1
30.18	30.00	1	75.45	75.50	0.8
35.21	35.25	0.9	80.48	80.50	1
40.24	40.25	1	85.51	85.50	0.2
45.27	45.25	1	90.54	90.50	1
50.30	50.25	0.3	95.57	95.50	0.8

Tab. 5. *List of frequencies associated with rotating shaft-lines and screw propeller*

Shaft-line			Screw propeller		
Frequency [Hz]		Coherence	Frequency [Hz]		Coherence
1	2	3	1	2	3
Left engine					
5.75	5.75	0.8	23.02	23.00	0.6
Right engine					
5.68	5.75	0.9	22.73	22.50	0.7

TESTS OF ELECTRIC GENERATING SETS

During the ship's mooring tests measurements of vibrations and acoustic pressure for four electric generating sets were performed. Results of the acoustic measurements were recorded by using the hydrophone located under the ship's hull in the place of seating a given generator. Vibrations were measured at the seating frame as well as the hull frames under a given electric generating set.

For signal recording the 2145 B&K analyzer fitted with a software for elaborating the spectrum of 200 [Hz] constant band width at 0.5 [Hz] resolution, was applied. The so recorded results were transmitted to an analyzing storing set. For further processing the signals the Microsoft Excel software was implemented.

The spectrum of underwater noise and vibrations recorded at the main engine's seating and the ship's hull is presented in Fig. 7. To better visualize the spectra the obtained values of vibrations were damped by 20 [dB].

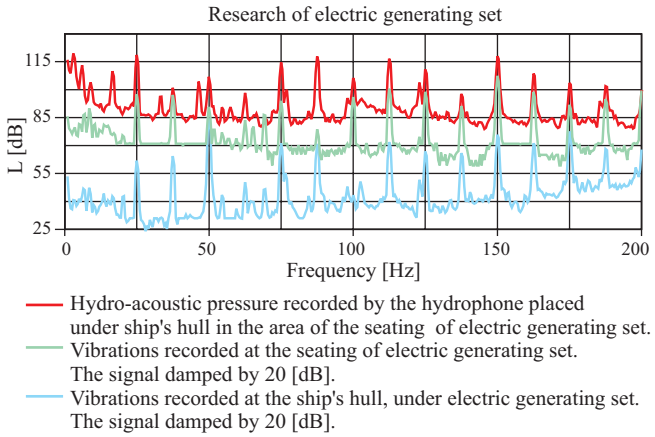

Fig. 7. *Spectrum of underwater noise and vibrations of electric generating set*

In the figure the upper spectrum marked red represents changes of acoustic pressure in function of its frequency. In green is presented the spectrum of vibrations recorded at the seating of electric generating set, and in black – the spectrum of vibrations recorded at the ship's hull.

In the spectra characteristic components occurring at the same frequencies can be observed, which leads to the conclusion that there is a relation between vibrations and underwater noise. The similarity between the obtained results was assessed by using the above described coherence function. In the function's diagram (Fig. 8 and 9) several stripes are observed whose values oscillate around one for the frequencies associated with operation of the tested electric generating set.

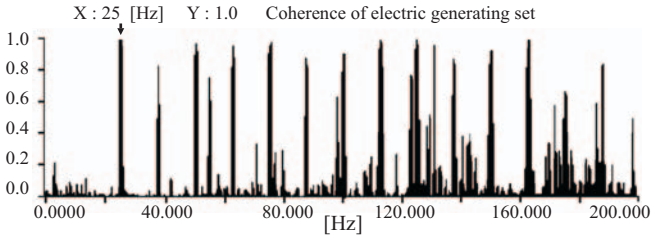

Fig. 8. *Coherence function of underwater noise and vibrations of electric generating set; the vibrations were recorded at the seating of the set.*

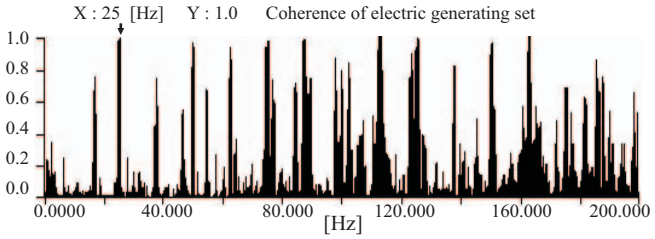

Fig. 9. *Coherence function of underwater noise and vibrations of electric generating set; the vibrations were recorded at the ship's hull just under the set.*

In Tab. 5 complete results obtained from the tests of the electric generating set no. 1 are presented. They contain values of hydro-acoustic pressure recorded by means of the hydrophone located under the ship's hull in the place of seating the electric generating set, as well as values of vibration velocity recorded at the engine's seating and ship's hull. The presented frequencies are associated with violent fuel combustion in cylinders. They were determined by using the same relations as in the case of the main engines' tests.

Tab. 5. *Results obtained from the tests of the electric generating set no.1*

Frequency [Hz]		Acoustic pressure [dB re 1μPa]	Vibration velocity		Coherence
			[μm/s]	[mm/s]	
1	2	3	4	5	6
25.00	119	4.8	80	1	1
37.50	101	3.0	69	0.8	0.9
50.00	107	1.1	537	1	1
62.50	99	0.4	8	1	1
75.00	115	1.1	76	1	1
87.50	118	0.16	64	0.9	1
100.00	106	1.0	2	1	0.9
112.50	117	1.5	54	1	1
125.00	111	1.1	28	1	1
137.50	99	0.4	23	0.9	0.9
150.00	118	2.4	67	1	1
162.50	109	0.8	36	1	1
175.00	104	0.3	68	0.7	0.9
187.50	101	0.4	23	0.8	0.9
200.00	100	0.7	20	0.9	1

Notation:
1 - frequency of electric generating set
2 - acoustic pressure level measured under the ship's hull in the place of seating the generator
3 - vibration velocity values measured at the generator's seating
4 - vibration velocity values measured at the ship's hull in the place of seating the generator
5 - values of the coherence function between vibrations measured at the seating and hydro-acoustic pressure
6 - values of the coherence function between vibrations measured at the ship's hull and hydro-acoustic pressure.

On the basis of the tests performed on electric generating sets, can be demonstrated occurrence of relations between vibrations and underwater noise since the values of coherence function between vibrations measured at the ship's hull and hydro-acoustic pressure are comprised within the range from 0.9 to 1, and for the vibrations measured at the engine's seating – within the range from 0.8 to 1. These values unambiguously confirmed the relation occurring between vibrations and underwater noise. However to unambiguously identify the waves in the dynamic testing range may be very difficult as the energy of waves associated with operation of electric generating sets, transferred to water, is much smaller than that of the waves associated with operation of the main engines, screw propeller and shafting.

RECAPITULATION OF THE MOORING TEST RESULTS AND DRAWN CONCLUSIONS

- In the mooring stage were performed the tests of two propulsion systems of the ship in question at the rotational speeds of the main engines : 600, 750, 800 [rpm] as well as the separate tests of the right and left propulsion system

operating at the speeds of 600, 750, 850 [rpm], and additionally the tests of electric generating sets.

- Results of the tests demonstrated that the identifying of hydro-acoustic waves associated with operation of those machines and devices is possible.
- The statement of frequencies resulting from operation of main engines, obtained from the tests, is contained in Tab. 6.

Tab. 6. *Frequencies resulting from operation of main engines at rotational speed values of 600, 750, 800, 850 [rpm], obtained from the tests performed in the mooring stage*

Source of vibrations	**Frequencies of propulsion system at main engine rotational speed of : [Hz]**		
	600 [rpm]	**750 [rpm]**	**850 [rpm]**
	One propulsion system under operation		
Left main engine (right one stopped)	10.25, 15.25, 20.50, 25.50, 30.75, 35.25, 41.00, 45.50, 51.00, 56.25, 61.00, 25.00, 66.50, 71.50, 75.75, 81.75, 87.00, 92.25, 97.25.	12.50, 18.75, 24.75, 31.00, 37.75, 43.50, 49.75, 56.00, 62.25, 68.25, 74.50, 80.75, 87.00, 93.25, 99.50.	14.25, 21.50, 28.75, 36.00, 43.25, 50.25, 57.50, 64.75, 72.00, 79.00, 86.25, 93.50.
Right main engine (left one stopped)	10.25, 15.55, 20.50, 25.75, 31.00, 36.00, 41.25, 46.50, 51.50, 56.75, 61.00, 75, 67, 72.25, 77.25, 82.50, 87.50, 92.75, 98.00.	12.75, 19.00, 25.25, 31.75, 38.00, 44.25, 50.50, 57.00, 63.25, 69.50, 76.00, 82.25, 88.50, 95.00.	14.25, 21.50, 28.50, 35.75, 43, 50, 57.25, 64.50, 71.50, 78.75, 85.75, 93.00.
Two propulsion systems under operation			
Main engine	**2*600 [rpm]**	**2*750 [rpm]**	**2*800 [rpm]**
Left one	10.25, 15.50, 20.50, 25.25, 30.75, 35.75, 40.75, 46.00, 51.00, 56.00, 60.00, 65.25, 71.25, 76.25, 81.50, 86.75, 91.75, 96.75.	12.50, 18.75, 25.00, 31.25, 37.50, 43.75, 50.25, 56.50, 62.75, 69.00, 75.25, 81.50, 87.75, 94.00.	13.00, 19.75, 26.25, 32.75, 39.25, 45.75, 52.50, 59.00, 65.50, 72.00, 78.50, 85.25, 91.75, 98.25.
Right one	10.25, 15.00, 20.00, 25.00, 30.00, 35.25, 40.25, 45.00, 50.25, 55.25, 60. 25, 65.25, 70.25, 75.50, 80.50, 85.50, 90.50, 95.50.	12.50, 18.75, 25.00, 31.5, 37.75, 44.00, 50.50, 56.75, 63.00, 69.25, 75.50, 81.75, 88.00, 94.25.	13.25, 19.75, 26.50, 33.00, 39.50, 46.25, 52.75, 59.50, 66.00, 72.50, 79.25, 85.50, 92.50, 99.00.

- On the basis of the rotational speeds of main engines basic frequencies associated with rotation of screw propeller and shafting were determined.
- Knowing frequencies of the tested system as well as those associated with operation of electric generating sets one is able to identify the waves associated with operation of the propulsion system, which propagate in surrounding water.
- From the above presented theoretical relationships it is possible to calculate frequencies of hydro-acoustic waves for all setting ranges of the propulsion systems in the frequency band up to 100 [Hz]. Such calculations were performed for the rotational speed values of main engines at which the ship in question usually operates.
- The statement of the so calculated wave frequencies of the systems is given in Tab. 7 in which the frequencies resulting from operation of electric generating sets are also included. It can be expected that the waves of those frequencies will propagate in surrounding water during measurements to be carried out on the ship in motion.

Tab. 7. *Frequencies resulting from operation of propulsion systems and electric generating sets, calculated by using theoretical relationships*

Source of vibrations	Frequencies of propulsion system at main engine rotational speed values of : [Hz]			
	600 [rpm]	750 [rpm]	850 [rpm]	950 [rpm]
Main engines	5.00, 10.00, 15.00, 20.00, 25.00, 30.00, 35.00, 40.00, 45.00, 50.00, 55.00, 60.00, 65.00, 70.00, 75.00, 80.00, 85.00, 90.00, 100.00.	6.25, 12.50, 18.75, 24.75, 31.00, 37.25, 43.50, 49.75, 56.00, 62.25, 68.25, 74.50, 80.75, 93.25, 99.50.	7.00, 14.25, 21.25, 28.25, 34.50, 42.50, 49.50, 56.50, 63.75, 70.75, 78.00, 85,92, 99.00.	8.00, 15.75, 23.75, 31.50, 39.50, 47.50, 55.50, 63.25, 71.25, 79.25, 87.00, 95.00.
Screw propeller	5.75, 11.25, 17.00, 22.5, 28.25, 33.75, 39.50, 45.25, 50.75, 56.50, 62.25, 67.75, 73.50, 79.00, 84.75, 93.25, 96.00.	7.00, 14.00, 21.25, 28.25, 35.25, 42.25, 49.50, 56.50, 63.50, 70.50, 77.75, 84.75, 91.75.	8.00, 16.00, 24.00, 32.00, 40.00, 48.00, 56.00, 64.00, 72.00, 80.00, 88.00, 96.00.	9.00, 18.00, 26.75, 35.75, 44.75, 53.75, 62.75, 71.50, 80.50, 89.50, 98.50.
Shafting	2.75, 5.75, 8.50, 11.25, 14.25.	3.50, 7.00, 10.50, 14.00, 17.50, 21.25.	4.00, 8.00, 12.00,16.00, 20.00, 25.00, 29.00.	4.50, 9.00, 13.50, 18.00, 22.50, 26.75.
Electric generating set	12.50, 25.00, 37.50, 50.00, 62.50, 75.00, 87.50, 100.00, 112.50, 125.00, 137.50, 150.00, 162.50, 175.00, 187.50, 200.00.			

- In order to confirm the results obtained from the tests carried out in the mooring stage it would be necessary to perform series of similar tests (but of a much wider scope) on the ship in a dynamic testing stage.
- Such stages are well adjusted to measuring and analyzing the underwater noise of ships in motion as well as to monitoring hydro-acoustic background. The acoustic methods applied to this aim are specially useful because of a very wide range of propagation of hydro-acoustic waves in surrounding water. For this reason it will be possible to early detect alien floating units during permanent monitoring the coastal water zone if only structure of acoustic noise field of own ships and acoustic background is known.

BIBLIOGRAPHY

1. Cempel Cz. : *Applied vibro-acoustics* (in Polish). State Scientific Publishing House (PWN), Warszawa 1989
2. Baranowska A Gloza I.: *Identification of underwater disturbance sources with the use of coherence function* (in Polish). Materiałs of 48th Open Seminar on Acoustics, Wrocław 2001.
3. Gloza I., Malinowski S. : *Identification of ship's underwater noise sources in the coastal region*, Hydroacoustics, Vol. 5/6, 2003.
4. Gloza I., Domagalski J., Malinowski S. : *Identification of sources of ship's hydro-acoustic field in a close surrounding* (in Polish). Materiałs of 49th Open Seminar on Acoustics, Warszawa-Stare Jabłonki 2002.
5. Grelowska G., Bittner P., Gloza I.: *Experimental research on noise generated by ship in motion* (in Polish). Materials of 9th Symposium on Hydroacoustics, Gdynia - Jurata, 1992.
6. Kozaczka E., Kiciński W., Nyszko G.: *Identifying investigations of acoustic signals emitted to water* (in Polish), Phase II, IV. Research reports, Gdynia 1995.
7. Urick R. J. : *Principles of Underwater Sound*. Mc Graw – Hill, New York 1975

CONTACT WITH THE AUTHORS

Prof. Eugeniusz Kozaczka
Faculty of Ocean Engineering
and Ship Technology
Gdansk University of Technology
Narutowicza 11/12
80-952 Gdansk, POLAND
e-mail : kozaczka@pg.gda.pl

— — — — — —

Grażyna Grelowska
Mechanic-Electric Faculty,
Polish Naval University
Śmidowicza 69
81-103 Gdynia, POLAND
e-mail : grelowska@amw.gdynia.pl

Photo: Cezary Spigarski

POLISH MARITIME RESEARCH 4(54) 2007 Vol 14; pp. 47-52
DOI: 10.2478/v10012-007-0039-4

Mean long-term service parameters of transport ship propulsion system

Part II
Propulsion engine service parameters of transport ship sailing on a given shipping route

Tadeusz Szelangiewicz
Katarzyna Żelazny
Szczecin University of Technology

ABSTRACT

During ship sailing on a given shipping route in real weather conditions all propulsion system performance parameters of the ship change along with changes of instantaneous total resistance and speed of the ship. In this paper results of calculations are presented of distribution function and mean statistical values of screw propeller thrust, rotational speed and efficiency as well as propulsion engine power output and specific fuel oil consumption occurring on selected shipping routes. On this basis new guidelines for ship propulsion system design procedure are formulated.

Keywords: thrust, efficiency and rotational speed of screw propeller, long-term prediction, shipping route, design working point of screw propeller

SERVICE PARAMETERS OF PROPULSION ENGINE OPERATION

The service parameters of propulsion engine operation, calculated below for a ship sailing on a given shipping route, are as follows:

- ☆ engine power output N
- ☆ engine speed (number of engine revolutions per time unit) n
- ☆ specific fuel oil consumption(SFOC), g, or hourly fuel oil consumption G.

The first two parameters (N, n) determine engine working point (if engine directly drives propeller without any reduction gear then $n = n_p$). During ship's sailing on a given shipping route in changeable weather conditions the engine working point changes its location. By controlling fuel charge (consequently also number of revolutions) a new engine working point is searched with the use of the criterion assumed below, so as to get it placed within engine layout area. Change of location of the engine working point makes fuel oil consumption changing: both the specific, g, and hourly one G.

ENGINE PERFORMANCE CHARACTERISTICS AND LOAD DIAGRAM

The propulsion engine load diagram consists of a few areas limited by appropriate characteristic lines. Working point of propulsion engine can be located in the areas but in some of them – only for a determined time of operation. The example load diagram of a Sulzer propulsion engine is shown together with depicted SFOC characteristics in Fig. 7.

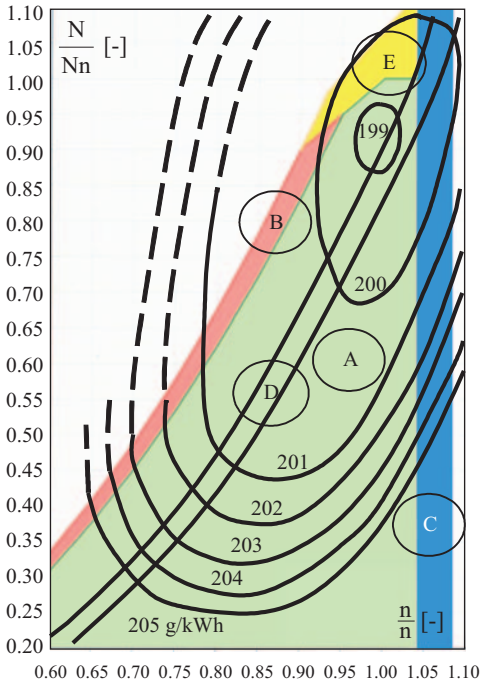

Fig. 7. *Load diagram of a Sulzer propulsion engine [8]. M_n – rated torque, **A** – continuous rating area (green); **B** – engine overload area (red); **C** – sea trial rating area (blue); **D** – still-water optimum rating area (...); **E** – instantaneous rating area (yellow)*

The particular areas are limited by engine performance characteristics of the following form:

$$N = k_m \cdot n^m \qquad (13)$$

where:
- N – engine power output
- k_m – coefficient for a given characteristic line
- n – engine speed
- m – exponent depending on an engine type and producer; for SULZER RTA 52, RTA 62, RT 72, RTA 84 slow-speed diesel engines:
  - m = 0 – for nominal continuous rating or maximum continuous rating,
  - m = 1 – for constant torque characteristics,
  - m = 2.45 – for overload characteristics.

Particular characteristics and range of engine speed are determined depending on an engine type (producer).

In Fig. 7, on the engine load diagram the SFOC characteristics, g, are shown. They are provided by engine producer and valid for a given engine and determined conditions (a given air temperature etc). There are also more general characteristics published by engine producers in the form of relevant nomograms, e.g. [8], which make it possible to calculate the SFOC depending on an engine type (producers), its nominal parameters (power and speed), instantaneous engine load as well as ambient conditions (temperature of air and cooling water). The way of making use of the nomograms to calculate the SFOC of engines is given in [5]. Fuel consumption can be also determined on the basis of measurements carried out with the use of special instruments (flow meters, calibrated tanks) during propulsion engine operation [1].

SHIP PROPULSION CHARACTERISTICS – PROPULSION SYSTEM'S PERFORMANCE IN CHANGEABLE WEATHER CONDITIONS

The ship propulsion characteristics are the following : curves of propulsion power, thrust, efficiency and torque at propeller's cone, fuel consumption and ship speed available for a given ship resistance characteristic. The characteristics are usually presented on the propulsion engine load diagram in function of propeller (engine) speed or ship speed (then characteristic of constant number of revolutions is attached). The propulsion characteristics published in the subject-matter literature are usually elaborated on the basis of:

- ⇨ model test results of free propellers or behind-the-hull ones
- ⇨ results of measurements carried out on ship board [2, 7]
- ⇨ results of measurements carried out on ship board with simultaneous use of free-propeller characteristics derived from model tests or numerically determined [3, 4, 5, 6].

For purposes of this work a numerical method for predicting the ship propulsion characteristics was elaborated (for a designed ship appropriate model tests are not to be performed), in the following form:

- T(V, n) - propeller thrust
- Q(V, n) - propeller torque
- η_0(V, n) - propeller efficiency
- P_D(V, n) - power output at propeller's cone
- V(P_D, n)- ship speed characteristic

where:
- V – ship speed
- n – engine speed (if the engine is of a slow speed then $n = n_p$, where n_p - propeller speed).

The ship propulsion characteristics for K1 ship (its parameters given in [9]), presented in Fig. 8, 9, 10, were calculated for the assumed additional resistance increments ΔR, resulting from the assumed constant values of the wind velocity V_A. As the power, thrust and torque were calculated at propeller's cone the engine power output was recalculated for the same point.

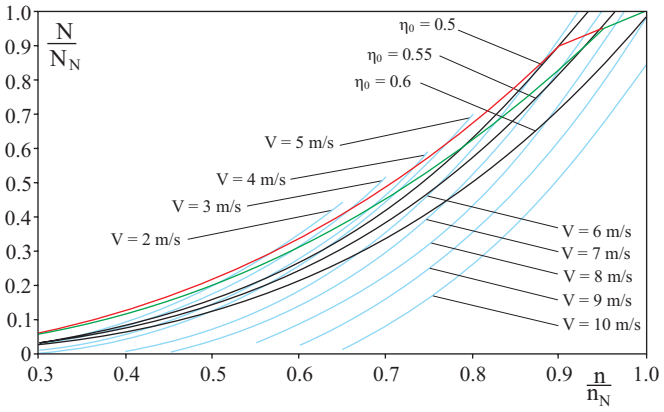

Fig. 8. Constant ship speed and constant propeller efficiency characteristics of K1 ship

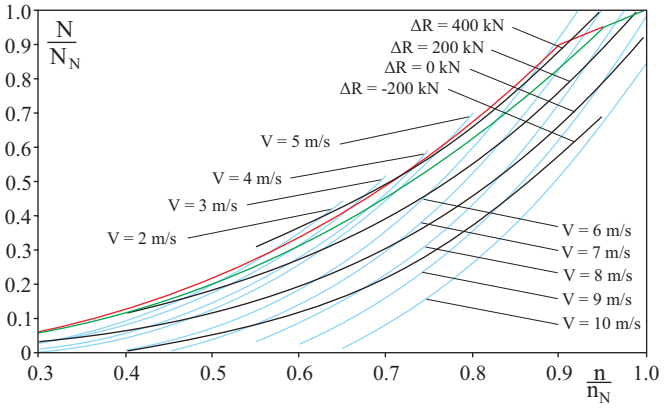

Fig. 9. Constant ship speed and constant additional ship resistance characteristics of K1 ship

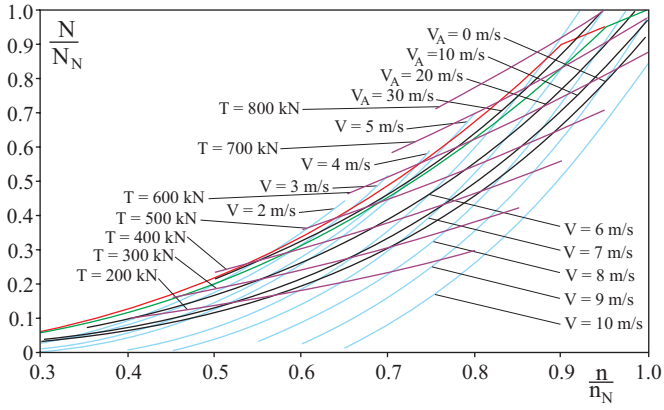

Fig. 10. Constant ship speed and constant propeller thrust characteristics of K1 ship, and constant wind velocity characteristic

In Fig. 10 are given the characteristics of constant velocity of wind blowing from a determined direction with respect to direction of ship motion (in the considered case the ship sails upwind –but such characteristics can be made for arbitrary wind and/or wave directions). They make it possible to correctly select a propulsion system's working point for changeable weather conditions or to predict, e,g., maximum ship's speed in the case of sea state worsening.

Possible change of propulsion system working point (for fixed pitch propeller) due to an additional resistance increase resulting from wind in the case in question (upwind motion of ship), is presented in Fig. 11.

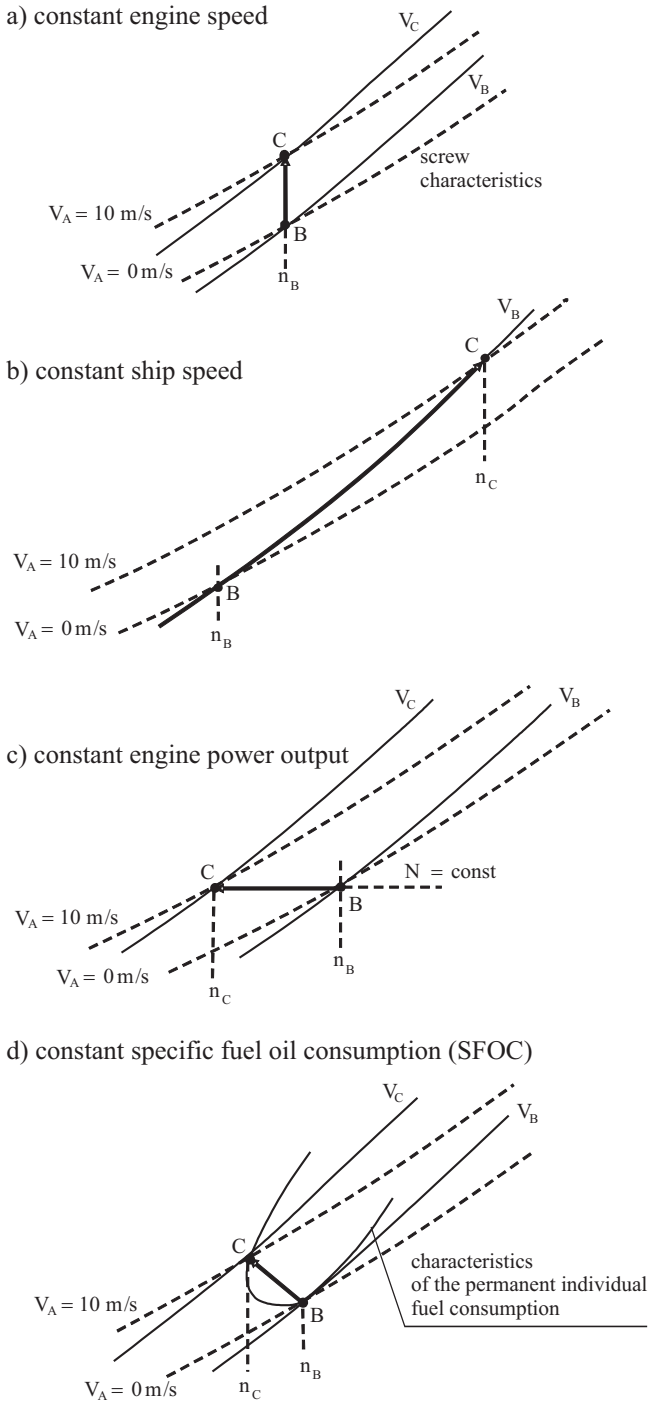

Fig. 11. *Examples of change of propulsion system working point, resulting from an increase of additional resistance due to changeable weather conditions*

In the described example the ship which starts from the point B, sails in still water with the speed V_B and propeller speed n_B, at the wind velocity $V_A = 0$ m/s. Then an additional resistance appears due to the head wind of the velocity $V_A = 10$ m/s. The following paths from the current propulsion system working point (B) to the new one (C) are possible (Fig. 11) :

a) at constant engine speed, n_B, fuel charge is increased (consequently also engine's power output) until the point C on the characteristic of V_A is reached, as a result the ship's speed drops to the value of V_C
b) at constant ship's speed V_B fuel charge is increased (consequently power output of the engine as well as its speed grow up to the value of n_C) until the point C is reached (the ship's speed can be kept constant up to the engine's limit curve)
c) at constant engine's power output the point C is reached, the ship's speed drops to the value of V_C as well as the engine's speed – to the value of n_C
d) at the SFOC kept constant the ship's speed and engine's speed is reduced until the point C is reached.

The four possible ways of reaching a new working point of propulsion system at resistance increasing – in this case due to wind velocity increasing– can be applied for different assumed criteria, e.g. : constant ship speed, maximum available ship speed, minimum fuel consumption, constant or maximum propeller efficiency.

For the determination of mean long-term service speed of ship at increasing resistance due to weather conditions the variant „b" will be used first, i.e. the initial ship's speed kept constant until the limiting characteristic is obtained (Fig.7).

When the additional resistance is further increasing the working point of the propulsion system will be searched on the limiting characteristic, i.e. the maximum available speed of the ship. The algorithm for searching the mean, long-term service speed of ship was so elaborated as to make it possible to apply also other variants (criteria) of selecting a new working point, presented in Fig. 11.

MEAN, STATISTICAL SERVICE PARAMETERS OF PROPULSION ENGINE OF SHIP SAILING ON A GIVEN SHIPPING ROUTE

Prediction of the mean, statistical service parameters of propulsion engine is performed in the same way as for screw propeller [10]. At first the instantaneous parameters which result from an instantaneous increase of ship resistance due to wind, waves, sea surface current and possible lay of rudder blade, are calculated and then probability of occurrence of relevant values of propulsion engine's output and speed and the SFOC is calculated.

The total probability of occurrence of given values of propulsion engine output and speed, P_T, is expressed as follows:

$$P_{Tn} = \sum_{A=1}^{n_A} \sum_{S=1}^{n_S} \sum_{\mu=1}^{n_\mu} \sum_{H,T=1}^{n_{HT}} \sum_{V=1}^{n_V} \sum_{\psi=1}^{n_\psi} p_{n_i} [n_i (\Delta R_i)] \qquad (14)$$

$$P_{TN} = \sum_{A=1}^{n_A} \sum_{S=1}^{n_S} \sum_{\mu=1}^{n_\mu} \sum_{H,T=1}^{n_{HT}} \sum_{V=1}^{n_V} \sum_{\psi=1}^{n_\psi} p_{N_i} [N_i (\Delta R_i)] \qquad (15)$$

where:

P_{Tn} – total probability of occurrence of a given value of the engine speed n_i (if the engine directly drives the propeller the occurrence probabilities of a given value of the engine and propeller speeds are the same: $P_{Tn} = P_{Tnp}$)

P_{TN} – total probability of occurrence of a given value of the engine power output N_i

n_i, N_i – instantaneous values of engine speed and output depending on an instantaneous value of the additional resistance ΔR_i

p_{ni}, p_{Ni} – instantaneous occurrence probabilities of given values of the engine's speed n_i and output N_i for an instantaneous situation resulting from ship sailing on a given shipping route, calculated according to (10), [10]

n_A, n_S, n_μ, n_{HT}, n_V, n_ψ – number of zones crossed by a ship, seasons of the year, values of wave direction, wave parameters, ship speed and course angle, respectively.

By applying the same technique as in the case of propeller, the mean statistical values of engine speed and output on a given shipping route can be expressed as follows :

$$\overline{n} = \frac{\sum_{i=1}^{n_n} P_{T_n} \cdot n_i (\Delta R_i = \text{const})}{\sum_{i=1}^{n_n} P_{T_n}} \tag{16}$$

$$\overline{N} = \frac{\sum_{i=1}^{n_n} P_{T_N} \cdot N_i (\Delta R_i = \text{const})}{\sum_{i=1}^{n_N} P_{T_N}} \tag{17}$$

where:

n_n, n_N – number of the intervals containing similar instantaneous values of engine speed and output, respectively.

During ship sailing on a shipping route in changeable weather conditions all the ship's service parameters result from its engine's working point which is to be located within the area of the engine's load diagram (Fig. 7) characterized by engine speed and power output.

Having the occurrence probabilities of given values of engine speed and output one is able to determine the occurrence probability of a given working point, i.e. of the pairs of values : engine speed – engine output (in the same way as for those of propeller speed – ship speed, Fig. 5 in [10]).

The calculated distribution function of engine speed – engine output makes it possible to calculate the distribution function of SFOC as a determined value of fuel consumption corresponds with each of engine's working point, Fig. 7. Having the distribution function one can calculate the mean long-term value of specific fuel oil consumption for a given shipping route, in a similar way as for engine speed and output.

RESULTS OF CALCULATIONS

Results of the calculations for the selected ship and shipping route (engine and shipping route parameters were specified in [9]), are presented in the form of :

- engine speed histogram and mean statistical value
- engine power output histogram and mean statistical value
- specific fuel oil consumption (SFOC) distribution function and mean statistical value
- probability distribution function of long-term occurrence of given values of engine speed and output (histogram of engine's working point)
- mean, long-term working point of propulsion engine.

In the figures the calculation results are presented - under the assumption that engine's output reaches at most 0.9 N_n - for K1 containership [9] and the two very different shipping routes : 5b - "easy" one and 2b - „difficult" one - in the sense of occurrence of long-term weather parameters.

Ship: K1 - assumed service speed = 8.44 [m/s]
- probability of maintaining a given speed, P_{VE}

Engine speed histograms

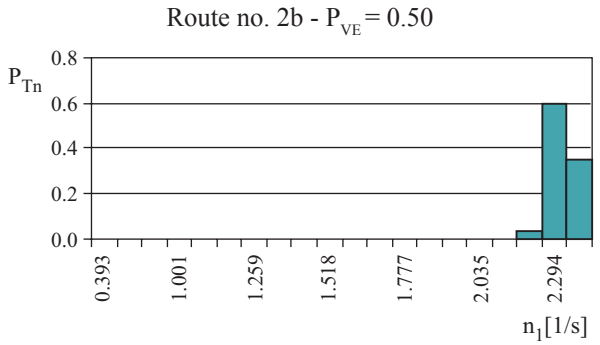

Nominal engine speed n_n = 2.330 [1/s]
Mean engine speed $\overline{n}$ = 2.335 [1/s]

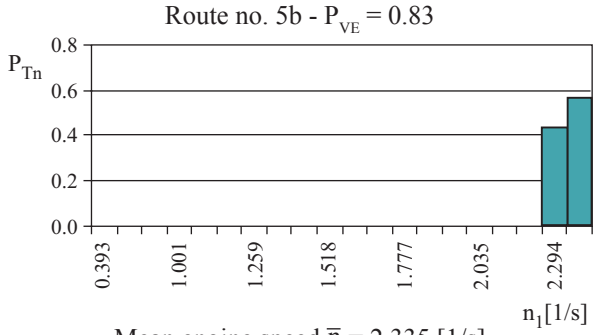

Mean engine speed $\overline{n}$ = 2.335 [1/s]

Power output histograms

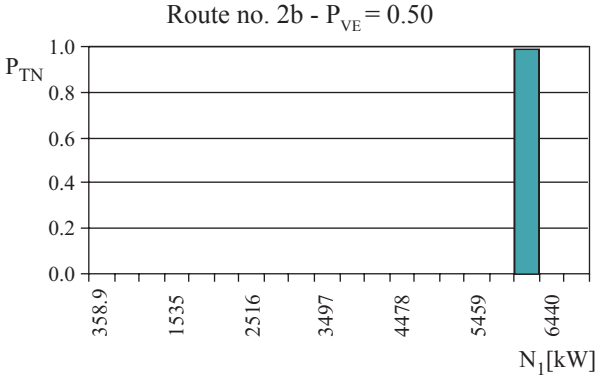

Nominal power output N_n = 6930 [kW]
Mean power output $\overline{N}$ = 6164 [kW]

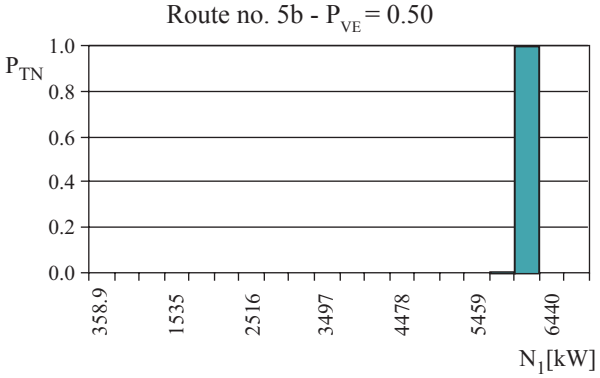

Mean power output $\overline{N}$ = 6156 [kW]

Fig. 12. *Histograms and mean statistical values of speed and output of propulsion engine of K1 ship sailing on shipping routes : 2b and 5b*

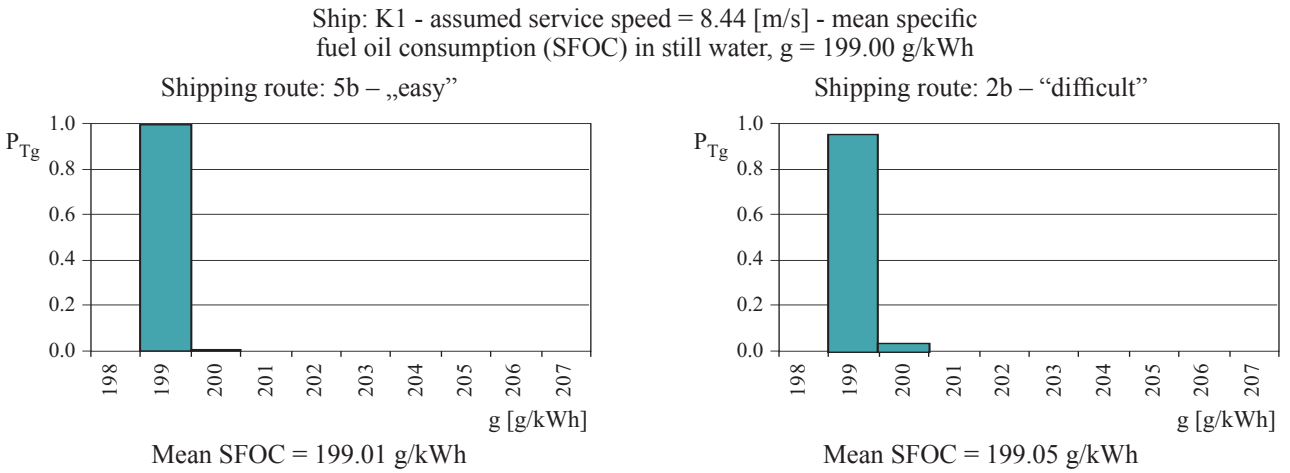

Fig. 13. *Histograms and mean statistical values of specific fuel oil consumption (SFOC) for K1 ship sailing on shipping routes : 2b and 5b*

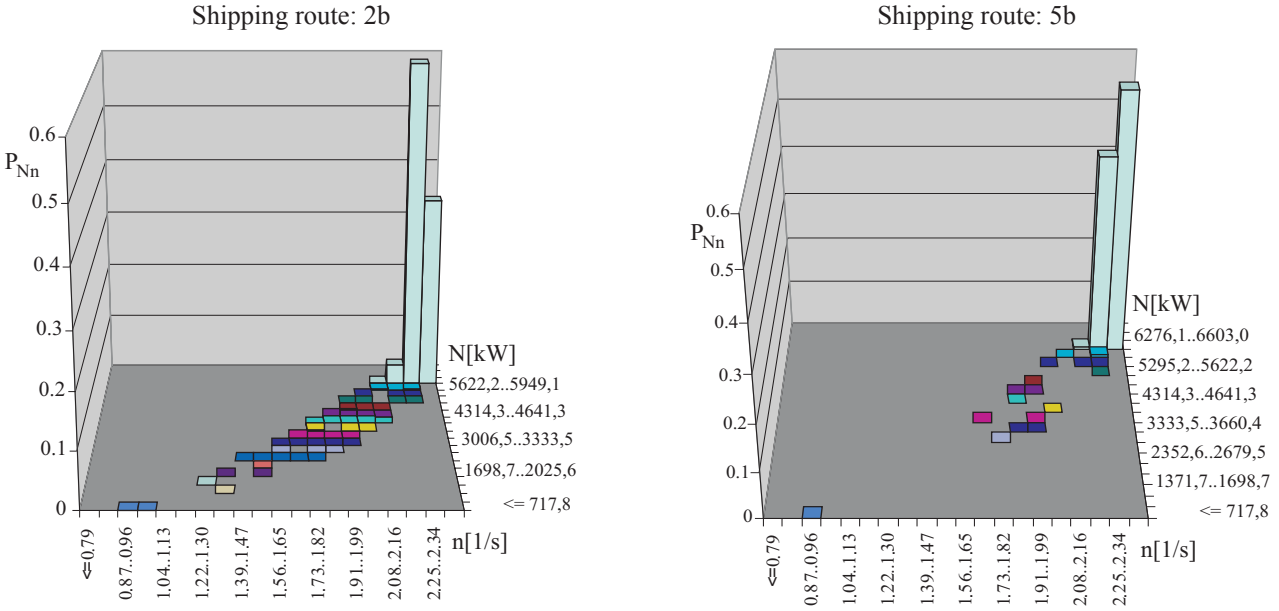

Fig. 14. *Probability of occurrence of the propulsion engine's working point (engine speed- output), P_{Nm}, for K1 ship sailing on shipping routes : 2b and 5b*

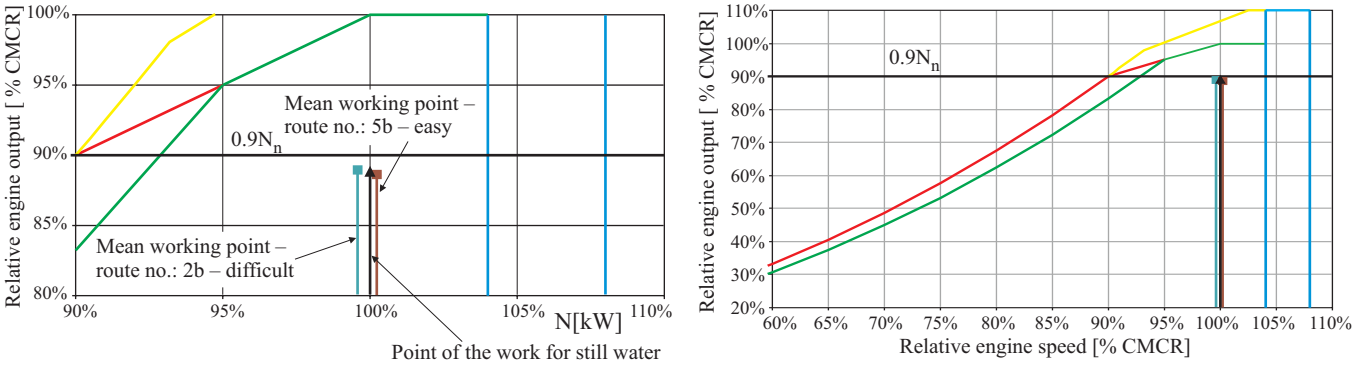

Fig. 15. *Mean, long-term working point of propulsion engine of K1 ship sailing on shipping routes : 2b and 5b*

FINAL CONCLUSIONS

- Conclusions resulting from the calculations of mean statistical service parameters of screw propeller were presented in [10]. Results of the calculations of the mean statistical parameters of propulsion engine operation (engine speed, output and specific fuel oil consumption - SFOC) in the form of histograms are very similar to those of screw propeller as the engine in question directly drives the propeller and the calculated power output is used only for propelling the ship (as no other power consumers were taken into consideration, e.g. shaft generators).
- The calculations of SFOC were performed for approximate characteristics under the assumption that the engine is new, air and cooling water parameters are standard and ship's hull and screw propeller are clean (un fouled). Therefore the calculation results should be assessed rather qualitatively but not quantitatively.

- The obtained histograms and mean statistical parameters depend not only on weather conditions on a given shipping route but also on an assumed criterion of propulsion control; the presented calculations were performed for the criterion of maintaining the ship speed constant (Variant "b", Fig. 11) and if it is not possible – for a maximum available speed at the engine power output of 0.9 N_n at the most. The assumed criteria of ship propulsion (engine) control highly influence service parameters of propulsion system. This can be observed in the case of the SFOC distribution as well as occurrence probability of a given working point of engine on a given shipping route.
- The condition of maintaining the assumed ship speed may result in a somewhat greater SFOC value on a shipping route where statistically more favourable weather conditions occur than on those of more harsh weather conditions. Hence not only weather conditions occurring on a shipping route are decisive of fuel consumption level. Therefore to obtain a possibly low SFOC level the propulsion control should be optimized by using various criteria (Fig. 11) depending on a given situation. In real conditions also ship course can be changed that consequently is equivalent to shipping route optimization.
- The elaborated computer software makes it possible to choose different control criteria of ship propulsion and optimize both its service parameters and entire shipping route.
- Calculations of probability of occurrence of propulsion engine working point (Fig. 14 and 15) may be also used for assessing the wear level of engine or its elements as well as for scheduling overhauls.

NOMENCLATURE

g – specific fuel oil combustion (SFOC)
G – hourly fuel oil combustion
k_m – coefficient of engine performance characteristic
N – engine power output
N_n – nominal engine power output
$\overline{N}$ – mean long-term engine power output
n – engine speed (number of revolutions per time unit)
n_n – nominal engine speed
n_p – propeller speed
$\overline{n}$ – mean long-term engine speed
n_A, n_S, n_μ, $n_{H\Gamma}$, n_V, n_ψ – number of : sea areas crossed by a ship, seasons, values of wave directions, wave parameters, ship speed and course, respectively
P_D – power delivered to propeller cone
P_{Nn} – probability of occurrence of a given working point of propulsion engine of the power output N and speed n
P_{VE} – probability of maintaining a given speed
P_{TN} – probability of occurrence of a given value of engine power output
P_{Tn} – probability of occurrence of a given value of engine speed
p_w – probability of ship being in a given situation
Q – propeller torque
ΔR – additional ship resistance due to weather conditions
T – propeller thrust
V – ship speed
V_A – mean wind velocity
V_E – ship service speed
η_0 – free-propeller efficiency.

BIBLIOGRAPHY

1. Balcerski A.: *Probabilistic models in the theory of design and operation of ship diesel engine power plants* (in Polish), Publ. by Foundation for Promotion of Shipbuilding Industry & Maritime Economy, Gdańsk 2007
2. Beukelman W., Buitenhek M.: *Full scale measurements and predicted sea-keeping performance of the containership "Atlantic Crown"*, International Shipbuilding Progress, Vol. 21, No. 243, 1974
3. Chachulski K.: *Power problems of operation of ship propulsion systems* (in Polish), Maritime Publishers (Wydawnictwo Morskie), Gdańsk 1991
4. Chachulski K.: Control of loading state of propulsion engine and its fuel combustion in any service conditions (in Polish). 14th International Symposium of Ship Power Plants, Szczecin, 1992
5. Chachulski K.: *Methods and algorithms for solving the operation problems of ship propulsion systems* (in Polish). Szczecin Maritime University, Szczecin, 1992
6. Chachulski K.: *Fundamental problems of ship propulsion systems* (in Polish), Maritime Publishers (Wydawnictwo Morskie), Gdańsk 1988
7. Ferdinande V., De Lembre R.: *Service - performance and sea-keeping trials on a car-ferry*, International Shipbuilding Progress, Vol. 17, No. 196, 1970,
8. SULZER : *General Technical Data for Marine Diesel Engines*, 1986
9. Szelangiewicz T., Żelazny K.: *Calculation of the mean long-term service speed of transport ship, Part III: Influence of shipping route and ship parameters on its service speed*, Polish Maritime Research, No 2/2007

CONTACT WITH THE AUTHORS
Prof. Tadeusz Szelangiewicz
Katarzyna Żelazny, D.Sc., Eng.
Faculty of Marine Technology,
Szczecin University of Technology
Al. Piastów 41
71-065 Szczecin, POLAND
e-mail : tadeusz.szelangiewicz@ps.pl

POLISH MARITIME RESEARCH 4(54) 2007 Vol 14; pp. 53-58
DOI: 10.2478/v10012-007-0040-y

Experimental research on effectiveness of the magnetic fluid seals for rotary shafts working in water

Zbigniew Szydło,
AGH University of Science and Technology
Leszek Matuszewski,
Gdansk University of Technology

ABSTRACT

This paper presents course of research on ferro-fluidal seals used in water. The tests were carried out for a hydrophobic magnetic fluid and specially selected profiles of sealing lips at various linear velocities in sealing unit. Though the tests were preliminary their results showed that the research on application of magnetic fluids to seals working in liquid environment should be continued. From the point of view of development of ring drives the most important advantage of ferro-fluidal seals is their smallest drag as compared with seals of other types.

Keywords: propulsion systems operating in water, magnetic fluids, tightness, seals

INTRODUCTION

Seals containing a magnetic fluid, known as Magnetic Fluid (MF) seals (or Ferro-Fluidic (FF) seals) in subject-matter literature, have taken firm place in seal engineering because of their simple structure, high reliability and operational effectiveness. They are used in many crucial mechanisms of machines working in gaseous environment at the pressure lower than 0.5 MPa, as well as in vacuum devices [1, 2].

However only a few publications can be found on application of MF seals to devices working in liquid environment. Difficulties associated with application of MF seals working in liquids are greater than in the case of their work in gaseous environment because of specific phenomena occurring at the interface of two liquids. Some of the problems which require to be experimentally tested separately, are discussed in [3].

Material and structural elaboration of MF seals capable of effective working in liquid environment could be of a great importance for many industrial branches where tightness of mechanisms being in permanent contact with liquid decides on correct operation of devices**.** It is also important for propulsion systems of floating units which are in permanent contact with water, hence limitation or elimination of leakage is essential for maintaining assumed operational parameters of the devices.

A research on seals with applied magnetic fluid, intended for operating in water was initiated by the Laboratory of Seals and Application of Magnetic Fluids, Department of Construction and Operation of Machines, Mining & Metallurgy Academy in Cracow in cooperation with the Department of Ship Theory and Design, Gdańsk University of Technology. A long-term aim of the research is to elaborate MF seals which will be capable of effective working also in shipborne devices.

In the previous publications of these authors [4] some aspects of application of MF seals in liquid environment were discussed and results of preliminary experiments carried out to assess possibility of effective operation of the seals submerged in liquid, were presented.

The experimental research on the problem has been continued and in further experiments other geometrical and structural versions of the seals and other kinds of magnetic fluid were used. In this publication is presented a summary of the tests have been performed so far with the use of the laboratory stand adjusted for testing MF seals in water.

The tests are still of a preliminary character, however in the opinion of these authors their results show directions in which further research on application of magnetic fluids to seals working in liquid environment, should be developed.

AIM AND SCOPE OF THE RESEARCH

The research was aimed at possible determination of effective operation of a MF seal installed on a rotating shaft immersed in a chamber full of tap water under pressure depending on the shaft's rotational speed, geometry of gap with magnetic fluid and construction of sealing unit.

The basic criterion of operational effectiveness of the seal was to maintain tightness of the testing chamber for an assumed operation time of the unit.

For all the investigations in the testing chamber the tap water was used as working medium.

For the tests two kinds of magnetic fluid and two sealing sleeves of different geometry were used at the following pressure values of the working medium :

- ⇨ 0.15 MPa - for the sealing sleeve of 0.1 mm gap and 8 sealing lips,
- ⇨ 0.05 MPa - for the sealing sleeve of 0.3 mm gap and 4 sealing lips.

The tests were carried out at various rotational shaft speeds within the range from 125 rpm to 6800 rpm.

A part of the tests was performed with the use of an additional protecting set of sealing rings : one of circular cross-section (O-ring) and another one of rectangular cross- section, placed from the side of working medium, before the basic MF seal. The test was aimed at making clear to which extent such design solution is effective, that was important for elaboration of further research program.

THE TEST STAND AND MEASUREMENT SYSTEM

The construction and mode of operation of the test stand was described in detail in [4].

Here are described only the testing head's elements crucial from the point of view of the investigations in question, as well as the measurement system used in the tests.

In Fig.1 is shown the drawing (half-cross-section and half –view) of the head for testing MF seals in liquid environment. The most important parts are shown in colours.

Compressed air is delivered through the channel (11) (in yellow) to the elastic recess (9), that makes pressure of the liquid (12) (in blue) which directly impacts the seal unit (1, 2, 3, 4), increasing.

Area of research versions shown in the picture number 3

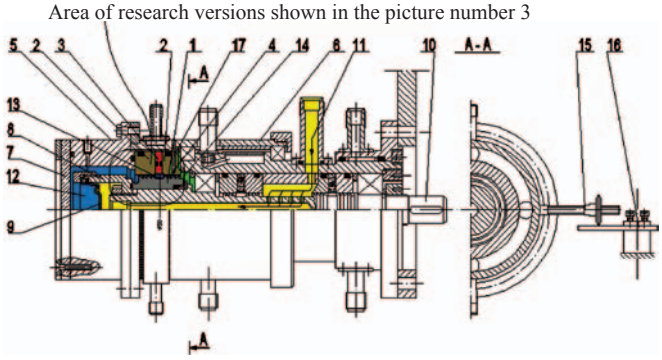

Fig. 1. *Construction of the head for testing MF seals in liquid environment.* ***Notation*** *: **1** – multi-lip sleeve, **2** – pole shoes, **3** – permanent magnets, **4** – magnetic fluid, **5** – testing head's casing, **6** – pivotable casing of head's bearings, **7** – transparent cover of testing head, **8** – rubber membrane holder, **9** – rubber membrane, **10** – rotating shaft, **11** – compressed air channel, **12** –zone of pressure set in liquid-filled chamber, **13** – zone of liquid penetration to the chamber, **14** – zone of liquid outflow due to leakage, **15** – pressing arm of torque-meter, **16** – extensometric beam for torque measuring, **17** – opening of magnetic fluid temperature indicator.*

In Fig. 2 the schematic diagram of the control-measurement system and overall view of the test stand is presented.

To produce pressure in the water-filled chamber, was used the compressed air delivered from the tank (17) fed by the air compressor (16), to the inlet socket (10). Compressed air pressure and rate of flow are controlled by the pressure reducing valve (18) and the throttle valve (19). Air pressure at the inlet socket (10) is measured by the MBS 32 Danfoss pressure transducer (21) of the measurement range of 0...1 MPa, as well as the indicating manometer of the measurement range up to 0.16 MPa. The cut-off valve (20) serves to close the compressed air channel when the set pressure is reached.

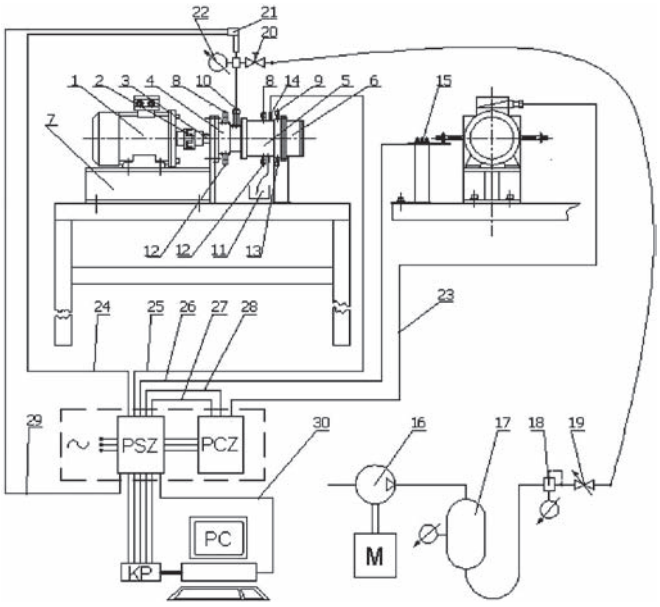

Fig. 2. *Overall view and schematic diagram of the control-measurement system of the stand for testing MF seals.* ***Notation*** *: **1** – driving motor, **2** – clutch, **3** – rotating shaft, **4** – casing of shaft bearings, **5** – pivotable casing of head's bearings, **6** – testing head's casing, **7** – testing stand's basement, **8** – inlet sockets of cooling system of shaft seals, **9** – inlet socket for cooling medium of the tested MF seal, **10** – compressed air supply socket, **11** – tank for leaks from the testing head, **12** – outlet sockets of cooling system of shaft seals, **13** – outlet socket for cooling medium of the tested MF seal, **14** – temperature gauge, **15** – extensometric beam for torque measuring, **16** – air compressor, **17** – compressed air tank, **18** – reducing valve, **19** – flow control valve, **20** – cut-off valve, **21** – pressure transducer, **22** – manometer, **23** – electric supply for driving motor, **24**, **25**, **26**, **27**, **28** – measuring lines for pressure, temperature, torque, rotational speed and power, **29**, **30** – electric supply of pressure transducer and computer measurement system, **PSZ** – control-supply panel, **PCZ** – frequency converter, **KP** – measurement chart.*

The testing stand is fitted with Pt 100 temperature gauge (14) for measuring magnetic fluid temperature in the seal, and the extensometric beam (15) for measuring the seal's anti-torque.

Rotational speed of the driving motor (1) is controlled by means of the frequency converter PCZ which makes it possible to measure rotational speed of the driving shaft and power absorbed by the driving motor.

Signals of pressure, temperature, torque, rotational speed and absorbed power are conducted through the measuring lines 24, 25, 26, 27 and 28 to the control- supply panel PSZ, and next to the five-channel measuring chart KP, of PCIA –71B type, cooperating with the PC by means of the ADVANTECH GENIE software of 2.12version.

MAGNETIC MATERIALS USED IN THE RESEARCH

In the previously conducted tests [4] dealing with the seal of version A (Fig. 2) the C2- 40M magnetic fluid produced in Russia, was used.

In the research on the seals of B and C version the BM-30 magnetic fluid, also of Russian origin, was applied.

In Tab. 1 the basic properties of the fluids are presented.

Magnetic field in the sealing system was generated by means of the set of permanent magnet discs. In the tests of the seal of A version (Fig. 2) samarium – cobalt (Sm-Co) alloy magnets were used, and to that of version B and C - neodymium (Nd)magnets.

Tab. 2 presents full characteristics of the permanent magnets used in the tests.

Tab.1. Characteristics of magnetic fluids used in the research on MF seals working in water.

Kind of fluid	C2-40M	BM-30
Basic fluid	Silicon fluid	Mineral oil
Magnetic particles	Magnetite : Fe_3O_4	Magnetite: Fe_3O_4
Density ρ [g/ml]	1.414	1.345
Magnetization saturation M_s [kA/m]	39.1	37.5
Plastic viscosity at 20°C, η_{pl} [Pa s]	0.520	0.386

Tab. 2. Basic properties and dimensions of the magnets used for the tests of MF seals in liquid environment

Magnetic material	Sm-Co alloy	Neodymium N38
Residual magnetic inductance B_r [T]	0.77	1.23
Coercive force H_c [kA/m]	540	912
Maximum energy density $(BH)_{max}$ [kJ/m^3]	55	294
Maximum working temperature [°C]	250	150
Dimensions of a single magnet [mm]	Φ16x5	Φ15x5

The remaining elements of the magnetic core, i.e. pole shoes and sleeves fitted with sealing lips, were made of a low-carbon steel of good magnetic properties.

DESIGN, GEOMETRICAL AND TESTING PARAMETERS OF THE SEALS

In Fig. 3 are shown details of geometry and design solutions applied to various versions of the tested seals.

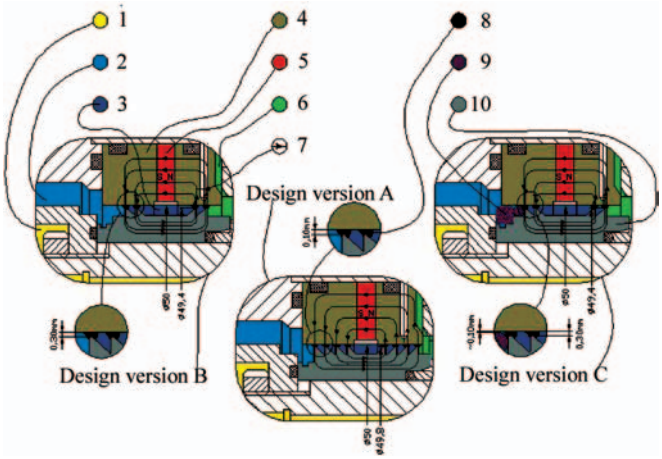

Fig. 3. *Geometry of sealing lips and construction of seals in various design versions used in the tests. Versions A and B – without protecting rings, version C - fitted with the set of rings protecting MF seal against direct influence of whole amount of water contained in the test chamber.* ***Notation*** *: **1** – zone of compressed air, **2** – zone of water under pressure, **3** – zone of water penetration, **4** – pole shoes, **5** – set of permanent magnets, **6** – zone of leakage, **7** – lines of magnetic force field, **8** – magnetic fluid, **9** – set of rings protecting MF sealing lips, **10** – multi-lip sleeve.*

For all the tests was used the same set of the pole shoes of 50 mm - diameter sealing hole, having the set of permanent magnets inserted between them. In the version A twelve Sm-Co magnets of Φ16mm x 5mm in size, and in the versions B and C twelve Nd magnets of Φ15mm x 5mm, were used (Tab. 2).

In the version A the multi-lip sleeve of 49.8 mm outer diameter and eight sealing lips filled with magnetic fluid, was used. Value of the height of the gap filled with magnetic fluid amounted to 0,1 mm. Such testing system was the subject of the preceding research described in [4].

In design versions B and C the multi-lip sleeve of 49.4 mm diameter and four sealing lips filled with magnetic fluid, was used. Value of the height of the gap filled with magnetic fluid amounted to 0.3 mm. The choice of the number of sealing lips smaller than in the above mentioned tests resulted from the assumed lower value of liquid pressure in the chamber to be sealed, whereas the greater height of the gap with magnetic fluid made operation of the seal in a non-coaxial position of the shaft against the sleeve with pole shoes, possible.

Moreover, in the design version C the set of rings protecting MF seal against direct influence of the whole amount of water contained in the test chamber, was installed from the side of water under pressure, before the first sealing lip. The protecting set was composed of two rubber rings placed in series : one of circular and other of rectangular cross-section. Dimensions of the rings were so selected as to obtain the gap between the outer diameter of the rings and the inner diameter of the pole shoe equal to about 0.10 mm (see relevant detail for the design version C, Fig. 3). Tests of such design solution was aimed at checking the influence of limitation of magnetic fluid contact with the water contained in the chamber on ultimate rotational speed for the seal in question.

In Tab. 3 geometrical parameters of the tested seals are given.

Tab. 3. Geometrical parameters of the tested seals.

Design version	A	B	C
Outer diameter of pole shoes [mm]	50	50	50
Number of sealing lips	8	4	4
Inner diameter of sealing lips [mm]	49.8	49.2	49.2
Height of the gap filled with magnetic fluid [mm]	0.1	0.3	0.3
Outer diameter of protecting rings [mm]	lack	lack	49.8

In the tests of the seals of A version the C2-40M magnetic fluid was used (Tab. 1).

Eight-hour lasting series of the tests were carried out for the following rotational speeds : 125; 250; 500; 750; 1,000; 1500; 2000; 3000 rpm. And, the test was performed of gradual continuous increasing the rotational speed up to the loss of tightness by the sealing unit. All the tests were carried out at the initial water pressure p = 0.15 MPa [4].

In the tests of the seals of B and C versions the BM-30 magnetic fluid was used (Tab. 1). For these seal versions was carried out one long test (lasting for over 200 h) of the sleeve (B version) at constant speed of 3000 rpm, as well as several tests of the sleeve at various rotational speeds within the range from 3000 rpm up to 6000 rpm and for different duration time from a few minutes up to a few dozen hours. For the tests of B and C versions of the seal the initial water pressure of 0.05 MPa was set.

RUN AND RESULTS OF THE TESTS

The way of preparation of the seals to testing, generation of water pressure in the chamber as well as starting and stopping procedures of the test stand are described in [4]. In the tests concerning A version of the seal the test's duration time and water pressure in the chamber was measured and amount of water leaking from the seal was monitored.

The procedures used in the tests of the seals of B and C versions were similar to those applied to the tests of the seals of A version. Also, the above mentioned measurements and observations were carried out, and in majority of the tests also the seal's anti-torque and temperature was measured. During the tests the measured quantities were read and recorded by the computer.

The test results of the particular seal versions are collected in Tab. 4, 5 and 6, for A, B and C seal versions, separately. In the tables are given basic operational parameters of the tests and values of anti-torque and temperature of the seal recorded during the tests. Results of the test run monitoring which concerned leakage quantity and changeability are also attached.

In the diagrams (Fig. 4 and 5) is presented comparison of changes of anti-torque and temperature of the seals of B and C versions operating in similar conditions during 2 h period.

In Tab. 4 are given parameters of the tests of seal of A version as well as results of the tests in the form of either occurrence of leakage or lack of it. The tests were aimed at checking correctness of the design concept of the test head and preliminary testing the MF seal's operation in water. The seal operated correctly during several-hour tests at various rotational speeds. Lack of its tightness appeared in the last test at the rotational speed of 6800 rpm (the circumferential speed of 17.80 m/s).

In Tab. 5 parameters of the tests of the seal of B version are given. In the tests the sleeve fitted with four sealing lips and of 0.3 mm gap height was applied. The cycle of tests was aimed at checking the operational effectiveness of the seal during a longer time period at the rotational speed of 3000 rpm commonly used in industrial practice, as well as at determining the rotational speed range leading to loss of tightness.

In the tests was used the BM-30 magnetic fluid based on mineral oil (Tab.1), other than that previously applied.

Tab. 4. *Parameters and results of the tests of the MF seal of A version. Magnetic fluid : C2-40M (Tab.1). Number of sealing lips : 8. Height of the gap filled with magnetic fluid : 0.10mm. Water pressure in the test chamber : 0.15 MPa.*

No. of test	Rotational speed [rpm]	Circum-ferential speed [m/s]	Duration time [h]	Comments / Leakage
A1	125	0.33	8.0	Replacement of MF / No leakage
A2	250	0.65	8.0	No replacement of MF / No leakage
A3	500	1.31	8.0	No replacement of MF / No leakage
A4	750	1.96	8.0	No replacement of MF / No leakage
A5	1000	2.62	8.0	No replacement of MF / No leakage
A6	1500	3.93	8.0	No replacement of MF / No leakage
A7	2000	5.24	8.0	No replacement of MF / No leakage
A8	3000	7.85	8.0	No replacement of MF / No leakage
A9	Uniformly increasing from 0 up to 6800	Uniformly increasing from 0 up to 17.80	0.30	No replacement of MF / Sudden leakage at 6800 rpm

Tab. 5. *Parameters and results of the tests of the MF seal of B version. Magnetic fluid : BM-30 (Tab.1). Number of sealing lips : 4. Height of the gap filled with magnetic fluid : 0.30 mm. Water pressure in the test chamber : 0.05 MPa.*

No. of test	Rotational speed, [rpm]	Circumferential speed, [m/s]	Testing time, [h]	Anti-torque, [Nm]		Temper. [°C]		Comments/ Leakage
				Initial	Final	Initial	Final	
B1	3000	7.85	201	Not measured		Not measured		Replacement of MF / No leakage
B2	4000	10.47	1.5	Not measured		Not measured		No replacement of MF / After 62 min. of tests – a leakage increasing from 2 drops per minute to continuous flow
B3	4000	10.47	0.25	Not measured		Not measured		Replacement of MF / After 2 min. of test –permanent leakage from 2 to 4 drops per minute
B4	3000	7.85	66	0.130	0.090	21	52	No replacement of MF / No leakage
B5	3500	9.16	0.10	Changing within the range from 0.140 to 0.06		22	56	No replacement of MF / After 1 min of test –permanent leakage from 1 to 2 drops per minute
	3000	7.85	5.00					Decrease of rotational speed – no leakage
	4000	10.47	0.25					Increase of rotational speed – a leakage of about 8 drops per minute

In the test carried out at the constant rotational speed of 3000 rpm for 201 h period (the test B1) no leaks were observed. They appeared in the tests B2 and B3 carried out at the rotational speed of 4000 rpm. In the test B2 carried out without replacement of the magnetic fluid used in the preceding test, extensive leakage occurred after one - hour operation, whereas in the case of the test B3 performed with the use of the replaced magnetic fluid a permanent but small leakage occurred just after starting the test, hence it was terminated after about 15 minutes of the seal's operation.

Interesting, that in the test B4 performed at the rotational speed of 3000 rpm without any replacement of the magnetic fluid used in the preceding test no leakage was observed for all the testing period of 66 h. After about 2 h the anti-torque value reached about 0,09 Nm, and the seal's temperature value – about 52°C. The values maintained constant up to the termination of the test.

The test B5 was carried out at various rotational speeds changeable during the test. The first symptoms of leakage was observed at the rotational speed value of about 3500 rpm.

In Tab. 6 are presented parameters and results of the tests of MF seal of C version, in which the additional set of rings protecting the seal against direct influence of the whole amount of water contained in the test chamber (Fig. 3, seal version C).

In majority of the tests performed in the series a significant increase of temperature of magnetic fluid in the seal occurred. The temperature increase was often accompanied by the increase of anti-torque of the seal, similar to that observed during the tests C1, C2, C5 and C6. In the range of the rotational speeds up to 4800 rpm (12.57 m/s) no leakage was observed. Attention should be paid to the relatively short duration time of the tests of the series, resulting from the increasing of the seal's temperature. In the test C6 performed at the rotational speed of 5400 rpm a small leakage was observed, and it was very intensive in the test C7 carried out at the rotational speed of 6000 rpm.

Tab. 6. *Parameters and results of the tests of the MF seal of C version fitted with an additional set of rings protecting the MF seal. Magnetic fluid : BM-30 (Tab.1). Number of sealing lips : 4. Height of the gap filled with magnetic fluid : 0.30 mm. Height of the gap of protecting rings : 0.10 mm. Water pressure in the test chamber : 0.05 MPa.*

In Fig. 4 are shown changes of seal anti-torque for two hours of testing the seals of B and C versions (Fig. 3) working in similar conditions. The anti-torque changes of B version of the seal are similar to those obtained during the tests of the seal in gaseous environment [5]. It can be observed that the anti-torque of the C version of the seal fitted with the additional protecting set of sealing rings is much greater than that of its B version without the additional elements.

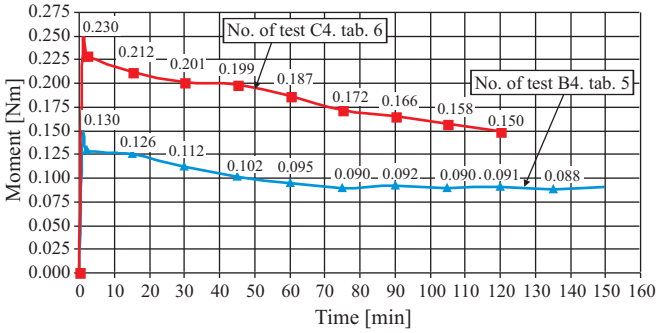

Fig. 4. *Changes of anti-torque of the tested MF seals in B version – without protecting rings, and in C version – with additional protecting rings, recorded during two hours of the test.*

In Fig. 5 are shown changes of seal temperature during two hours of testing the seals of B and C versions (Fig. 3) working in similar conditions. It can be observed that temperature of

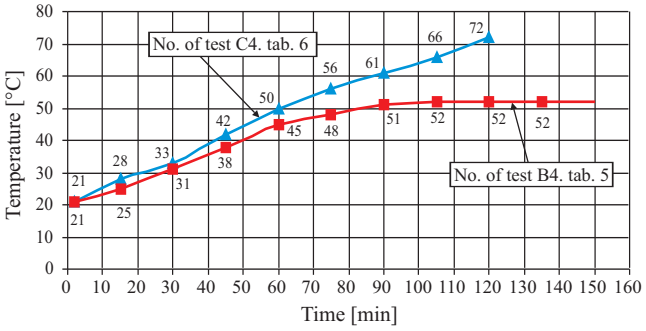

Fig. 5. *Temperature changes of the tested MF seals of B version – without protecting rings, and of C version – with additional protecting rings, recorded during two hours of the test.*

No. of test	Rotational speed. [rpm]	Circumferential speed. [m/s]	Testing time. [h]	Anti-torque. [Nm]		Temper. [°C]		Comments/ Leakage
				initial	final	initial	final	
C1	4000	10.47	2.30	0.128	0.500	23	78	Replacement of MF. Sudden increase of temperature and anti-torque / No leakage
C2	4000	10.47	1.70	0.140	0.500	23	70	No replacement of MF. Sudden increase of temperature and anti-torque / No leakage
C3	4200	11.00	0.80	0.150	0.220	23	70	No replacement of MF. Sudden increase of temperature and anti-torque / No leakage
C4	3000	7.85	2.00	0.230	0.150	21	72	Replacement of MF/ No leakage.
C5	4800	12.57	0.45	0.190	0.501	23	71	No replacement of MF. Changeable anti-torque; its sudden increase within the last min./ No leakage
C6	5400	14.14	0.50	0.175	0.320	27	75	No replacement of MF. Stable anti-torque; its sudden increase within the last 30 sec / Total leakage : 5 drops.
C7	6000	15.71	0.07	0.180	0.150	23	28	No replacement of MF / Dropping leakage evolving to continuous flow.
C8	4200	11.00	1.00	0.200	0.150	23	60	Replacement of MF/ No leakage.
C9	4800	12.57	3.50	0.170	0.090	22	75	No replacement of MF / Sudden leakage of 14 drops within 4-th min.; no leakage up to the end of the test.
C10	5400	14.14	1.17	0.150	0.077	23	73	No replacement of MF / After one minute – a leakage increasing to 11 drops per minute at the end of the test.

the seal of C version fitted with the additional protecting set of sealing rings, was continuously increasing, and that of the seal of B version without any protecting elements, became stable on the level of 52°C.

FINAL REMARKS

- The presented results of the tests of the seal of 50 mm diameter at 3000 rpm rotational speed show that MF seal can effectively work for a long time in water, at geometrical and operational parameters usually met in industrial devices.

- Loss of tightness of MF seal working in liquid occurs after exceeding a determined value of seal's rotational speed at which the sealed fluid starts penetrating through the sealing magnetic fluid. The performed tests indicate that the process of loss of tightness can be reversible. A decrease of rotational speed makes tightness of the system recovered.

- Application of a simple set of rings protecting MF seal resulted in the distinct increase (by about 1000 rpm) of the speed at which leakage occurred. It shows that it is possible to increase limiting values of geometrical and operational parameters of MF seals working in water by applying appropriate design solutions.

- However attention should be paid to the fact that in all the tests the application of the protecting set of sealing rings resulted in fast increase of seal's temperature. As the correct work temperature of magnetic fluids is limited to about 100°C a research to disclose causes of the phenomenon and its consequences should be undertaken.

NOMENCLATURE

MF - Magnetic Fluid Seals
FF - Ferro Fluidic Seals

BIBLIOGRAPHY

1. B. M. Berkovsky: *Magnetic fluids engineering applications*, Oxford University Press, Oxford-New York-Tokyo,1993.
2. Z. Szydło, W. Ochoński, B. Zachara: *Experiments on magnetic fluid rotary seals operating under vacuum conditions*, Tribotest Journal, 2005 vol. 11 no. 4.

J. Kurfess, H.K. Müller: *Sealing Liquids with Magnetic Fluids,* Journal of Magnetism and Magnetic Materials 85, 1990.

3. Z. Szydło, L. Matuszewski: *Ring driving unit – preliminary investigations on optimization of ferro-fluidal seals and drives* (in Polish).
4. W. Ochoński, Z. Szydlo, B. Zachara: *Experimental study of frictional characteristics of magnetic fluid shaft seals*, Proc. Int. Tribology Conf., Nagasaki, Japan (2000)

CONTACT WITH THE AUTHORS

Leszek Matuszewski, Ph. D.
Faculty of Ocean Engineering
and Ship Technology
Gdansk University of Technology
Narutowicza 11/12
80-952 Gdansk, POLAND
e-mail : leszekma@pg.gda.pl

Zbigniew Szydło, Ph. D.
AGH University of Science and Technology
Al. Mickiewicza 30
30-059 Kraków, POLAND
e-mail : zszydlo@uci.agh.edu.pl


Photo: Cezary Spigarski

POLISH MARITIME RESEARCH 4(54) 2007 Vol 14; pp. 59-63
DOI: 10.2478/v10012-007-0041-x

An analysis of lubricating medium flow through unsymmetrical lubricating gap of conical slide bearing

Mariusz Koprowski,
Gdynia Maritime University

ABSTRACT

This paper presents a computer analysis of lubricating medium flow through unsymmetrical lubricating gap of conical slide bearing. Numerical calculations were carried out with the use of the software Matlab 7.1 and Mathematica 5.2 for example conical slide bearings of different values of cone apex angles of pin and sleeve and set values of relative eccentricity and skewing angle as well as dimensionless bearing length equal to 1.

Keywords : unsymmetrical lubricating gap, conical slide bearing, numerical calculations, hydrodynamic pressure distribution, load carrying capacity

INTRODUCTION

Conical bearings were considered as sliding friction units by the following authors: [1, 3, 4, 6, 7, 11, 13, 15]. In the literature sources [4, 6, 11, 13, 15] a simplified one-dimensional theoretical flow model of oil as lubricating medium in gap of conical slide bearings was considered. The papers [1] and [7] dealt with gas lubrication of conical slide bearings. In all the above mentioned papers their authors assumed axially symmetrical flow of lubricating medium. Such assumption is a rough simplification of real lubrication conditions as it does not take into account two crucial facts. Firstly, cones of the pin and sleeve forming the conical bearing can have different values of apex angle. Secondly, a skewing of the pin within the sleeve may occur as a result of their non-parallel axes. The skewing results from inaccuracy of machining and assembling operations or deformation of sleeve and pin due to mechanical and thermal loading. In the opinion of this author the facts should not be neglected in analysing the lubrication process of conical slide bearings as they significantly impact the lubricating medium flow through the gap of slide bearing, which changes this way its operational parameters.

In the presented lubricating gap model a novelty is the taking into consideration of the above mentioned aspects. Moreover, the presented mathematical models concerning lubrication analysis of conical slide bearings make it possible to directly pass from the elaborated model of conical slide bearings to the known models of cylindrical journal slide bearings.

GEOMETRICAL AND MATHEMATICAL MODEL OF LUBRICATING GAP

Fig. 1 presents geometry of the conical slide bearing considered in this paper, where the pin and sleeve axes are inclined to each other by the angle υ and the pin and sleeve centres are shifted by the bearing eccentricity e. The angles γ and γ_1 are the inclination angles of generatrices of pin and sleeve cones.

In order to prevent contact of metal surfaces of pin and sleeve and resulting seizure of the bearing the following condition is to be satisfied : $\gamma - \gamma_1 \geq 0$

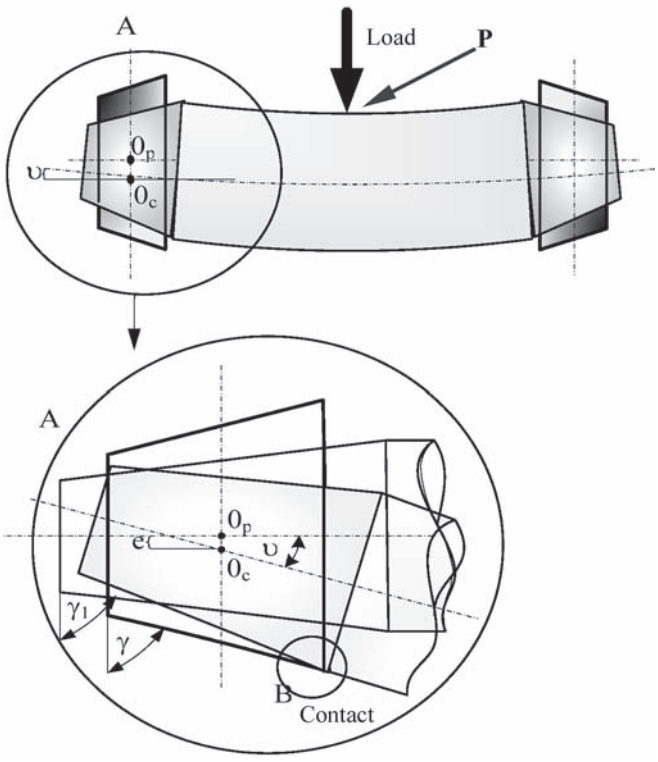

Fig. 1. *Geometrical model of conical slide bearing,* ***υ*** *[0°] – skewing angle,* O_p, O_c *– centres of sleeve and pin, respectively, e [m] – bearing eccentricity*

The skewing shown in Fig. 1 results from the applied load P. Fig. 1 simultaneously serves as a graphical illustration of the considered model of conical slide bearing. In the model the axis

skewing angle occurs in the plane consisting the centre line of pin and sleeve. The point B (Fig. 1) is the theoretical contact point of pin and sleeve. Simultaneously, its position determines the maximum value of skewing angle of a given bearing.

The dimensional equation which describes the lubricating gap in the conical slide bearing and takes into consideration the skewing of the sleeve as well as that the pin and sleeve cones forming the bearing can have different values of cone apex angles, is expressed as follows :

$$h(\varphi, x, \gamma, \gamma_1, \upsilon) = c(1+\lambda\cos\varphi)\Gamma + \\ + x(tg\upsilon)(\cos\varphi) + (x+L)\sin(\gamma-\gamma_1) \quad (1)$$

where :
c [m] – radial clearance
$\Gamma = 1/\sin(\gamma)$, $0 \le \gamma \le \pi$
$\lambda = e/c$ [–] – relative eccentricity
φ, x – conical coordinates
L [m] – half-length of the pin cone generatrix.

To generalize the equation (1) which describes gap height change the relationships connecting together dimensionless and dimensional quantities are assumed as follows:

$$h_1 = \frac{h}{c} \; ; \; L_1 = \frac{L}{R_0} \; ; \; x = L\,x_1 = L_1 R_0 x_1 \quad (2)$$

where:
L_1[-] – dimensionless length of bearing,
x_1 – dimensionless conical coordinate,
R_0 [m] – radius measured along the coordinate x at the half-height of pin cone.

On insertion of the relations (2) into the equation (1) which describes the gap-height change the following dimensionless form of the gap height is obtained:

$$h(\varphi, x_1, \gamma, \gamma_1, \upsilon) = \underbrace{(1+\lambda\cos\varphi)\Gamma}_{1} + \\ + \underbrace{\Psi L_1 x_1 \cos\varphi}_{2} + \underbrace{Y L_1 x_1}_{3} \quad (3)$$

where:
$\Psi \equiv (tg\,\upsilon)/\psi$, $0 \le \Psi \le 1$, $\gamma \equiv [\sin(\gamma - \gamma_1)]/\psi$, $0 \le \gamma \le 1$,
$\Gamma = 1/\sin\gamma$, $\gamma \ne 0$, $\psi = c/R_0$, $\psi \approx 0.001$

The gap model (3) can be compared with that of the slide bearing whose pin and sleeve surfaces are assumed perfectly smooth and stiff. Also, deformations of bearing surfaces, which result from oil pressure and temperature , are not taken into consideration.

The term 1 of the gap-height mathematical model (3) for Γ=1 describes the lubricating gap relevant for typical journal slide bearings in the case when the inclination angles of pin and sleeve generatrices against the vertical are equal to 90º

If value of the angle is less than 90º the term describes the gap of the journal bearing whose pin is skewed. The term 2 determines influence of the skewing angle on the lubricating gap height in the conical slide bearing (Fig. 3a). If the angle $\upsilon = 0$ then $\Psi = 0$ and in consequence the term equals zero. The term 3 of the lubricating gap equation (3) describes solely influence of the cone apex angles of pin and sleeve on the lubricating gap height in conical slide bearing. If the angles γ and γ_1 are equal to each other then the term equals zero and the lubricating gap height is constant along the coordinate x_1.

Fig. 2 and 3 graphically illustrate changes of lubricating gap height of conical slide bearing, depending on the relative eccentricity λ, the pin skewing angle υ against the sleeve axis, and different values of the inclination angles γ and γ_1 against the vertical, of generatrices of pin and sleeve cones.

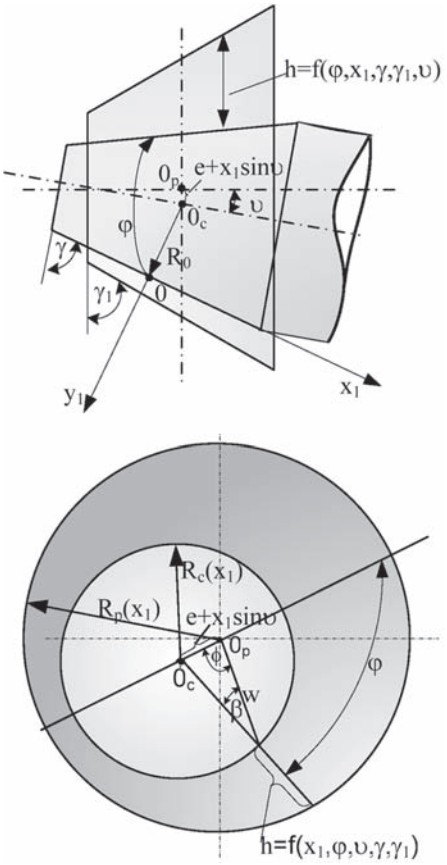

Fig. 2. *Geometrical model of conical slide bearing in the conical coordinate frame:* ***a)*** *Longitudinal cross-section,* ***b)*** *Transverse cross-section;* ***0*** *– the centre of the coordinate frame;* $\boldsymbol{R_0}$ *– pin radius measured in the point 0 ;* $\boldsymbol{\varphi}$, $\boldsymbol{\beta}$ *– auxiliary angles ;* $\boldsymbol{R_p(x_1)}$, $\boldsymbol{R_c(x_1)}$ *– sleeve and pin radiuses in function of the coordinate* $\boldsymbol{x_1}$ **.**

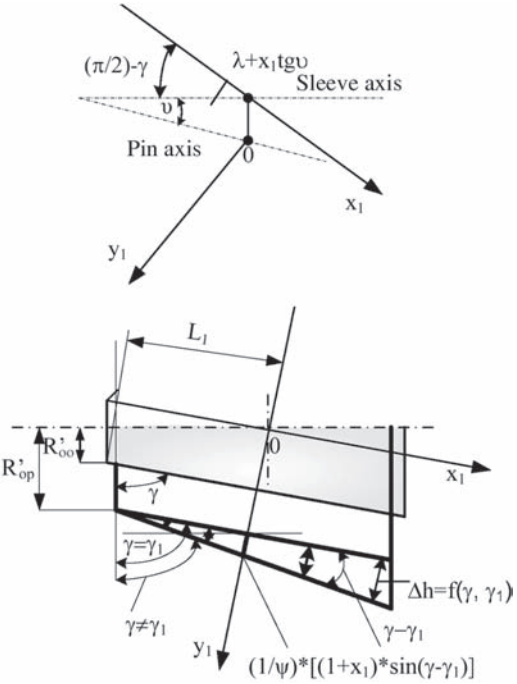

Fig. 3. *Details of the angles appearing in the conical slide bearing :* ***a)*** *influence of the skewing angle on the lubricating gap;* ***b)*** *influence of the apex angles of generatrices of pin and sleeve cones on the lubricating gap;* $\boldsymbol{\Delta h}$ *– lubricating gap increase due to difference of the pin and sleeve apex angles ;* $\boldsymbol{R'_{oc}}$, $\boldsymbol{R'_{op}}$ *– pin and sleeve radiuses measured in the cut-off places of the cones.*

ANALYSIS OF SKEWING IN THE LUBRICATING GAP MODEL

Allowable values of the skewing angle υ (Fig. 2) of the pin and sleeve axes in conical slide bearing depend on values of the relative eccentricity λ and the pin and sleeve cone apex angles. The limit value of the skewing angle υ at which metal-to-metal contact of the pin and sleeve occurs in the bearing (Fig. 1), can be determined by using the following expression :

$$\upsilon = \operatorname{arctg}\left\{\frac{\psi}{L_1}\Gamma[(1-\lambda)+2Y\sin\gamma]\right\} \qquad (4)$$

where:

$$\Gamma = 1/\sin\gamma\ ,\ \gamma \neq 0\ ,\ \Psi \equiv [\sin(\gamma - \gamma_1)]/\psi$$

To check correctness of the mathematical model of lubricating gap , (3) , as well as the expression (4) a computer analysis was performed by means of the software Mathematica 5.0. The simulation was carried out for several selected values of the eccentricity λ, angles γ, γ_1 and skewing angle υ. The calculated results of gap changes , obtained this way are graphically presented in Fig. 4. The limit values of the skewing angle υ for the assumed values of the parameters λ, γ and γ_1 are presented in Tab. 1.

Tab. 1. *Values of the pin skewing angle in the conical slide bearing, determined from the formula (4) for the assumed values of the slide bearing parameters*

No.	λ [-]	γ [°]	γ_1 [°]	γ - γ_1 [°]	υ [°]
1.	0.2	90	90	0	0.0458366
2.	0.2	88.2	88.2	0	0.0458584
3.	0.4	87.37	86.5	0	0.0344135
4.	0.4	87.37	86.49	0.01	0.0544135
5.	0.6	86.53	86.53	0	0.0229602
6.	0.6	86.53	86.529	0.01	0.0429602
7.	0.8	85.71	85.71	0	0.0114913
8.	0.8	85.71	85.70	0.01	0.0314913

LOAD CARRYING CAPACITY OF SLIDE BEARING

Apart from friction force and friction coefficient, load carrying capacity is the main parameter which characterizes operational features of slide bearings. To determine slide bearing's capacity it is necessary to analyze equilibrium conditions of normal and tangential forces acting within oil film (Fig. 5).

According to the notation used in Fig. 5 and the known definitions of bearing capacity forces [2], [5] the following expressions for the capacity force components can be given:

- The dimensionless transverse component of capacity force, C_{1p} :

$$C_{1p} = \sqrt{C_{1pX}^2 + C_{1pY}^2} \qquad (5)$$

where:

$$C_{1pX} = \int_{-1}^{+1}\int_{0}^{\varphi_k} p_1 \cos\varphi \sin(\gamma - \upsilon)\, d\varphi dx_1 \qquad (6)$$

$$C_{1pY} = \int_{-1}^{+1}\int_{0}^{\varphi_k} p_1 \sin\varphi \sin(\gamma - \upsilon)\, d\varphi dx_1 \qquad (7)$$

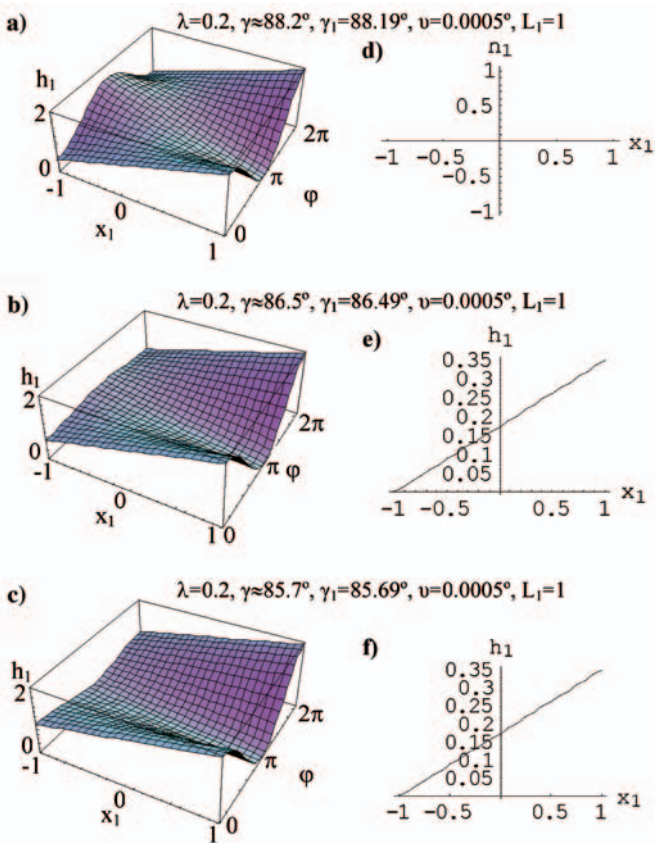

Fig. 4. *Lubricating gap changes in conical slide bearing for several values of the relative eccentricity λ ;* ***a), b), c)*** *– developed view of the gap height,* ***d), e), f)*** *– increase of the lubricating gap height due to difference of the angles γ and γ_1.*

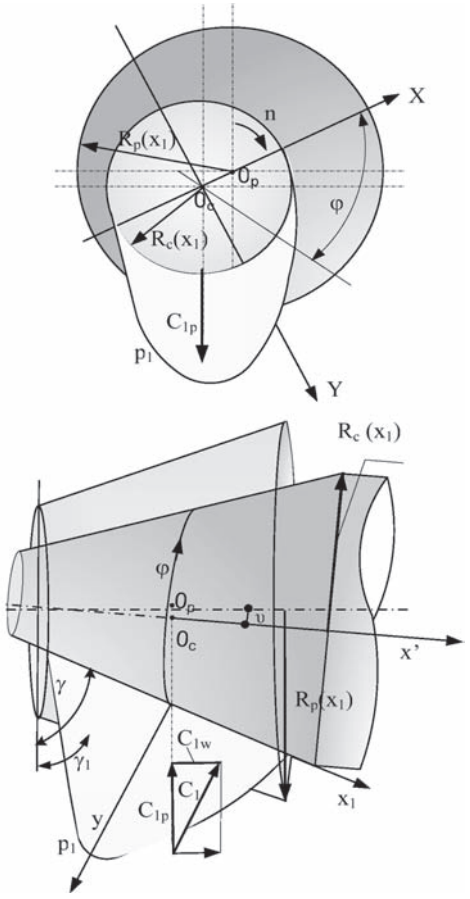

Fig. 5. *Schematic diagram of position of resultant capacity force in conical slide bearing ;* C_{1p} *- dimensionless transverse component of capacity force ;* C_{1w} *- dimensionless longitudinal component of capacity force .*

➢ The dimensionless longitudinal component of capacity force, C_{1w}:

$$C_{1w} = \sqrt{C_{1wX}^2 + C_{1wY}^2} \tag{8}$$

where:

$$C_{1wX} = \int_{-1}^{+1}\int_{0}^{\varphi_k} p_1 \cos\varphi \sin(\gamma - \upsilon)\, d\varphi dx_1 \tag{9}$$

$$C_{1wY} = \int_{-1}^{+1}\int_{0}^{\varphi_k} p_1 \sin\varphi \sin(\gamma - \upsilon)\, d\varphi dx_1 \tag{10}$$

The total (resultant) capacity force of conical slide bearing, C_1 , is the geometrical sum of the transverse force C_{1p} and longitudinal force C_{1w}:

$$C_1 = \sqrt{C_{1p}^2 + C_{1w}^2} \tag{11}$$

And, values of the forces C_{1p} i C_{1w} depend on the pin cone apex angle, skewing angle and hydrodynamic pressure.

To determine the total force C_1 (11) of a given bearing it is necessary to know value of the dimensionless hydrodynamic pressure p_1 which can be determined from the following formula [9]:

$$\frac{1}{U_1^2}\frac{\partial}{\partial\varphi}\left(\frac{h_1^3}{\eta_1}\frac{\partial p_1}{\partial\varphi}\right) + \frac{1}{L_1^2}\frac{\partial}{\partial x_1}\left(\frac{h_1^3}{\eta_1}\frac{\partial p_1}{\partial x_1}\right) = 6U_1\frac{\partial h_1}{\partial\varphi} \tag{12}$$

where:

$$U1 = L1(1 + x1)\cos\gamma$$

The differential equation (12) obtained by imposing relevant boundary conditions on the transverse component of velocity vector (measured perpendicularly to pin's conical surface) in the set of fundamental equations describes lubricating medium flow through the conical slide bearing gap [9].

Values of the distribution of the hydrodynamic pressure p_1 and the capacity force C_1 were numerically calculated by means of the software MATLAB 7.1 [8, 10]. The calculations were based on the finite differences method and the author's calculation procedures. The example calculation results of the hydrodynamic pressure distribution for the relative eccentricity $\lambda = 0.2$ are presented in Fig. 6, where Fig. 6a) shows hydrodynamic pressure changes within the journal slide bearing gap, and Figs. 6 b,c present the pressure distribution within the journal slide bearing gap. Fig. 7 presents changes of the capacity force C_1 in function of the relative eccentricity λ for several selected values of the cone apex angles of pin and sleeve at a constant value of the skewing angle υ.

FINAL REMARKS AND CONCLUSIONS

- From Fig. 1 and the numerical calculation results it can be observed that the pin skewing in the conical slide bearing sleeve leads to concentration of pressure, especially on its edge. The greater values of the skewing angle υ , the relative eccentricity λ and the difference of the cone apex angles γ and γ_1 (for conical slide bearings), the greater pressure in question.
- The presented mathematical model of lubricating gap (3) is general as it determines the lubricating gap of both the conical slide bearings and journal slide bearings (when the angles γ and γ_1 are assumed equal 90°) (Fig. 6 and 7).

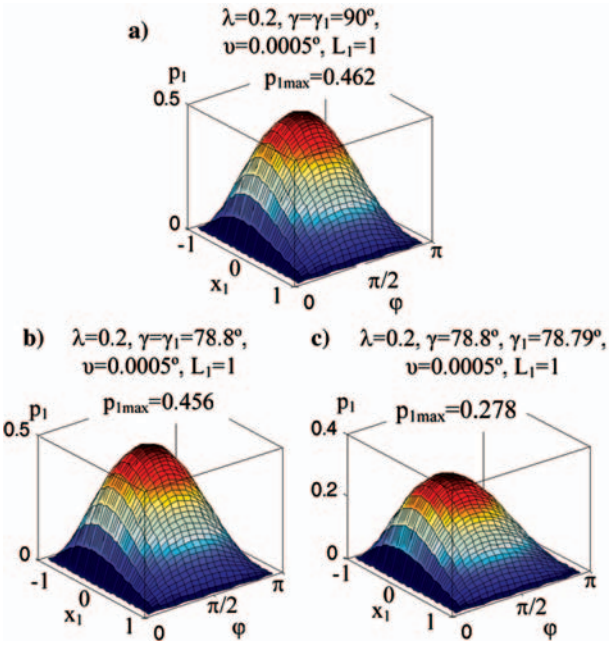

Fig. 6. *Pressure distribution in slide bearing:* ***a)*** *journal one;* ***b), c)*** *– conical one.*

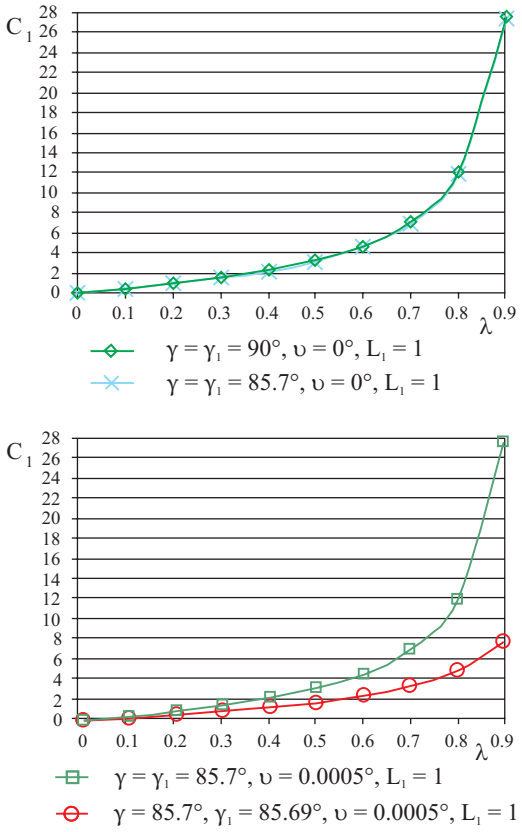

Fig. 7. *Diagram of changing values of the total capacity force C_1 in slide bearing*

- The data presented in Tab. 1 show that the conical slide bearings having an unsymmetrical lubricating gap ($\gamma - \gamma_1$) make greater limit values of the skewing angles υ acceptable as compared with those for conical slide bearings having symmetrical gap constant along the gearing ($\gamma - \gamma_1$). The phenomenon results from an additional increase of lubricating gap height by the value Δh (Fig. 3) resulting from difference of the angles γ andγ_1.
- Fig. 6 shows that the hydrodynamic pressure distribution within journal slide bearings s well as conical ones having the gap symmetrical and constant along the bearing take

similar values at the same relative eccentricity λ. Increasing difference of the cone apex angles of pin and sleeve results in decreasing the pressure p_1 within conical slide bearings (Fig. 6 c). The phenomenon is associated with a suction action of conical pin rotating within the bearing exerted onto lubricating medium flowing through the gap.

- From the diagram of lifting forces (Fig. 7) it results that the load carrying capacity of conical slide bearings significantly decreases along with increasing the difference of the cone apex angles of pin and sleeve.

NOMENCLATURE

$c = R_p - R_c$ – radial clearance [m]
C_1 – dimensionless value of slide bearing capacity force [-]
C_{1p} – dimensionless value of transverse component of slide bearing capacity force [-]
C_{1pX} – dimensionless value of transverse component of slide bearing capacity force along X - direction [-]
C_{1pY} – dimensionless value of transverse component of slide bearing capacity force along Y- direction [-]
C_{1w} – dimensionless value of longitudinal component of slide bearing capacity force [-]
C_{1wX} – dimensionless value of longitudinal component of slide bearing capacity force along X - direction [-]
C_{1wY} – dimensionless value of longitudinal component of slide bearing capacity force along Y - direction [-]
$e = O_p - O_c$ – eccentricity [m]
h – dimensional value of lubricating gap height [m]
h_1 – dimensionless value of lubricating gap height [-]
L – dimensional value of slide bearing length [m]
$L_1 = L/R_o$ – dimensionless value of slide bearing length [-]
O_c – pin centre
O_p – sleeve centre
p_1 – dimensionless value of hydrodynamic pressure in bearing gap [-]
p_o – characteristic value of hydrodynamic pressure [MPa]
$R_ş$ – radius of slide bearing pin [m]
R'_{oc} – pin radius measured at the cut of slide bearing cone [m]
R'_{op} – sleeve radius measured at the cut of slide bearing sleeve cone [m]
R_0 – pin radius measured at the height of the assumed centre of coordinate frame [m]
R_p – radius of slide bearing sleeve [m]
$U_1 = L_1(1 + x_1)\cos\gamma$ – dimensional value of circumferential velocity of pin [-]
X, Y – coordinates of auxiliary coordinate frame
$Y \equiv [\sin(\gamma - \gamma_1)]/\psi$

φ, y_1, x_1 – dimensionless conical coordinates
φ, y, x – conical coordinates
γ – vertical slope angle of generatrix of bearing pin cone [º]
γ_1 – vertical slope angle of generatrix of bearing sleeve cone [º]
$\Gamma = 1/\sin\gamma$
$\lambda = e/c$ – relative eccentricity [-]
η_1 – dimensionless value of oil dynamic viscosity [-]
η_o – characteristic value of oil dynamic viscosity [Pas]
υ – skewing angle of pin axis relative to sleeve axis [º]
ω – angular velocity of pin [1/s]
ψ – dimensionless value of the ratio $R_o/c \approx 0.001$.

BIBLIOGRAPHY

1. Apanasewicz S., Kazimierski Z., Lewandowski J, Szaniewski A.: *The flow of the gas layer between two conical surfaces.* Fluid Dynamics Transactions Vol. 5, Part II, PWN, Warszawa 1971
2. Burcan J.: *Bearing of hyperboloidal sleeve* (in Polish). ZEM no. 3-4, 1973
3. Fuller D.D.: *Theory and practice of lubrication* (in Polish). PWT, Warszawa 1960
4. Gottwald I.,Vieveg R.: *Berechnung und Modellversuche an Wasser-und Luftlagern*. Zeit. Angewandte Physik Bd. II, H. 11.1950,
5. Hebda M., Wachal A.: *Tribology* (in Polish). WNT, Warszawa 1980
6. Janiszewski R.: *Theoretical analysis of magneto-hydrodynamic flow of lubricating medium through conical slide bearing* (in Polish). Doctoral thesis, Lublin University of Technology –Mining & Metallurgy Academy (AGH), Kraków 1980
7. Kazimierski Z.: *Unsteady flow in thin layer of viscous gas between two non-coaxial cones* (in Polish). Publ. of Lodz University of Technology, Heat Machines 75, 1972
8. Kazimierski Z.: *Essentials of fluid mechanics and methods of computer simulation of flow* (in Polish). Publ. of Lodz University of Technology, Łódź 2004
9. Koprowski M.: *Hydrodynamic models of lubrication of conical slide bearings in magnetic field* (in Polish). Trybologia no. 3, 2006,
10. Majchrzak E., Mochnacki B.: *Numerical methods. Essentials of theory, practical aspects and algorithms* (in Polish). Publ. of Wrocław University of Technology, 1996
11. Szaniewski A.: *Flow of viscous incompressible liquid through conical slide bearing gap* (in Polish). Publ. of IPP PAN, 15, Warszawa 1970
12. Walicki E.: *Load carrying capacity of conical slide bearing* (in Polish). Scientific Bulletins (Zeszyty Naukowe) no.7, Mechanics and Structures (Mechanika- konstrukcje) 4, Bydgoszcz High School of Engineering (WSI), 1973
13. Wierzcholski K .: *Flow of non - Newtonian power law lubricant through the conical bearing gap*. Acta Mechanica 50, 1984,
14. Wierzcholski K.: *Theory of unconventional lubrication of slide bearings* (in Polish). Publ. of Szczecin University of Technology (Wydawnictwo Uczelniane Politechniki Szczecińskiej), Szczecin, 1995
15. Wierzcholski K., Nowak Z.: *Influence of a temperature dependent lubricant consistency on the capacity of a conical journal bearing*. Proc. of the Congress on Rheology, Acapulco 1984

CONTACT WITH THE AUTHOR

Mariusz Koprowski, Ms. C.
Cathedral of Bases of the Technique,
Gdynia Maritime University
Morska 81/87
81-225 Gdynia, POLAND
e-mail : mkoprows@am.gdynia.pl
tel.: (058) 6901-483

POLISH MARITIME RESEARCH 4(54) 2007 Vol 14; pp. 64-67
DOI: 10.2478/v10012-007-0042-9

The influence of organic polymer on properties of mineral concentrates

Part I

Marzenna Popek,
Gdynia Maritime University

ABSTRACT

The property is evaluated when acceptance for loading of solid bulk cargoes is judged prior to shipment. The liquefaction can be prevented by means of limiting the moisture content of the cargo by introducing the safety margin, regardless of the condition of stresses. It is rational to limit the moisture content of cargoes, which may liquefy, because liquefaction is not liable to occur when the degree of saturation is low, even if the permeability of the material is low. To prevent sliding and shifting of ore concentrates in storage biodegradable thermoplastic materials were added to the ore. The polymer absorbs water from the particle pore in mineral concentrates and its moisture content goes down. In consequence, polymer prevents: drainage of water from the particle pore, sliding and shifting of ore concentrates in storage.

Keywords: polymer, mineral, water, cargo

INTRODUCTION

Liquefaction is a phase transition of initially solid, but water–saturated, loosely packed granular material into a liquid. The coupled processes which take place in fluid–saturated granular material lead to liquefaction.

The following chain of events can describe the liquefaction process. When the cyclic load is applied to such material, particles of the material may move in microscopic scale. The deformation of the mineral concentrates leads to a change in the pore space. During liquefaction the pore space generally decreases. The reduction of the pore space leads to an increased pore pressure. If the fluid cannot migrate the increase in the pore pressure follows from the pore fluid compression due to reduction of the pore volume. However, the fluid migration associated with drainage reduces in general the maximum values of the pore pressure. The increased pore pressure reduces shear stress the grains can support, and leads to a reduction of their elastic shear strength [1, 2].

Shear strength of granular materials is maintained by friction force between particles and by cohesion. Friction force is a product of effective compressive force between particles and friction coefficient. When pressure of water in void becomes high then effective compressive force between particles becomes small. In such cases, if the cohesion is negligible, shear strength of the granular material becomes very low and the material flows.

Many factors influence liquefaction of solid bulk cargoes under dynamic sea loading. One of them is the property of the cargo which contains moisture.

The moisture content which allows for passing the bulk cargoes from solid into liquid state, is called critical. One of its possible measures is the *Flow Moisture Point –FMP.*

Chapter VI of the SOLAS Convention requires that "cargoes which may liquefy shall only be accepted for loading when the actual moisture content of the cargo is less then its *Transportable Moisture Content*" [3].

Large group of organic polymers is used in mineral industry to fulfil specific functions such as depressants, dispersants or flocculent [4]. Organic polymers can be used in a wide range. These polymers can be used as absorbers of water from mineral concentrates before their transportation by sea. Particularly attractive are the new materials based on natural renewable resources, which prevent from further impact on the environment.

In this work the results of investigation on possible using new biodegradable thermoplastic materials, are presented. To prevent the sliding and shifting of ore concentrates in storage, biodegradable thermoplastic materials are added to the ore. The used materials are based on starch. Y Class polymer is composed of starch and natural cellulose. Starch can be destructurized and compatibilized with different synthetic polymers such as polycaprolactone (Z Class polymer) [5]. The polymers are hydrophilic, tend to absorb moisture and prevent drainage of water from the ore particle pores. Cellulose is one of those polymers which has been used in many applications. Starch is an inexpensive abundant product available annually from corn and other crops. It is totally biodegradable in many environments and makes development of totally degradable products possible.

EXPERIMENTAL TESTS

Material

A sedimentary lead concentrate was used for the tests in question.

The main component of the concentrate was the mineral galena (PbS). The sedimentary galena is a product of gravimetric separation, of large mineral particles. The lead content in sedimentary galena amounts to about 80 %. The water content in sedimentary concentrate is equal to 1-2 % The sedimentary galena is a fine material described as that " which may liquefy if shipped above the TML".

The following material was tested:

- Y Class polymer – made - by Novamont S.P.A.- of thermoplastic starch and cellulose derivatives from natural origin
- Z Class polymer–made - by the same company - of starch and polycaprolactone

The sample of polymer was in a granular form.

Testing methods

The influence of the adding of polymer to the ores on their parameters determining ability for safe shipment by sea, was assessed on the basis of determination of the following parameters:

Grain size content

For liquefaction to occur, the concentrate should have a permeability low enough that excess pore pressures cannot drop before sliding occurs.

From the viewpoint of grain size distribution, criteria of the grain size were introduced based on the effective size of D10 which is derived from the grain size accumulation curve and represents permeability. The materials other than coals can be regarded as non-liquefaction ones in the case when D10 is bigger than 1 mm. Here D10 constitutes such value provided the maximum grain size of the material is not greater than 9.5 mm.

In soil mechanics literature the requirement is usually expressed as 0.006 mm < D_{10} <0,3 mm for liquefaction to be likely, where D_{10} represents the particle size for which only 10% of the material mass is finer [6].

The grain size distribution was measured for both samples of concentrates: i.e. those without polymers and for mixtures with the polymers Y and Z (polymer content in mixture : 0.5%, 1.0%, 1.5% and 2%).

Estimation of FMP

The evaluation of TML was performed with the use of the Proctor Fagerberg Method according to the recommendations given in the Code of Safe Practise for Solid Bulk Cargoes [7].

Water absorption of polymers added to the concentrates

The polymers Y and Z were added to the concentrates in wet state (water content corresponding to the TML of sedimentary galena). Then the samples were tested for estimation of moisture content at several time intervals [8].

RESULTS AND DISCUSSION

Grain size content

In the sedimentary lead concentrate the amount of particles smaller than 0.3 mm is as low as 45 % and content of particles greater than 1mm exceeds 20 %. This is the reason why the lead concentrates may liquefy.

The results of grain size analysis are presented in Fig. 1 through 8 in the form of the grain size distribution curves.

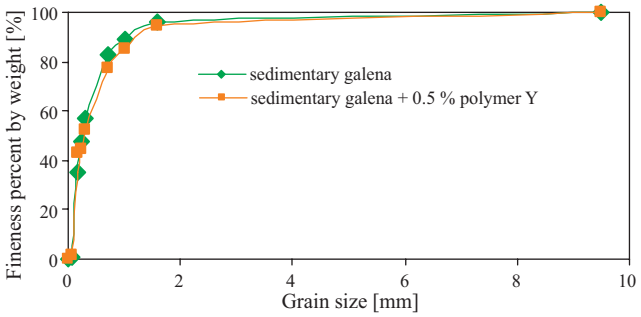

Fig. 1. *The grain size distribution in sedimentary galena + 0.5 % of polymer Y*

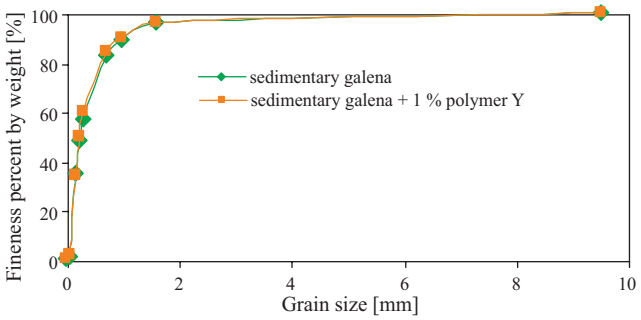

Fig. 2. *The grain size distribution in sedimentary galena + 1 % of polymer Y*

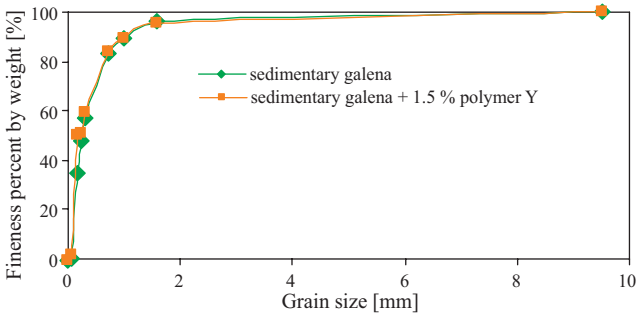

Fig. 3. *The grain size distribution in sedimentary galena + 1.5 % of polymer Y*

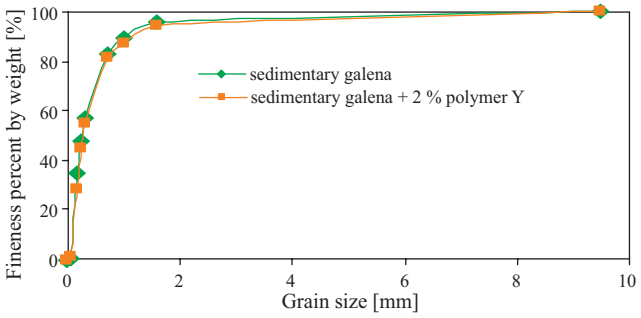

Fig. 4. *The grain size distribution in sedimentary galena + 2 % of polymer Y*

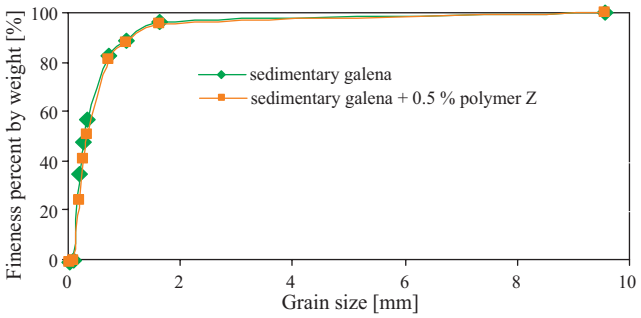

Fig. 5. *The grain size distribution in sedimentary galena +0.5% of polymer Z*

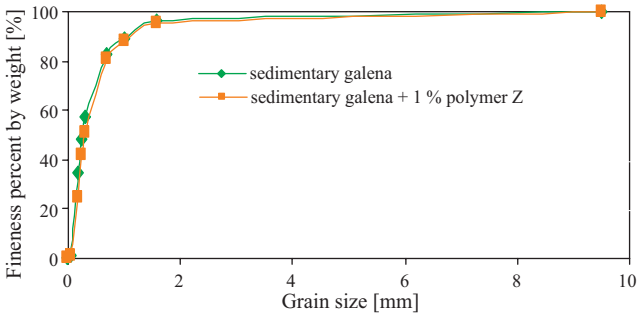

Fig. 6. *The grain size distribution in sedimentary galena +1% of polymer Z*

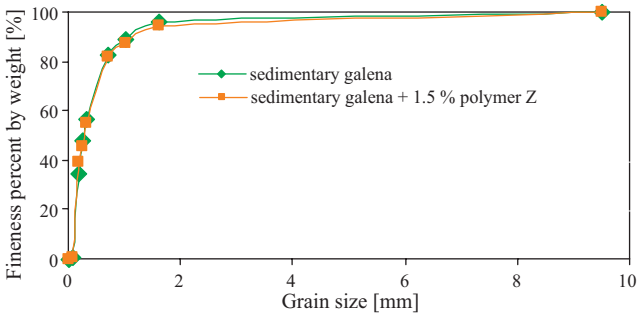

Fig. 7. *The grain size distribution in sedimentary galena + 1.5% of polymer Z*

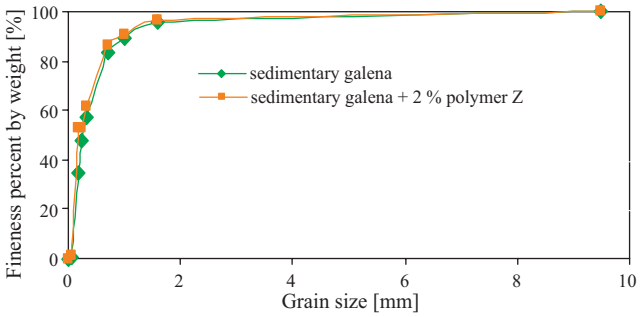

Fig. 8. *The grain size distribution in sedimentary galena + 2 % of polymer Z*

The course of grain size distribution curves indicates that all the tested concentrates are susceptible to liquefaction in sea transportation conditions as in each case the content of grains smaller than 0.3 mm is above 10%.

The percentage values of content of the grains (below 0.3 mm in size) in mixtures of concentrates and polymers are presented in Tab. 1.

Tab.1. *The content of the grains of size below 0.3 mm in concentrates*

Sample type	Content of grains [%]	
	Added polymer Y	Added polymer Z
Sedimentary galena +0.5% content of polymer	52.51	49.03
Sedimentary galena +1.0% content of polymer	58.85	51.04
Sedimentary galena +1.5% content of polymer	59.85	54.88
Sedimentary galena +2.0% content of polymer	54.66	61.72

The above presented results of the grain size analysis indicate that the addition of polymers does not significantly change grain size distribution.

Estimation of TML

Tab. 2. *Transportable Moisture Limit (TML) determined by Proctor C/Fagerberg Method*

Sample type	TML [%]				
	Content of polymer				
	0%	0.5%	1.0%	1.5%	2.0%
Sedimentary galena + added polymer Y	6.20	6.15	6.16	6.22	6.19
Sedimentary galena + added polymer Z	6.20	6.23	6.24	6.19	6.21

Despite the presence of a polymer in tested concentrates the values of estimated TML are similar because liquefaction is tightly related to the grain size content values.

Water absorption of polymers added to the concentrates

The results of estimation of water content in concentrates with added polymers are presented in Fig. 9 through 12.

The water uptake of the blend containing starch and cellulose (polymer Y) was higher than that of the blend containing starch and polycaprolactone (polymer Z).

The mixtures containing 1.5 % of polymers Y and Z absorbed water the most and for them the greatest decreasing content of moisture in tested concentrate was observed.

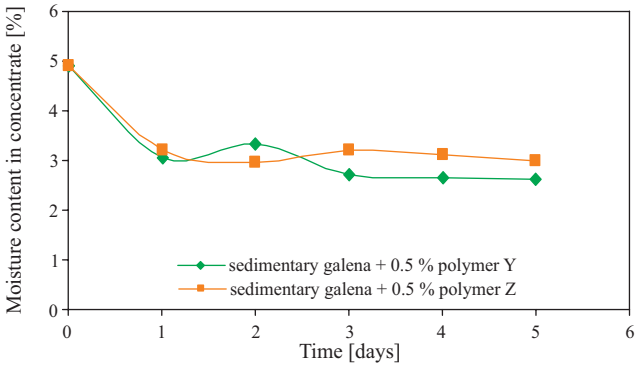

Fig. 9. *The influence of polymer on concentrate moisture content in sedimentary galena + 0.5 % polymer*

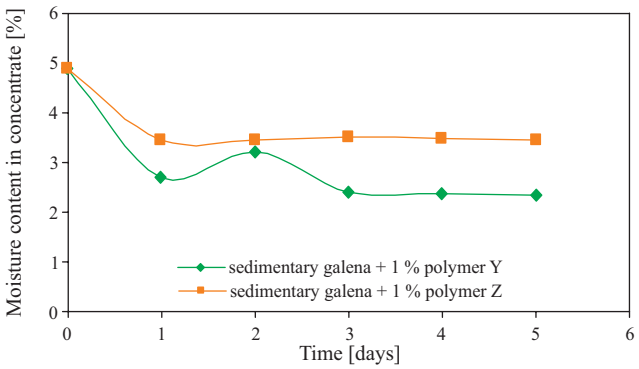

Fig.10. *The influence of polymer on concentrate moisture content in sedimentary galena + 1 % polymer*

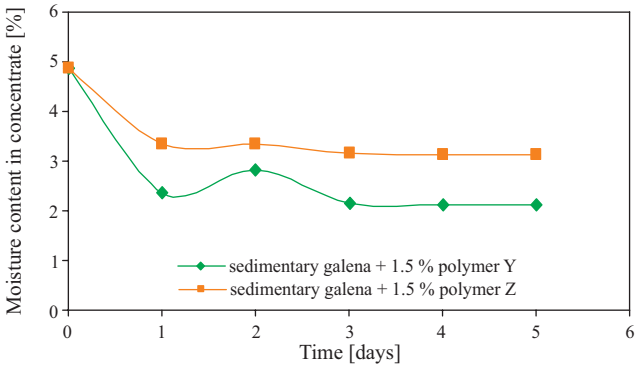

Fig. 11. *The influence of polymer on concentrate moisture content in sedimentary galena + 1.5% polymer*

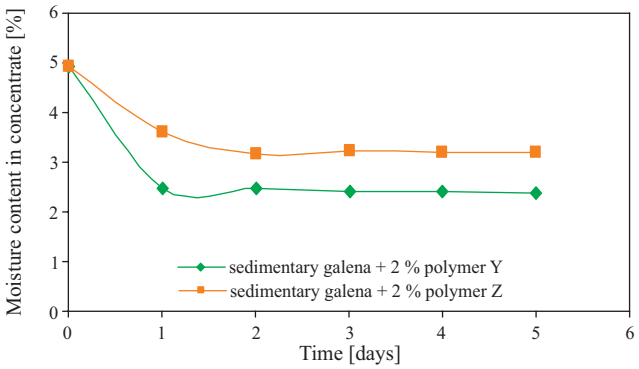

Fig. 12. *The influence of polymer on concentrate moisture content in sedimentary galena + 2% polymer*

The time required for reaching the lower moisture content in ore concentrates (below TML) was very short.

For the first 2 days moisture of ore concentrates decreased significantly and after 4-5 days it became stable reaching 2.4 % content for the tested concentrate.

After two days the slight increasing of moisture content of concentrate (mixture with polymer Y) was observed. It could indicate an insignificant leaching of starch during the experiment. The decreasing of moisture content after next day could be connected with the swalling of cellulose.

CONCLUSIONS

- The grain size analyses indicate that polymers do not significantly change grain size distributions.
- The comparison of the TML values confirms that the correlation between the grain content and TML value occurs.
- As to the results of the performed tests it can be stated that polymers absorb water from the pores between particles of mineral concentrate and its moisture content decreases.
- The type of polymer affects water uptake. In general, the polymer made of starch and cellulose absorbed more water than that made of starch and polycaprolactone. The equilibrium absorption of polymers was reached in 48 hours.
- The new solution of liquefaction problem is very promising because the used polymers are considered to be products of a low environmental impact.

BIBLIOGRAPHY

1. Youd T. L.: *Liquefaction mechanisms and induced ground failure*. In W. H.K. Lee, H. Kanamori, P.C.Jennings & C. Kisslinger,(Ed.) : International Handbook of earthquake and engineering seismology, Part B, Academic Press, (2003)
2. Sieder R., van den Beukel A.:*The liquefaction cycle and the role of drainage in liquefaction,* Granular Matter 6, (2004)
3. International Maritime Organization: *International Convention for the Safety of Life at Sea – SOLAS 1974/1978,* 2001
4. Bulativic, S. M.: *Use of organic polymers in the flotation of polymetallic ores: A Review*. Minerals engineering 12/4 (1999)
5. Bastoli C., Belloti V., Baerel L., 1286, (1990)
6. Eckersley J.D., *Coal cargo stability*, TheAusIMM Proceedings, No1(1997)
7. International Maritime Organization: *Code of Safe Practise for Solid Bulk Cargoes,* London, 2005
8. Ramaswamy M. & Bhattachary M.: *Properties of Injection Moulded Blends of Starch and Modified Biodegradable Polyesters,* European Polymer Journal 37, (2001).

CONTACT WITH THE AUTHOR

Marzenna Popek, Ph. D.
Department of Chemistry
and Industrial Commodity Science,
Gdynia Maritime University
Morska 83
81-225 Gdynia, POLAND
e-mail: marzenap@am.gdynia.pl

POLISH MARITIME RESEARCH 4(54) 2007 Vol 14; pp. 68-73
DOI: 10.2478/v10012-007-0043-8

Shooting resistance of non-metallic materials

Lesław Kyzioł
Polish Naval Academy,
L.Kyziol@amw.gdynia.pl

ABSTRACT

This paper presents test results of shooting resistance of non-metallic materials such as ceramics, rubber, glass reinforced plastic (GRP), natural and modified wood. It was demonstrated that GRP samples 16 mm thick protected with ceramic plates 10 mm thick can be considered bullet-proof against bullets of 7.62 mm caliber. And, multi-layer plate with a core of natural or modified wood cannot be taken as a bullet-proof material against 7.62 mm bullets.

Keywords: glass reinforced plastics (GRP), wood-polymer composites, ceramics, rubber, shooting, shooting resistance, ballistic plate

INTRODUCTION

Polyester laminates can be reinforced with fabrics or mats of glass, carbon or kevlar fibres, and strips or grids of amorphous metals. Such structures applied in shipbuilding are of a small thickness and show low resistance to machine-gun shots of 7.62 mm caliber, 9.5 g mass and 830 m/s initial velocity [1÷5]. Therefore to ensure sufficient shooting resistance against 7.62 mm bullets the GRP laminates should be covered by appropriate shields. As Polish standards in this field are lacking the tests of shooting resistance of shields are carried out in compliance with the requirements of DIN 52290 Standard or EUROPEAN STANDARD CEN, shown in Tab.1.

Tab. 1. *Requirements of DIN 52290 Standard and European Standard CEN for shooting tests of shields against 7.62mm bullets*

Lp	Kind of hazard	Kind of bullet	Bullet mass [g]	Bullet velocity V_{50} [m/s]	Shooting distance [m]
1	4	VMS/ WK	9.45±0.1	785÷795	10
2	5	VMS/HK	9.75±0.1	800÷810	25
HK- hard-core bullet, WK- soft- steel- core bullet, V_{50}- velocity at which 50% of bullets are stopped in shield					

New structural and protecting materials are necessary for building and modernizing the ships. To this end shooting tests are carried out in view of application of such materials for building and/or modernizing the locally - armoured ships, as well as military and police land vehicles. Preparation of bullet-proof materials was focused on the condition that the gun-bullets hitting the material's surface could fully dissipate their energy during penetration or even at the end of erosive perforation of shields.

In this paper are presented test results of shooting resistance of selected materials. Behaviour under shooting was tested of GRP laminates covered with ceramic shields and rubber layers, used in building superstructures of naval ships. And, possible application of natural and modified wood as one of ballistic shield layers was investigated. Description of the investigations was presented in detail in [5].

The tests carried out in the Institute of Fundamentals of Construction of Ship Machines, Polish Naval University, Gdynia, were aimed at determining overall ballistic resistance of shields made of various materials. In the subject-matter literature the data on application of non-metallic materials to shields of a higher resistance to bullets and bits, are lacking.

This paper is aimed at experimental determination of ballistic features of samples of 50 mm diameter formed with a few layers of non-metallic materials under shooting with the use of 7.62 mm bullets. The samples were installed in a tube fitted with an extensometric force meter, fixed in a ballistic pendulum. The relative effectiveness of the sample was assessed by means of the following formula :

$$\left(\frac{\text{deflection angle of pendulum}}{\text{deflection angle of pendulum with steel sample}}\right)^2 \cdot 100\%$$

The average deflection angle of pendulum at shooting tests of 12mm thick samples amounts to 6.19° [8].

Capability of absorbing bullet's kinetic energy, revealed by different samples can serve as a measure of their ballistic resistance and the basis to assess their usefulness in designing shields of a higher shooting resistance to bullets and their fragments.

Because of the specific features of the available test stand the force in the tube in which sample is fixed as well as the ballistic pendulum deflection angle in which the tube is fixed, were measured [8] instead of measuring the maximum impact force of bullet and amount of energy absorbed by the sample.

DESCRIPTION OF THE TEST STAND

The tests were performed in the test stand (Fig. 1) consisted of the ballistic pendulum (6) and two sets of the fixing frames (3), piezo-ceramic detectors (2) replaced after every shot, tube (5) fixed in the pendulum together with extensometric force meter, and the indicator (7) for measuring the pendulum

deflection angle. After penetrating the first set of two frames the bullet (1) impacts the sample (4) and - after penetrating it - affects the next two piezo-ceramic detectors. The impulse from the first detector triggers the time meter in the oscilloscope (9) which records the instant of bullet's impact in the second detector. This makes it possible to determine the bullet's velocity before hitting the sample. Similarly, the bullet's velocity behind the sample is determined by means of the second set of frames with detectors and the oscilloscope (10). The sample is rested on the tube (5) and tightened with the nut. To ensure a greater overall susceptibility of the sample the pressure exerted on it is so low as to allow its edges to displace against the nut and tube during shooting through the sample. No investigations on possible influence of the sample rigid support in the tube were performed.

The maximum value of the pendulum deflection angle φ resulting from a given shot [Tab. 2, column (6)] was read from the indicator's scale. The greater the bullet's impact the greater the pendulum deflection angle (and - in consequence- the amount of energy absorbed by the tested sample).

The bullet's trajectory deviation from the sample axis was equal to about 9 mm thus the bullet turned up close to the supporting edge of the sample leaving it unpenetrated. Therefore the entire kinetic energy of the bullet was absorbed by the sample and the pendulum inclined up to the angular position $\varphi_{max} = 9^o$.

As the potential energy of the pendulum in the top position, amounting to :

$$E_{pot} = mgl\,(1 - \cos\varphi) \tag{1}$$

where :
m – mass of the equipped pendulum
g – gravity acceleration
l – distance of mass centre from the pivoting axis
φ – maximum deflection angle of the pendulum

is equal to the amount of the energy transferred to the pendulum during shooting, the following formula was assumed to be a measure of the effectiveness of particular samples :

$$\varepsilon = \frac{1-\cos\varphi}{1-\cos 9^\circ}\cdot 100\% = \frac{\sin^2 0.5\varphi}{\sin^2 0.5\cdot 9^\circ}\cdot 100\% \tag{2}$$

For small angles, values of their sines are practically equal to their arguments hence in Tab. 6, col. 9 the following values are introduced :

$$\varepsilon = \left(\frac{\varphi}{9}\right)^2 \cdot 100\% \tag{3}$$

TESTED LAMINATES AND SHIELDS

The GRP laminate was tested of 16 mm and 17 mm in thickness (marked L16 or L17) applicable to construction of superstructures on special vessels. The GRP laminate additionally reinforced with layers of 1 x 0.032 mm stripes of canvas fabric of amorphous alloy of 39% Fe, 40% Ni, 1% Al and 20% B content, of the tensile strength R_m=1560 MPa, was marked L18. To stick the metal reinforcement into the laminate, Epidian-5 resin and Z-1 curing agent were used. The GRP laminate additionally reinforced with layers of mat made of the cut amorphous-alloy fibres stuck with the above mentioned resin and curing agent, was marked L22 or L24 depending on its thickness.

To the GRP laminate, D23-E polyester resin was applied as a resinoid bond, and it was also used for the shields - smooth plates of the ballistic ceramics (Al_2O_3+SiC), having

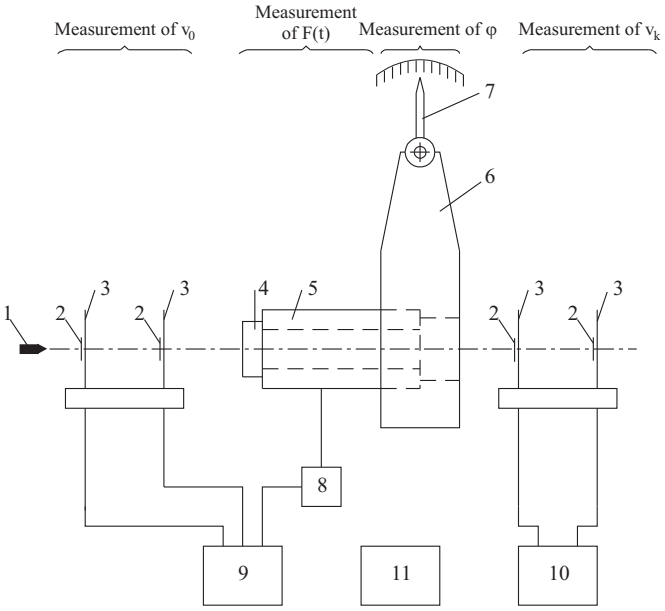

Fig.1. *Schematic diagram of the test stand.*
1 *– bullet,* ***2*** *– piezoelectrical detector,*
3 *– damping frame with detector stuck on it,*
4 *– shot sample,* ***5*** *– tube with extensometric force meter,*
6 *– ballistic pendulum,* ***7*** *– indicator of pendulum angular deflection,*
8 *– amplifier,* ***9*** *– digital oscilloscope with register,*
10 *– digital oscilloscope with recorder of F(t) and Δt;*
$\boldsymbol{v_0}$, $\boldsymbol{v_k}$ *– velocity of a bullet in front of and behind the sample;*
Δt *– time of the flight of the bullet between two first detectors*

5x50x50 mm or 10x50x50 mm dimensions, and x-relief plates of 5x45x159 mm and 10x45x159 mm dimensions, stuck onto the laminate plates. The laminate samples with ceramic shields were marked C5 or C10, depending on shield thickness, or C5x or C10x, where the shields were made of x-relief ceramic plates. The laminate samples in which 5.5 mm rubber layer was stuck between the laminate and ceramic shield, were marked /g/, whereas those without rubber layer were marked /-/. Examples of marking the laminate plate samples are shown in Fig. 2 and 3.

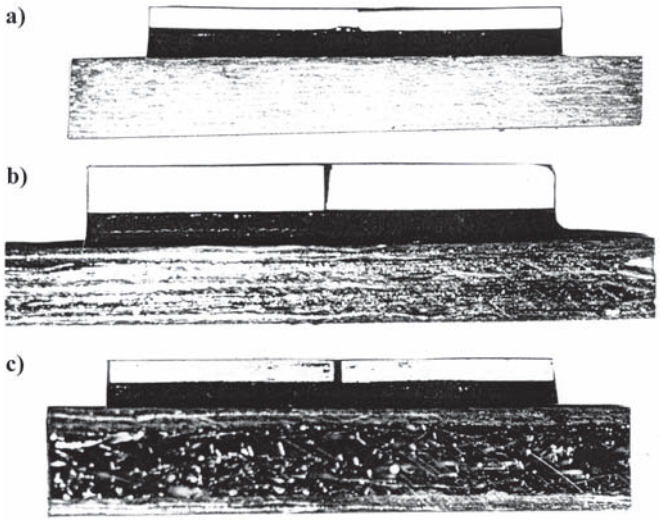

Fig.2. *Examples of CGL ballistic composites (ceramics + rubber + + laminate):* ***a)*** *Al ceramics of 5x50x50 mm dimensions + 5.5 mm rubber layer + GRP laminate of 16x140x140 mm dimensions, marked : C5/g/L16,* ***b)*** *Al ceramics of 10x50x50 mm dimensions + 5.5 mm rubber layer + GRP laminate of 16x140x140 mm dimensions, reinforced with amorphous alloy fabric, marked : C10/g/L18,* ***c)*** *Al ceramics of 5x50x50 mm dimensions + 5.5 mm rubber layer + GRP laminate of 24x140x140 mm dimensions, reinforced with amorphous alloy mat, marked : C5/g/L24.*

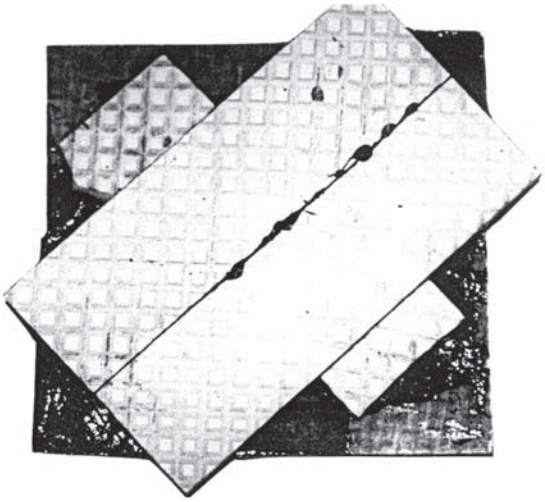

Fig. 3. CGL ballistic composite of the structure : Al x-relief ceramics of 10x45x159 mm dimensions + 5.5 mm rubber layer + GRP laminate of 16x140x140 mm dimensions, marked : C10x/g/L16/.

Nine laminate plate samples fitted with ballistic shields, marked: C5/-/L16, C10/-/L16, C10/g/L16, C5/g/L17, C10/g/L17, C10x/g/17, C10/g/L18, C5x/-/L22 i C5x/g/L24, were tested.

RESULTS OF SHOOTING RESISTANCE TESTS

The tests were carried out on the standardized stand for testing ballistic resistance of materials [6]. The 140mm x 140 mm laminate samples were fixed in the head of the tube dynamometer, with ballistic shields heading the shooting direction. The plates were shot with 7.62 mm bullets of 9.5 g mass and 830 m/s initial velocity, fired from PK rifle from 3 m distance. The dynamometer recorded course of force changes during bullet's penetration into the sample plate. After shooting image of damage was photographically recorded.

An example of the recorded damage resulting from bullet's impact :

★ the sample plate C10/g/16. The course of force due to bullet's impact is shown in Fig. 4. The greatest impact force F_{max} = 88.6 kN.

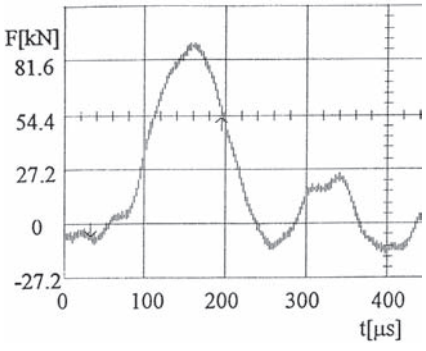

Fig.4. The course of impact force due to 7.62 mm AP bullet striking with 830 ms^{-1} velocity into C10/g/16 ballistic plate composed of : Al ceramic plate of 10x50x50 mm dimensions + + GRP laminate plate of 16x140x140 mm dimensions ; F_{max} = 88.6 kN

The bullet damaged the ceramic plate, ballistic erosion of the rubber layer occurred, and small prints of the bullet's size appeared on the struck side of the GDP plate. At the edge of the GRP plate local under-surface shear deformations, and on its rear side shallow delaminations, occurred. (Fig. 5).

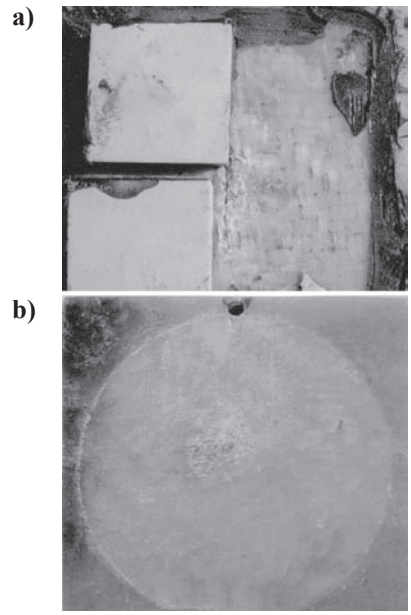

*Fig. 5. Effects of shooting the C10/g/16 ballistic composite plate by using 7.62 mm AP bullet with 830 ms^{-1} velocity. **a)** view from the bullet's inlet side, **b)** view from the GRP rear side.*

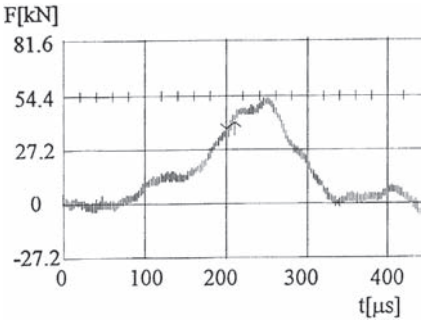

Fig. 6. The course of impact force due to 7.62 mm AP bullet striking with 830 ms^{-1} velocity into CGL ballistic plate composed of : Al ceramic relief plate of 5x45x159 mm dimensions + laminate plate reinforced by amorphous metallic mat of 22x140x140 mm dimensions, marked C5x/-/L22; F_{max} = 47.5 kN

★ CGL C5x/-/L22 plates. The course of force due to bullet's impact is shown in Fig. 6.
The greatest impact force F_{max} = 54 kN.
The bullet penetrated the GRP laminate plate. A partial delamination occurred on the contact surfaces of the amorphous metallic mate with laminate and on the rear side of the laminate (Fig.7).

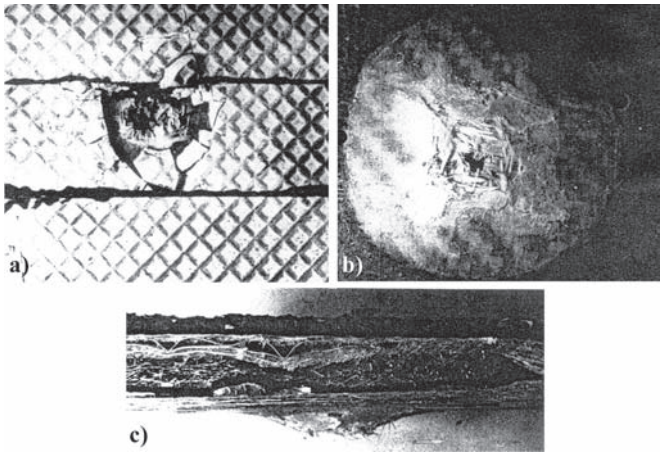

*Fig. 7. Effects of shooting the CGL ballistic composite plate by using 7.62 mm AP bullet with 830 ms^{-1} velocity, marked C5x/-/L22 : **a)** view from the side of bullet's inlet and outlet, **b)** cross-section of the composite plate **c)** cross section of the composite*

TESTS OF SAMPLES CONTAINING NATURAL OR MODIFIED WOOD

Research on modification of wood performed in the Basic Engineering Institute, Polish Naval University, Gdynia, inspired this author to determine shooting resistance of such material applicable to ship structures, assuming that modified wood is used for one of the ballistic plate layers .

In Tab. 2 are presented results of shooting tests of the layered samples in which the inner layer was made of natural or modified wood (16 mm thick) and the outer layers of steel or aluminium disks (6 mm thick). The detailed results of the tests were published in [7]. For the samples under shooting values of the bullet's initial velocity were contained within the range of 790 ÷ 909[m/s].

Tab. 2. *Results of ballistic tests.* ***Notation****: St - hull structural steel of A grade, Al - AlZn5Mg2CrZr alloy, Ds - pine wood, Dm - modified pine wood, Fs_{max} - maximum compressive force, Fr_{max} - maximum tensile force*

Number of series	Kind sample	Number of sample	Velocity of bullet		Angle of pendulum deflection	Impact force		Effectiveness of sample
			Before sample	Behind sample		max.	min.	
			V_0 [m/s]	V_k [m/s]	φ [deg]	Fs_{max} [kN]	Fr_{min} [kN]	ε [%]
1	2	3	4	5	6	7	8	9
1	6 16 6 St Ds St	14.1	806	370	6	57	-21	44
		14.2	862	394	6	49	-18	44
		14.3	793	366	5.5	52	-16	37
		average	**820**	**377**	**5.8**	**53**	**-18**	**42**
2	6 16 6 St Dm St	26.1	877	434	6	64	-29	44
		26.2	892	374	6.5	72	-33	52
		26.3	885	410	6	67	-34	44
		average	**885**	**406**	**6.1**	**68**	**-32**	**47**
3	6 16 6 Al Ds Al	18.1	851	781	1.5	13	-5	2
		18.2	888	745	2	21	-6	4
		18.3	888	765	1.5	19	-6	2
		average	**876**	**764**	**1.6**	**18**	**-6**	**3**
4	6 16 6 Al Dm Al	30.1	869	714	2.9	41	-19	10
		30.2	909	704	2.8	38	-17	9
		30.3	888	666	2.2	34	-16	5
		average	887	695	2.6	37	-17	8
5	6 16 6 Al Ds St	22.1	869	609	4	34	-8	19
		22.2	869	632	4.1	30	-5	20
		22.3	869	645	4.2	32	-6	20
		average	**869**	**629**	**4.1**	**32**	**-6**	**20**
6	6 16 6 Al Dm St	34.1	888	526	4	49	-18	19
		34.2	869	625	4	50	-23	19
		34.3	869	543	4.5	46	-15	25
		average	**876**	**564**	**4.1**	**48**	**-19**	**21**

The maximum values of the force in the tube reached from Fs_{max} = 68 [kN] and Fr_{max} = -32 [kN] (steel-modified wood-steel) to Fs_{max} = 18 [kN] and Fr_{max} = -6 [kN] (aluminium-natural wood-aluminium). Shooting resistance of the aluminium-modified wood-aluminium layers is comparable to that of aluminium-sand-aluminium and aluminium-glass-aluminium composites. In each case where the outer layers were made of steel and the inner ones of sand, crushed glass or modified wood the lowest shooting resistance was shown by those whose inner layer was made of modified wood. The samples whose inner layer was made of natural wood showed the lowest shooting resistance [7].

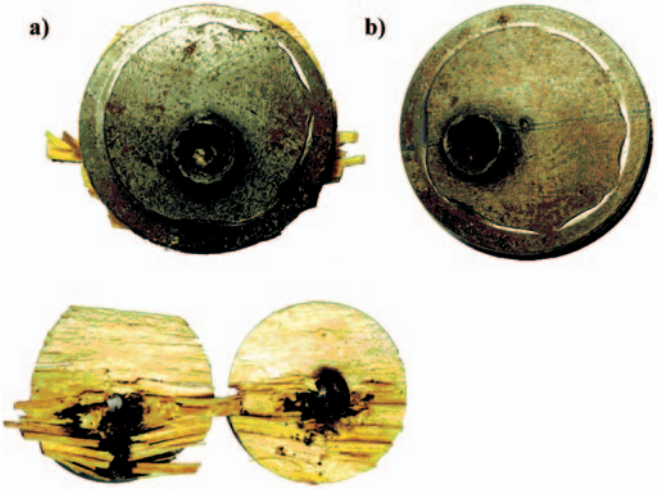

Fig. 8. *Example view of the sample having the inner layer made of :* ***a)*** *modified wood,* ***b)*** *natural wood*

In Fig. 8 the image is shown of the damaged inner layer made of : a) modified wood and b) natural wood. It can be observed that in the case of damaging the inner layer of modified wood (Fig.7a) fragmentation mode prevailed. The resisting inner layer failed. The material fragments observed on the photograph illustrate mode of the damage. The inner layer made of natural wood (Fig.7b) sustained perforation. The bullet faced no resistance from the side of the layer.

DISCUSSION OF RESULTS

The obtained results of the shooting tests of GRP laminate plates indicate that the thickness of ballistic shield plays crucial role. It was revealed that the application of 10 mm ceramic shields made the plates consisted of ceramic shields and GRP laminate resistant to shooting. The bullet's energy was mostly absorbed by a single ceramic plate of 10x50x50 mm or 10x45x159 mm dimensions (Fig.5). In the case when the bullet destroyed a few ceramic plates (Fig.7) they absorbed more impact energy and the bullet penetrated the ceramic shield to a smaller depth. If such plates are thicker they will probably absorb more energy and bullet's impact force will drop faster. Positive results were obtained in the case of application of 5,5 mm rubber layer between ceramic shield and laminate. The rubber so much absorbed energy of impact of fragments of the bullet and ceramics into laminate that their strikes left only small prints on the laminate surface. It was also showed that the additional reinforcement by means of the layers of metallic fabric or mat introduced to the GRP was not purposeful as it only increased extent of delamination of the laminate, resulting from the bullet's impact. Hence it can be assumed that the GRP laminates additionally reinforced with metallic mat or fabric are less resistant to shooting than the GRP laminate itself. Extent of the delamination of the bullet-penetrated laminate plates was smaller than that in the plates not penetrated by the bullet and it appeared mainly on the rear side of the GRP plates.

To sum up the tests results it can be stated that the highest resistance to shooting with the use of PK rifle and the steel-core bullet of 7.62 mm caliber, 9.5 g mass, at its initial velocity of 830 m/s, was obtained for the laminate plates protected by (Al_2O_3 + SiC) ballistic ceramic plates of 10 mm thickness and rubber layer of 5.5 mm thickness.

CONCLUSIONS

On the basis of the obtained test results the following conclusions can be offered :

- The best protection of the GRP laminate plates of 16-24 mm in thickness against shooting with the use of 7.62 mm AP bullets of 9.5 g mass and 830 m/s initial velocity is provided by the 10 mm plates made of (Al_2O_3 + SiC) ballistic aluminium ceramics combined with 5.5 mm rubber layer.
- In order to reduce impact energy of bullet fragments striking GRP and ceramics it is purposeful to introduce a rubber layer of about 5 mm in thickness between the ceramic plates and GRP laminate.
- The reinforcing of the GRP with the use of metallic reinforcement is unreasonable as it increases degree of GRP delamination resulting from shooting.
- A modified wood layer is more effective than that of natural wood. It provides a greater absorption of bullet's energy and greater maximum force in the tube.
- Destruction process of the intermediate layer made of modified wood due to impact of 7.62 mm bullet is of entirely different character (fragmentation dominates) than that observed in the case of application of natural wood (perforation dominates).

BIBLIOGRAPHY

1. Kim S.J., Goo N.S.: *Dynamic contact response of laminated composite plates according to the impactors shapes*. International Journal of Impact Engineering, vol.65, No 1, 1997.
2. Chun I., Lam K.Y.: *Dynamic response of fully clamped laminated composite plates subjected to low velocity impact of a mas.* International Journal of Solids and Structures, vol.35, No 11, 1998.
3. Zhu G., Goldsmith W., Dharan C.K.H.: *Penetration o laminated kevlar by projectiles.* International Journal of Solids and Structures, vol.29, No4, 1992.
4. Goldsmith W., Dharan C.K.H., Chang H.: *Quasi-static and ballistic perforation of fiber laminates*. International Journal of Solids and Structures, vol.32, No 1, 1995.
5. Zatorski Z.*: Resistance to penetration of uniform plates* (in Polish). Proc. 7th Domestic Conference on Fracture Mechanics (VII Kraj. Konf. Mechaniki Pękania). Kielce-Cedzyna 23-25.09.1999. Scientific Bulletins of Swietokrzyski University of Technology (Zeszyty Naukowe Politechniki Świętokrzyskiej), Mechanics (Mechanika), vol. 68,Part 2, 1999.
6. J.Fila, Z.Zatorski (authors) : *A unified stand for testing ballistic resistance of materials, especially for ship protection and armoured structures* (in Polish). Patent UP RP no. 0641 AMW, 1999
7. Kyzioł L.: *Tests of ballistic resistance of composites containing modified wood* (in Polish). Scientific Bulletins of Polish Naval University (Zeszyty Naukowe AMW), No. 3, Gdynia 2004
8. Kolenda J., Kyzioł L. *et al*. : *Impact and ballistic resistance of a new aluminium alloy and composites containing it* (in Polish). Wydz. Mech.–Elektr. Research raport No2 (IPBMO), 2000

POLISH MARITIME RESEARCH 4(54) 2007 Vol 14; pp. 74-82
DOI: 10.2478/v10012-007-0044-7

An overview of the didactic and scientific activity at the faculty of mechanical and electrical engineering of the Polish Naval Academy

Zbigniew Korczewski, D.Sc., PNA Prof.
Polish Naval Academy

ABSTRACT

The article characterises the didactic and scientific activity at the Faculty of Mechanical and Electrical Engineering of the Polish Naval Academy. The current didactic offer and the areas of current research work are presented, along with main characteristics expected from the naval-specialisation graduate majoring in mechanics and machinery construction, in the context of the Polish Navy technical staff education system. Discussed are the subjects of research activities initiated in particular Faculty units, and leading scientific problems which have been studied for years within the field of widely understood utilisation of naval technology.

Keywords: Polish Naval Academy, Faculty of Mechanical Engineering, Faculty of Electrical Engineering, Didactic, Scientific

INTRODUCTION – HISTORICAL BACKGROUND

The Polish Naval Academy, bearing the name of Westerplatte heroes, is the only military naval academy in Poland, which since 1922 has permanently trained officers wanting to serve on Navy ships and offshore units.

The beginning of activity of the PNA Faculty of Mechanical and Electrical Engineering dates to November 1, 1931, when Commander Karol Korytowski, the then Commandant of the Naval Officers School in Torun, admitted as freshman cadets 12 candidates for naval technical officers [1].

The earliest formulated general mission of the Faculty of Mechanical and Electrical Engineering was training mechanical engineers ready to perform their duties as naval officers responsible for operation and professional service of all machinery and systems situated in the ship's engine room.

During 75 years of Faculty's existence its organisational structure was changed several times, always to follow the development of naval sailing techniques. In the most difficult years of the Second World War, when the Academy was moved to the United Kingdom (Plymouth, Davenport, Okehamptom), the organisational structure of the Faculty reflected the requirements resulting from war activity conducted in alliance with the Royal Navy. In those days the then Faculty of Technology graduated 23 mechanical officers ready to command, during war operations, power plants on both Polish Navy's ships and those obtained from the United Kingdom [2,3].

After the Second World War the activity of the Faculty was continued in a new situation of geopolitical reality. On January 18, 1946, in Gdynia-Oksywie the Naval Officers School, the predecessor of the present Polish Naval Academy, started its activity, with the Faculty of Technology as part of it. Since then to now the headquarters of the Academy have been situated in the block of buildings designed in 1924 by Professor Marian Lalewicz - a lecturer of architecture at the Lvov and Warsaw Universities of Technology (Photo 1a). Until 1939, the Centre of Experts Training of the Polish Navy had had its headquarters in there, and during Hitler's occupation - the Kriegsmarine. The present sight of the Academy is given in Photo. 1b.

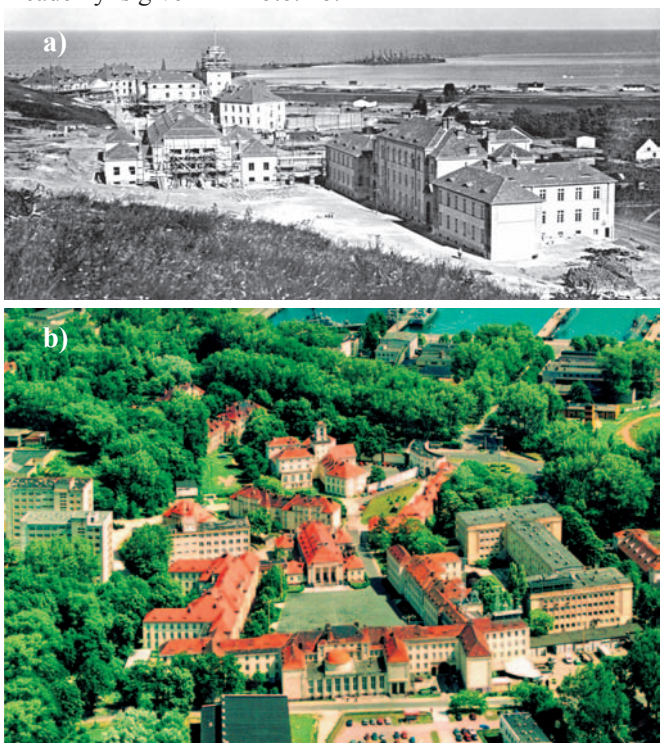

Photo. 1. Campus of the Polish Naval Academy in Gdynia
***a)** Academy under construction - 1925, **b)** present sight of Academy.*

The most recent change in the organisational structure of the Academy was made in 2003. It resulted in restructuring the Faculty of Mechanical and Electrical Engineering which, preserving its previous name transformed its structure formerly consisting of four faculty institutes and two separate Departments of Mathematics and Physics into that consisting of two faculty institutes and one Mathematics and Physics Department. The present structure of the Faculty is given in Fig. 1.

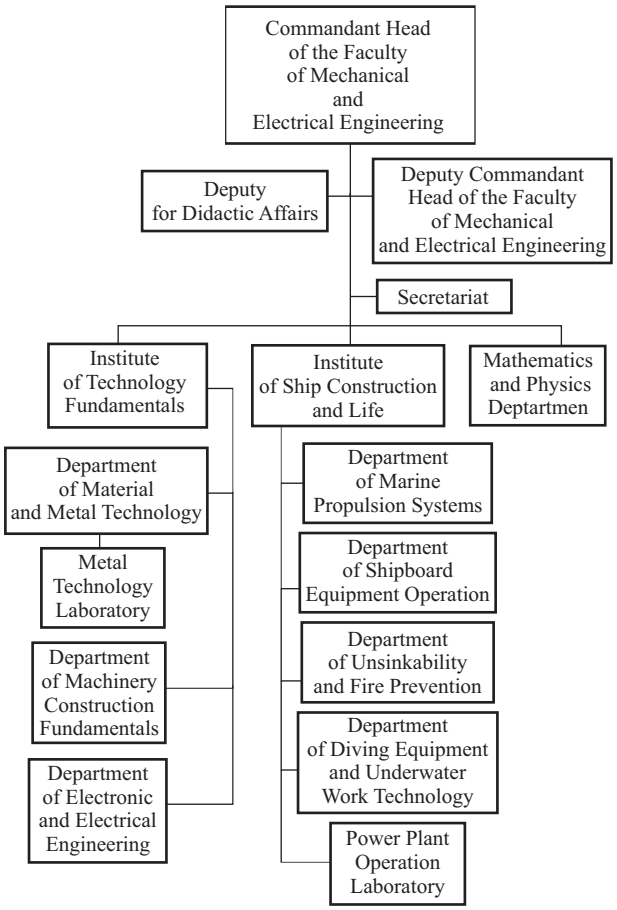

Fig. 1. *Organisational structure of the PNA Faculty of Mechanical and Electrical Engineering*

At present the Faculty employs 53 academic lecturers, including 12 independent research workers (6 full professors and 6 associate professors) and 41 assistant research workers (28 assistant professors and 13 masters of science). To conduct BS studies, MS studies, and unified intramural studies of mechanics and machine construction, the Faculty has the relevant minimum staff for the home unit (5 independent research workers representing the discipline identical or very close to the education major, i.e. machine design and operation, and 3 independent research workers representing similar, or basic disciplines being in some relation with the education major) and for running an outside didactic centre. In the latter case the requirements for the home unit include: 8 independent research workers and 7 assistant professors, including 5 independent research workers and 6 assistant professors representing the discipline of concern, with the remaining academic lecturers representing related disciplines. A complementary requirement which is met by the Faculty is to have 9 assistant professors with professional practice. At present the Faculty has 184 students in total, including: 60 intramural military students, 31 intramural civilian students, and 93 extramural civilian students. All this gives an extremely high ratio of education quality, as compared to other higher-education institutions in Poland. This ratio, understood as the proportion of independent academic lecturers to students, is equals to 1:15 in PNA.

Admission limits for military studies are decided, year by year, by the Minister of National Defence, and the Academy cannot change them. This year the admission limit for the major of mechanics and machinery construction was equal to 18 persons. Such a small number of military students allows these studies to be treated as privileged, individual in practice, and completely adequate to professional requirements expected from the graduates – future Navy officers and operators of marine power plants.

Until the academic year 2004/2005 the admission limit for civilian studies had been decided by the Ministry of Science and Higher Education, and was equal to 20 candidates for intramural studies for the entire Academy. In the recent year, i.e. for the academic year 2005/2006 this limit was increased to 100 persons (out of which 30 persons for the Faculty of Mechanical and Electrical Engineering). At present, the admission limit for civilian studies is decided by the Academy Senate, depending on the scale of the financial support obtained from the Ministry of Science and Higher Education. The number of young people starting civilian intramural studies, initiated for the first time in the Faculty in academic year 2005/2006, have been doubled to 60 people in the present year.

Since 1987 the Faculty is authorised to confer scientific degrees in the field of technical sciences and the discipline: machine building and operation. Since the authorisation to confer doctors degree was obtained, 44 doctor's theses were successfully defended at the Faculty. Eight Faculty graduates were conferred the degree of associate professor and four - of full professor.

TRAINING TECHNICAL STAFF FOR WORK AT SEA

The Faculty of Mechanical and Electrical Engineering conducts studies preparing for work at sea. It trains candidates for Navy officers at five-year uniform graduate studies, with the major in mechanics and machinery construction, and major specialisations in marine power plant operation and electrical equipment operation, as well as (since 2005) civilian students for candidates for merchant marine officers, with the same major and the specialisation in marine power plant operation. The future officers are taught general-education subjects, including English, psychology, sociology, mathematics, physics, physical education, and job-oriented subjects, such as, for instance, thermodynamics, mechanics, electrotechnics, turbine engines, piston engines, marine power plants, marine power plant control systems, theory of operation, and ship equipment repair technology. The graduates are conferred the title of an engineer - ship mechanic and (candidates for Navy officers) the degree of Navy Ensign. Civilian graduates receive the diploma of the merchant marine watch officer.

As well as that, since 1998 the Faculty has conducted extramural BS studies in the major of mechanics and machinery construction, and the major specialisations in marine power plant operation and electrical equipment operation. After these studies the graduates are conferred the title of an engineer - mechanic with relevant specialisation.

As a consequence of including naval academies to the Act on Higher Education, extensive work is conducted in the Naval Academy towards its fast adaptation to the requirements of this Act. Following the Bologne Convention, starting from the academic year 2006/2007 a system of two-level education of civilian students has been introduced, which will also apply

to military students since the academic year 2007/2008. New programmes of two-level studies conducted in the intramural and extramural modes take into account all programme and time requirements defined in relevant teaching standards for the course of mechanics and machinery construction, as well as standard requirements concerning marine staff education, defined in the STCW Convention. With respect to military students – relevant directives of the Ministry of National Defence are also taken into account. The studying programmes take into account ranking by the ECTS evaluation system, concerning transfer and accumulation of ranks, and include detailed check of ability to communicate in English. According to NATO standards in force in the Academy, our military graduates have to meet language requirements defined in STANAG 6001 - level 3, which corresponds to standard C1 requirements according to the criteria of the European Council.

Characteristics of the military graduate

The military graduate of the PNA Faculty of Mechanical and Electrical Engineering has to possess knowledge, skills and professional attitude which will allow them to take duties of Navy officer commanding the electromechanical section of the ship. Professional dispositions for doing this duty by the graduate are warranted by the possession of Quality Certificate ISO 9001:2000 by the Faculty, and conducting the studies in accordance with Education Quality Standards defined by the Ministry of Science and Higher Education, and the International Convention Concerning Requirements in Training Sea Vessel Crews, STCW 78/95. In recognition of high quality of education in the two abovementioned areas, the Faculty was granted the following accreditations:

- Quality Certificate ISO 9001:2000 confirmed for three years, i.e. until 21.09.2008. The range of the certification covers:
  - teaching students in intramural and extramural modes at the first and second level, and at postgraduate studies
  - conducting scientific research in the field of military, technical, and human sciences
  - conducting specialist courses, including those concerning activities named in the resolutions of the STCW Convention, and professional improvement courses.
- Certificate of the Commission of Accreditation of Technical Academies for the major of mechanics and machinery construction, for academic years 2002/2003 to 2007/2008
- Certificate of the National Accreditation Commission for the major of mechanics and machinery construction, for academic years 2005/2006 to 20011/2012
- Certificate of Acknowledgement of the Minister of Marine Economy for training marine staff at the operating level in the engineering department, within the range covered by STCW resolutions - in force until July 1, 2011.

An essential property of the process of education is ability to form appropriate professional attitude by direct contact of Academy graduates with the didactic personnel, members of which, along with university titles and degrees, also reveal vast sea-war practice confirmed by relevant professional degrees.

As far as military studies are concerned, the Faculty conducts training in two major specialisations: marine power plant operation, and marine equipment operation.

The graduate in the major specialisation of marine power plant operation possesses basic general and job-oriented education obtained following the studying programme relevant for the major of mechanics and machinery construction and necessary for understanding scientific fundamentals of engineering knowledge within the area of the construction and technology of ship machine production. Moreover, they possess versatile specialist knowledge required for independent running of marine power plants, including the use of weapons, and meeting at the same time ship sailing safety and sea environment protection requirements. This, in turn, allows them, just after the graduation, to take independent officer's posts on Navy vessels and merchant marine ships. They also have thorough knowledge on how to solve technical problems in mechanics, and design ship machinery and equipment with the use of modern computer-aided methods invented to support engineering work.

The graduate in the major speciality of electrical equipment operation possesses versatile knowledge and skills concerning the construction and operation of mechanical and electrical systems on the ship. They acquire ability to work in engineering teams consisting of specialists in mechanics, machine building, electrotechnics and electronics. High attention is paid to syntonic cooperation of the future engineer-mechanic with the computer environment, both within the range of its operation, and the integration of ship machines with elements providing opportunities for computer control, digital recording and processing of operating data. Programme essentials included in particular lectured subjects are a warranty that the graduate in this specialisation is well prepared to solve technical problems connected with the operation of ship machines and systems containing electronic, electrical and mechanical components. The studying programme includes interdisciplinary problems within the fields of modern machinery industry and advanced electrical and electronic technologies, studying of which requires linking basic knowledge of mechanics, and machine construction and operation, with widely understood experience in informatics, automatics, electrotechnics and electronics.

The graduate of military studies is prepared to :

- command the crew of the ship department
- make rational operational decisions in difficult situations taking place in marine power plant operation at sea and in extreme battle conditions
- manage material resources on the ship according to the regulations in force
- run research projects and scientific investigations in scientific and research institutions
- continue education at third-level studies.

In particular, specialist qualifications of the graduate include:

- ability to operate and design marine power plants and general vessel systems
- familiarity with the construction and principles of operation of ship propulsion systems, and electrical and electronic equipment
- ability to use computer systems to support design of ship machines and equipment
- familiarity with marine power plant control systems and electric power generation systems on the ship
- theoretical and practical knowledge of problems of diagnostics and control of marine power plant machines and systems.

The graduate is ready to work:

- ⇨ on Polish Navy ships – as the commander of the electromechanical department
- ⇨ on sea merchant ships – ad the watch officer

- ⇨ at technical universities, in scientific research institutes, or research and development centres with ship oriented specialisation, respectively, as academic lecturer, or research worker
- ⇨ in institutions involved in industrial consultancy and promotion of knowledge on mechanics and machinery construction.

Characteristics of the civilian graduate

Within the framework of civilian studies, the Faculty conducts teaching in two major specialisations: marine power plant operation (marine specialisation) and technical applications of computers (polytechnic specialisation without marine rights).

The major specialisation of marine power plan operation is oriented on training marine experts able to do a duty of an engineer-mechanic – watch officer on merchant vessels, while the specialisation of technical applications of computers - specialist in naval computer systems.

Among the subjects lectured in the naval specialisation, special attention is paid to the construction and practical use of general ship systems and power plant systems on civilian watercraft. The studying programme covers the area of interdisciplinary problems concerning modern machine industry and advanced electric technologies, studying of which requires basic knowledge of mechanics, and machine construction and operation linked with wide experience in electrotechnics. During their education the students get familiar with the structure and operation of marine power plants and general ship's systems, as well as mechanical and electrical systems. They gain ability to work in engineering teams consisting of specialists in mechanics, machine building and electrotechnics. The essentials of particular lectured subjects are the warranty that the graduate with this major specialisation is well prepared to solve technical problems connected with the operation of marine power plants, and ship's machines and systems having pneumatic, hydraulic and mechanical components.

Specialist qualifications of the graduate with the civilian marine specialisation are identical to those obtained after military studies. Beside already mentioned sea-going ships, employment prospects for these graduates also include shipyards and design-and-production plants having connections with the shipbuilding industry.

Studies in the major specialisation of technical applications of computers focus on problems of widely understood applications of computer systems for solving present-day problems on naval engineering. The studying programme includes all standard subjects in the major of mechanics and machinery construction, extended by problems of computer engineering systems in operation in naval applications. During their studies the students get familiar with basic problems of mechanics and naval machinery construction, with selected problems concerning principles of operation of naval mechanisms and equipment, as well as with the structure and control of computer systems. The studying programme includes computer aided design, realisation of engineering computations with the aid of specialist software, graphical data presentation and their processing using multimedia techniques, as well as the use of internet resources.

The thematic structure of the subjects offered in the studying programme pays attention to theoretical and practical preparation of the graduate to easy implementation and practical use of new achievements of computer technique in numerous applications of naval engineering. We expect that these abilities may turn out very useful on the present-day and future work market.

Specific qualifications of the graduate include:

- ➲ ability to use computer software as the aid in designing elements of naval machinery and equipment
- ➲ knowledge of the structure and basic principles of operation of naval machinery and equipment
- ➲ practical ability to use available computer software for engineering analyses
- ➲ practical knowledge of present-day ship propulsion control systems and electric power generation systems
- ➲ theoretical and practical knowledge of problems of steering and control of ship's engines.

The graduate in this speciality has the following employment opportunities:

- ☆ shipyards, design offices and production plants having connections with the shipbuilding industry
- ☆ technical and marketing departments in companies offering measuring instrumentation for naval machinery and equipment, among other destinations
- ☆ companies offering industrial control and measuring equipment
- ☆ companies developing marine power plant computer control systems.

Professional training

Professional training is integral part of the education process. Depending on the type and year of studies, it is conducted on Navy ships, in Navy training centres, on sea-going vessels, and in shipyards and repair or production plants working for shipbuilding industry. Ship training courses, lasting 6 months, aim at familiarising the trainees with the conditions of work at sea, ceremonials and customs cultivated by the sailors, and principles of operation of a marine power plant with the power output above 750 kW.

At the same time technological training courses, conducted in the production plants and shipyards, are oriented on gaining by the trainees more knowledge on the ship repair technology used in shipyards and the naval equipment production technology.

Didactic offer

Within the framework of the course of mechanics and machinery construction, the didactic offer of the Faculty includes vast variety of specialisations. While the specialisations of the military studies are strictly defined by MOD regulations, those offered in the civilian studies are the effect of permanent analyses of the work market, performed by the Faculty, and reflect the recognised educational needs. In our attempt to follow these needs, every year we extend our didactic offer by new specialisations, to meet in our projections the expectations of alumni of the secondary schools.

A serious organisational problem is relatively low, so far, popularity of intramural civilian studies offered by the Faculty. The Academy is well known in Poland but rather because of its military studies. In this-year recruitment for military studies there were 6 candidates for 1 place. The problem of recruitment for civilian studies, and the resultant poor mathematical and physical knowledge represented by the admitted young people, make it necessary to organise additional compensating courses oriented on minimisation of disproportions between the requirements of the studying

programmes to be realised by the Faculty and intellectual abilities of the young people starting their studies. The problem is becoming even more important in the light of the fact that the thematic range of didactic lessons conducted in English is more and more extended from year to year.

At present the Faculty offers the following specialisations:

- marine power plant operation (military and civilian studies)
- electrical equipment operation (military and civilian studies)
- technical applications of computers (civilian studies)
- mechatronics of oceanotechnical objects (civilian studies)
- diagnostics and repair technology of oceanotechnical equipment (civilian studies).

Such a wide variety of specialisations brings, however, some drawbacks. Namely, in case of high differentiation in specialisations in particular years of studies a situation may happen in which a student who failed to account for one year will not have an opportunity to repeat it, or even to finish studies in the specialisation which he or she started studying (the specialisation is selected during the second semester of studies). But we believe that the nearest future will bring long expected revival of shipbuilding industry in Poland, and the work market will stabilise which will allow us to reduce the list of offered specialisations.

SCIENTIFIC RESEARCH

The scientific potential of the Faculty, growing in successive years of the existence and development of the Academy, was the basis for more and more dynamic scientific activity, oriented on both fundamental and applied research, as well as on development activities and innovative initiatives taken to solve key research problems stated by the Polish Navy, MOD, and shipbuilding industry. Some activities focus on interdisciplinary issues connected with technical aspects of human activity at sea. A noteworthy feature of the scientific activity is that the research conducted in individual teams is strictly related with the didactic process, within the framework of mechanics and machinery construction, the major taught by the Faculty. The results of our scientific research make the basis for large part of the contents of the lectured subjects, while the research rigs, constructed as the result of research activities conducted by the Faculty, are used in laboratory work not only by students, but also by shipbuilding experts of various management levels.

At present, the Faculty of Electrical and Mechanical Engineering has the second scientific category granted by the State Committee for Scientific Research. The Institutes and the Department conduct scientific investigations attributed to various SCSR groups. The Faculty accounts in the group T10 for the scientific activity and the financial support gained for the statute activity.

When characterising the range of scientific research conducted at the Faculty, 7 basic research areas can be named, which, with different intensity, were undertaken throughout the history of its existence as part of the institute structure, i.e. since 1978:

1. Construction and operation of naval machines, in particular the construction and operation of marine propulsion systems and power plants, operation of electrical naval equipment, diagnostics of marine engines, emission of toxic compounds in exhaust gases of marine engines, and statistical methods in operation, reliability and diagnostics of naval machines and equipment. At present these subjects are the objects of basic research activity at the Institute of Ship Construction and Life. The subject matter of the conducted activities mainly focuses on issues connected with widely understood diagnostics of marine piston and turbine engines. This activity was continuously developed since 1982 in four esteemed research teams, out of which the team headed by Prof. Adam Charchalis, D.Sc., was focused on turbine engines, two teams headed by Prof. Leszek Piaseczny, D.Sc., and Dr. Stanisław Polanowski, Ph.D., were involved in studying internal combustion engines, and that headed by the author of the present article performed diagnostic studies of flow systems of piston and turbine engines. A key role in the conducted investigations was also played by the team of specialists in applied mathematics, headed by Prof. Franciszek Grabski, D.Sc., Head of the Mathematics and Physics Department. Realisation of over 20 research programmes made it possible to develop the Basic Diagnostic System for marine internal combustion (piston and turbine) engines. The system provides opportunities for a comprehensive on-line and off-line diagnosis of the current state of the engines being under the diagnostic control, and makes it possible to work out horizons of the prognosis of their faultless work. The developed measurement and control system was used for analysing toxicity of the exhaust gases emitted by marine engines in the aspect of meeting requirements of the MARPOL 73/78 convention. This made it possible to prepare methods of effective reduction of the level of toxic compounds and solid particles emitted in exhaust gases by marine engines and boilers, which goes towards the announced introduction of international standards and regulations limiting the levels of those emissions with respect to engines installed on navy ships.

Recent introduction of a new type of propulsion engine, with relatively low control flexibility, on Polish Navy ships is the motivation for looking for new, so called alternative diagnostic methods, which would make it possible to perform a comprehensive analysis of the technical state of such an engine independently of very expensive producer's service. The methods of diagnostic actions developed in numerous doctor's and qualifying theses base on the following measurements:

a. high- and low-frequency gasodynamic parameters of the working medium
b. lateral and torsional vibrations, along with their spectrum and correlation analyses
c. metallic impurities in the lubricating oil
d. emission of toxic compounds in exhaust gases
e. parameters of the delivered fuel
f. endoscopic inspections.

At present, the Faculty conducts two grants in this area:

- Method of diagnosing engines on military vessels, with limited space for measuring inner cylinder pressure, on the basis of the results of investigations of the gasodynamic processes in the turbocharging system,
- Models for identifying the technical state of an engine from the evaluation of its exhaust gas components.

The results of these grants are being introduced on Navy vessels, among other places.

It is noteworthy that part of the diagnostic instrumentation, such as the endoscope set or gas analysers for instance, can be successfully used for assessing the technical state of both piston and turbine engines. At the same time procedures that realise the diagnostic tests are different - more precisely they

are each time adapted to a particular type of engine. The strategic goal of the presented diagnostic methods, which are continuously developed and modernised, is to provide opportunities for running Navy's marine engines based on their actual technical state. The presently conducted research make it possible to perform technical state based operation of over 150 engines, of total output power exceeding 500 MW. The research rigs, data base, and diagnostic programmes are continuously updated and extended taking into account factory repairs and resultant changes of characteristics of the engines introduced to operation. For the time being, over 1000 expertises of ship's propulsion systems with piston and turbine engines have been done.

The presently conducted research activities are oriented on the development and modernisation of the Basic Diagnostic System, to allow diagnostic supervision of marine piston and turbine engines to be used on American frigates Oliver Hazard Perry (Detroit Diesel, type 16V149TI, and General Electric, type LM-2500), introduced to our Navy in recent years.

2. Technology of underwater activities, construction and operation of diving equipment. Working activities in the area of underwater engineering have been carried out at the Faculty since 1976 in research teams headed by successive commanders of the Department of Diving Equipment and Underwater Work Technology, established in that year as part of the Institute of Ship Construction and Life. They were: Captain Medard Przylipiak, M.Sc., Captain Marian Pleszewski, M.Sc., Captain Stanisław Skrzyński, Ph.D., and recently – Captain Ryszard Kłos, Ph.D. The subject matter of the initiated research activities was connected with the construction and operation of hyperbaric chambers and the construction of life-support systems in real marine diving systems, including submarines. Depending on the type and construction of the underwater object, these systems secure controlled change of parameters of the breathing atmosphere (composition, purity, smell, state parameters such as: temperature, humidity and flow velocity), or intensive exchange of the atmosphere without changing the pressure inside the object. As part of those activities, a hyperbaric unit for saturated diving was modernised to provide opportunities for long-lasting diving experiments, performed using breathing mixtures based on three gases: helium, nitrogen and oxygen, or two gases: nitrogen and oxygen, or helium and oxygen, down to the diving depth of 120 m. Using this unit numerous long-lasting cases of "diving" were executed to prepare and train teams of test-divers for diagnosing modern oceanotechnical objects. Moreover, as part of the studies of oceanotechnical problems, a system examining breathing apparatuses and robots used in the diving equipment was introduced to operation. The basic commissioner of the research activities in the area of underwater engineering is the Polish Navy and the exploratory company PETROBALTIC.

The presently conducted activities are connected with diagnosing underwater objects with the aid of vision systems, and are oriented on working out a method for dimensioning damages of underwater objects. This problem is of high significance when inspecting underwater constructions and Navy vessels, in particular with the aid of the unmanned underwater vehicle ROV SUPER Achilles owned by the Department of Diving Equipment and Underwater Work Technology.

Research activities closely connected with the technology of underwater work are also conducted in other Faculty's organisational units. In particular, the research work conducted by the team headed by Jerzy Garus, Ph.D., in the Institute of Technology Fundamentals refers to, among other topics, methods of recognising underwater objects based on their visual representations. The work aims at developing systems of three-dimensional visualisation of underwater objects, with their further identification and classification. The results to be obtained are expected to make the basis for working out a system of automatic detection of sea mines based on their visual representation. A simulator for remote control of an unmanned deep-water vehicle is being built to provide opportunities for effective examination of methods selecting a trajectory for the vehicle, and controlling its motion along the assumed trajectory.

3. Ship theory and construction. After years of stagnation caused by unexpected resignation of one of Faculty's professors in 1991, long expected revival in the field of model investigations of ship stability and unsinkability has been observed. Subjects were formulated in the Institute of Ship Construction and Life which integrated together the research team headed by Captain Waldemar Mironiuk, PhD, involved in building the research rig to examine in the model tank the behaviour of the physical model of a ship in various emergency states. The range of experimental investigations and numerical studies covers both static and dynamic stability of the ship.

The collected measuring instruments make it possible to record physical processes observed when a ship grounds, or some compartments are flooded in the model of a selected surface or underwater ship in operation in Polish Navy. Moreover, the rig provides opportunities for analysing the effect imposed on the initial ship stability by the free surface of the liquid transported in compartments or tanks, and/or by weight loading, moving, and unloading. Another planned option is examining the effect of wind on stability parameters of the ship in motion.

The expected results of the investigations will make it possible to work out new procedures of ship protection against failures, thus contributing to the prolongation of life of battleships in operation.

4. Material engineering. The objects of investigations are modern construction materials, including composites, splinter resistant steels, aluminium alloys and modified wood used in ship constructions. Material tests aim at working out the technology for their production in the context of their possible use in shipbuilding. This refers in particular to the activities connected with developing and introducing amagnetic steels and cast steels used for marine constructions, including methods for increasing ballistic strength of external and internal shields protecting most important battle stations and ship's quarters.

In recent few years, a new subject of scientific research has been developed in the Institute of Technology Fundamentals which is oriented on comprehensive examination of possible use of wood in shipbuilding. Within the framework of a broad research programme headed by Prof. Lesław Kyzioł, D.Sc., a research rig was built and put in operation. The rig is used for studying wood saturation and polymerisation, processes which make it possible to shape physical and chemical properties of the designed construction elements (Polish National Patent). After introducing genuine technological processes it was proved that the mechanical properties, fatigue, and abrasion resistance of the wood can be significantly increased by its modification consisting in surface saturation with a synthetic polymer (methyl methacrylate). The investigations also confirmed high impact strength of the composites making use of the modified wood, which allows them to be used in real ballistic protection shields on ships.

In recent years, the Faculty has also conducted material investigations connected with the degradation of mechanical properties of austenitic steels and the degradation of shipbuilding properties of aluminium alloys resulting from corrosive electrochemical action of sea water. A separate group of topics comprises vacuum-plasma based methods of refining steel surfaces of deck gear elements. For years these issues have been the object of investigations of specialists in material engineering involved in search for qualitatively new materials to be used in shipbuilding, i.e. materials tightly resistant to the action of corrosive environment at varying loads. The research team headed by Commander Wojciech Jurczak, Ph.D., has recently been strongly reinforced by employing Professor Witold Precht by the Faculty, a person recognised both in Poland and abroad as a specialist in material engineering.

5. Mechanics, in particular impact strength of ship constructions, and computer aided design of elements of ship machines and equipment. The presently conducted research activities include issues relating to general and local strength of ship's hull, resistance of naval devices and equipment, especially at pulse loads. The research includes both theoretical studies of the action of underwater shock wave on the ship hull, and experimental tests leading towards determining the resistance of ship's equipment to underwater detonations. Experiments are carried out which simulate loads of naval objects by contactless underwater detonations. This problem directly results from the need to know load characteristics of ship hulls and marine objects, generated during contactless underwater detonations. For obvious reasons these characteristics are not published, or they are not relevant to specific constructions of ships used by Polish Navy. The characteristics cannot be examined experimentally using real detonations, which is the reason why simulation models are to be developed and used to provide data which then can be transposed to real objects - after evaluating the range of model adequacy. The team, headed by Professor Stanisław Dobrociński, D.Sc., that studies these problems has methodological experience unique in Poland, and the preliminary test of the already developed models allows us to expect real and positive results of those investigations. Direct application of those investigations will consists in introducing constructional changes and modifications to improve impact strength of real ships in operation, and in formulating general conditions on how to preserve this property in the constructions of newly built ships.

An important position in this area of research is occupied by numerical methods applied to solve problems of ship construction hydro-elasticity. Moreover, graphical assistance systems are worked out to be used in numerical calculations, both for controlling input data preparation, and interpreting the obtained results. The latter task is realised using graphical visualisation of the output functions of displacement, stress, temperature and pressure.

6. Steering and numerical automation, in particular: identification and modelling of multi-dimensional objects, artificial neurone networks in steering, fuzzy steering, processing, transfer and visualisation of information data in naval systems, operation of electric power systems and electric drives of the ship. The developed research directions also include the computer system of ship control and measurements, modelling and identification of coefficients in dynamics equations for multi-dimensional objects, and steering the objects sailing along a given trajectory. An important position in the conducted research is occupied by unmanned underwater vehicles equipped with a camera and sonar to identify objects of danger (like mines, for instance).

7. Ship command assistance, including research activities within the field of computer integration of general ship systems, automatic ship control systems, graphical visualisation systems, marine power plant control systems, and marine stabilisation platforms. The studies under way refer to systems that visualise and store ship position and motion, along with its trajectory and the navigational situation for the purposes of Navy ships, and also make it possible to transmit the recorded data via radio to a land-based control centre or the depot ship.

LABORATORIES AND RECORDING EQUIPMENT

The Faculty owns various laboratories and working rooms to support the didactic process at the studies of mechanics and machinery construction, and the realisation of research activities conducted in particular organisational units of the Faculty. The specialist equipment and instrumentation of the didactic laboratories reflect present scientific achievements in the relevant scientific discipline, i.e. machine construction and operation. Detailed data on the laboratory equipment owned by the Faculty are given in Table 1.

Tab. 1. *Recording equipment used in laboratories and working rooms of the Faculty of Mechanical and Electrical Engineering*

Name of laboratory/ working room	Purpose and brief characteristic
Laboratory of marine power plant operation	Equipped with 2 turbine engines, 3 marine piston engines, and all machinery and equipment elements used on Polish Navy ships. Opportunities are also provided for installing recording instruments such as vibration analysers, endoscopes, specialised digital recorders recording high- and low-frequency parameters, etc. The following experimental stands are situated in the laboratory: • stand for testing operating parameters of the engine, equipped with the marine engine SULZER, type 6AL20/24, and the Froude water brake, type DPY6D • didactic stand equipped with the marine engine WOLA, type 57 H6A • marine, single-piston, high-speed internal combustion engine • piston engine S312C • turbine engine GTD–350 • current generating set with the turbine engine TG–16 • stand with an auxiliary marine boiler, type VX506A-10 • oil centrifuge stand equipped with the self-cleaning centrifuge ALFA-LAVAL, type MAPX 207 -24S and the centrifuge ALFA-LAVAL, type MB 1424 F • rotating pump stand equipped with the rotordynamic liquid ring pump, type SK6-01-1 and S-21-4-1 • hydrophore stand • stand for adjusting multi-section injection pumps, type MOTORPAL

Name of laboratory/ working room	Purpose and brief characteristic
Laboratory of marine power plant operation	• air compressor stand equipped with marine piston air compressors, type K2-150 and S2W-50 • fuel injector control and adjustment stand, equipped with a sampler for controlling PRW-3 injectors • refrigerated store stand with a marine compressor • stand for examining FKM–250 van • stand for examining a gear pump • stand for aligning the shaft line and adjusting the timing gear.
Laboratory of metal technology	Equipped with w strength, fatigue and hardness testers, cryostats, impact hammers with relevant cooperating instrumentation, scanning microscopes, etc. The following experimental stands are situated in the laboratory: • stand for mechanical working, equipped with lathes TSB 16; TSB 20; TUM 2117 and two millers Fu2 • stand for manual working, equipped with machines and tools for manual working • welding stand, equipped with: 3 electric welders SPM 200; welding apparatus PSP 251; welders RZP 2A and Mini-Mag 161 • stand do casting and plastic working, equipped with the electric muffle furnace 4kW; lithium box-type furnace KS 520/14; sylithium box-type furnace PSK-1; laboratory dryer KC 100/200 • stand for strength tests, equipped with strength testers MTS 810-12; 1231Y-10 INSTRON and Fu1000 • stand for fatigue strength tests, equipped with the fatigue tester DSO150; and a horizontal machine for fatigue tests in liquid environment • stand for abrasion tests, equipped with a machine for measuring the rate of abrasion of the construction • stand for impact tests, equipped with the pendulum hammer PS-30; PS-5; the rotating impact hammer RSO and the drop-weight hammer MBO for testing large material samples • stand for hardness tests, equipped with hardness testers HPO 3000, PW 106, HPO 250 and the micro hardness tester, type PMT-3 • stand for testing corrosion and corrosion-stress resistance, equipped with the static stretcher – 12 pcs, the four-stand strength tester UMB 6000 and the brine chamber • stand for corrosion-cavitation tests • stand for metallographic tests, equipped with the transmission electron microscope BS- 540, the scanning electron microscope BS- 300, the metallographic microscope Neophot-2 and the vacuum sublimator B302 • wood modification stand, equipped with a saturation autoclave and a polymerisation autoclave; • stand for workshop measurements, equipped with the universal workshop microscope, type ZKMO0.2/150, a small workshop microscope; the Schmalz surface analyser, the Hommel surface analyser - Tester P3, slide callipers, and other small-scale measuring instruments.
Non-permanent laboratory of marine power measurements	The laboratory is equipped with the following instruments: • set for testing mechanical impurities in the lubricating oil ZBZ-1 • signal analyser FFT T2143 • set of HORIBA analysers, type MEXA 9000 • four-gas analyser HORIBA 544J • sound level meter MEDIATOR • levelling laser device OPTALIGN • exhaust gas and admission air flow meter • optical dynamometer DO 9500 • meteorological station • surface roughness meter SUTRO • coating thickness meter MINITEST 60 • portable set for calibrating measuring converters based on the MCX II calibrator and the calibrating pump PV 411 made by DRUCK • torque meter MT – 200 with the torque and rotational speed meter IMFA 20005 • set for endoscope tests, and for recording and visualisation of their results, based on baroscopes and the fibroscope made by OLIMPUS and STORZ.
Non-permanent working room of diving apparatuses	Stands for breathing equipment tests, done according to the EU directive 89/686/EEC.
Non-permanent working room of hyperbaric chambers	Equipped with the experimental deep-diving unit DGKN – 120, which provides opportunities for full exposition and realisation of investigations connected with long lasting stay of a human being under water.
Non-permanent physical and chemical laboratory	Equipped with a gas chromatograph with the mass spectrometer AGILENT 5973, the laboratory shaker LAB – 11 – 200, the gas chromatograph Varian Aerograph 1400, and the laboratory scales AD 500.

Name of laboratory/ working room	Purpose and brief characteristic
Non-permanent laboratory of unmanned underwater vehicles	Underwater vehicle ROV SUPER Achilles, underwater navigation system for ROV type vehicles.
Marine power plant simulator	Equipped with: • corvette power plant simulator - 4 stands with access to internet • simulator of marine low-speed engine - 1 stand with access to internet • computer system for training operation on marine auxiliary installations - 4 stands with access to internet • stand for computer-aided diagnostics of the combustion process in a marine engine, with access to internet.
Didactic room of electronics, automatics and digital systems	Equipped with universal meters, general purpose and specialised oscilloscopes, and didactic computer stands.
Non-permanent didactic laboratory of visualisation systems.	Equipped with a radiolocation situation simulator which delivers information to the data visualisation systems, to be used for steering the ship, groups of ships, and tactic unions (within the framework of the subject entitled Automated Systems of Command and Sea Situation Visualisation). Moreover, the laboratory has the system that simulates the motion of a ship.
Non-permanent didactic laboratory of electric machines	Equipped with 10 sets of machines and measuring stands providing opportunities for conducting basic laboratory activities with electric machines.
Non-permanent laboratory of electric ship propulsion systems	Equipped with 3 sets of electric machines and 5 laboratory stands equipped with specialised meters to conduct laboratory activities on electric ship propulsion systems.
Non-permanent didactic laboratory of fundamentals of electrotechnics and electric measuring	Equipped with 13 laboratory stands providing opportunities for conducting Laboratory activities on electric measurements, and other ship measurements.
Non-permanent laboratory of marine power plant	Equipped with three generating sets and necessary instrumentation, along with digital system of control measurements and visualisation of power plant operation states.
Working room of computer design	Equipped with 10 CAD/CAM stands.

CONCLUSIONS

The state of didactic and scientific achievements observed in the jubilee 75-th year of the existence of the Faculty of Mechanical and Electrical Engineering obliges its authorities to take relevant actions towards starting at the Faculty the second major of civilian studies, and towards submitting for the rights to confer D.Sc. degrees in technical sciences, in the discipline: machine building and operation.

The performed analysis of the employment structure of independent and assistant research workers in the context of represented scientific specialisations and professional experience, along with the prognoses on further didactic development of the Faculty make the basis for expecting that since the academic year 2007/2008 all rights will be obtained for conducting first-level intramural and extramural studies (with further possible extension to the second level) on the second major of mechatronics, in the following specialisations: „Identification and diagnostics of naval technical systems" and „Computer assistance in mechatronics".

Having analysed the present composition of the Faculty Council, and individual and collective achievements of particular research workers in the context of the regulations in force of the Minister of Science and Higher Education concerning conditions for obtaining habilitation rights, we can expect that within the next 3-4 years the intellectual potential and research base of the Faculty will entitle the Dean to submit for granting the Faculty Council these rights. It is noteworthy that as far as the number of research workers with relevant titles is concerned, the Faculty has already met these criteria.

BIBLIOGRAPHY

1. Nawrot D.: *Navy officers in the II Republic of Poland*. Bellona Publishing House, Warsaw 2005 (in Polish).
2. Komorowski A., Nawrot A., Przybylski J.: *Graduates of Polish naval academies in years 1922 – 1995*. PNA Publications, Gdynia 1995 (in Polish).
3. Czyż W.: *Faculty of Mechanical and Electrical Engineering* (*Faculty of Technology*) *at OSMW*, WSMW and PNA in years 1946 –1991 (in Polish).

CONTACT WITH THE AUTHOR
Assoc. Prof. Zbigniew Korczewski
Mechanic-Electric Faculty,
Polish Naval University
Śmidowicza 69
81-103 Gdynia POLAND
e-mail: zkorczewski@wp.pl

The Ship Handling Research and Training Centre at Ilawa is owned by the Foundation for Safety of Navigation and Environment Protection, which is a joint venture between the Gdynia Maritime University, the Gdansk University of Technology and the City of Ilawa.

Two main fields of activity of the Foundation are:

- Training on ship handling. Since 1980 more than 2500 ship masters and pilots from 35 countries were trained at Iława Centre. The Foundation for Safety of Navigation and Environment Protection, being non-profit organisation is reinvesting all spare funds in new facilities and each year to the existing facilities new models and new training areas were added. Existing training models each year are also modernised, that's why at present the Centre represents a modern facility perfectly capable to perform training on ship handling of shipmasters, pilots and tug masters.

- Research on ship's manoeuvrability. Many experimental and theoretical research programmes covering different problems of manoeuvrability (including human effect, harbour and waterway design) are successfully realised at the Centre.

The Foundation possesses ISO 9001 quality certificate.

Why training on ship handling?

The safe handling of ships depends on many factors - on ship's manoeuvring characteristics, human factor (operator experience and skill, his behaviour in stressed situation, etc.), actual environmental conditions, and degree of water area restriction.

Results of analysis of CRG (collisions, rammings and groundings) casualties show that in one third of all the human error is involved, and the same amount of CRG casualties is attributed to the poor controllability of ships. Training on ship handling is largely recommended by IMO as one of the most effective method for improving the safety at sea. The goal of the above training is to gain theoretical and practical knowledge on ship handling in a wide number of different situations met in practice at sea.

For further information please contact:
The Foundation for Safety of Navigation and Environment Protection

Head office:
36, Chrzanowskiego street
80-278 GDAŃSK, POLAND
tel./fax: +48 (0) 58 341 59 19

Ship Handling Centre:
14-200 IŁAWA-KAMIONKA, POLAND
tel./fax: +48 (0) 89 648 74 90
e-mail: office@ilawashiphandling.com.pl
e-mail: office@portilawa.com